Aus dem Institut für klinische Pharmakologie
Direktor: Prof. Dr. med. Ali El-Armouche

FUNCTIONAL CHARACTERIZATION AND EVALUATION OF THE THERAPEUTIC POTENTIAL OF POLO-LIKE KINASE 2 IN CARDIAC FIBROBLASTS AND FIBROSIS

D i s s e r t a t i o n s s c h r i f t

Zur Erlangung des akademischen Grades

Doctor of Philosophy (Ph.D.)

Vorgelegt

Der Medizinischen Fakultät Carl Gustav Carus

Der Technischen Universität Dresden

Von

Dr. med. Stephan R. Künzel

Aus Bautzen

Dresden 2019

1. Gutachter: Prof. Dr. med. Ali El-Armouche

2. Gutachter:

Tag der mündlichen Prüfung:

Gez.:……Vorsitzender der Promotionskommission

Imagination is the source of all human achievement.

Sir Ken Robinson

To my parents Kerstin and Reinhard and my fiancée Karolina.

Thank you for putting the extra into the ordinary every day.

Table of contents

List of figures

List of tables

List of abbreviations

Abbreviation	Explanation
°C	Degree Celsius
ACB	Aortocoronary bypass
ACE	Angiotensin converting enzyme
ACTA	Alpha-actin
AF	Atrial fibrillation
AT1	Angiotensin 1
cDNA	Complementary Deoxyribonucleic acid
CO_2	Carbon dioxide
Col1	Collagen 1
CRISPR/cas	Clustered regularly interspaced short palindromic repeats/ CRISPR-associated
CSQ	Calsequestrine
CX	Connexine
DAPI	4′,6-diamidino-2-phenylindole
DDR2	Discoidin domain-containing receptor 2
DMEM	Dulbecco's Modified Eagle Medium
DMOG	Dimethyloxaloylglycine
DMSO	Dimethyl sulfoxide
DNA	Deoxyribonucleic acid
ECM	Extracellular matrix
EDTA	Ethylenediaminetetraacetic acid
EEF2	Eukaryotic elongation factor 2
ERK1/2	Mitogen-activated protein kinase 3/1

FAP	Fibroblast activation protein
FCS	Fetal calf serum
FIH-1	factor inhibiting HIF
GAPDH	Glyceraldehyde 3-phosphate dehydrogenase
gDNA	Genomic Deoxyribonucleic acid
GFR	Glomerular filtration rate
HFpEF	Heart failure with preserved ejection fraction
hFSP	Human fibroblast surface protein
HIF	Hypoxia-inducible factor
iPSC	Induced pluripotent stem cell
KO	Knockout
LV	Left ventricular
MAPK	Mitogen-activated Kinase
MMP	Matrix metalloproteinases
Morphea	Localized skin fibrosis
mRNA	Messenger Ribonucleic acid
MS	Mass spectrometry
NSAID	Nonsteroidal anti-inflammatory drugs
O_2	Oxygen
OPN	Osteopontin
OSAS	Obstructive sleep apnea
p42/44 MAPK	Mitogen-activated protein kinase 3/1
p53	Tumor protein p53
PCR	Polymerase chain reaction

PHF	PHD finger protein
PLK2	Polo-like kinase 2
PPARγ	Peroxisome proliferator-activated receptor gamma
PPI	Proton-pump inhibitors
PRKRA	Protein kinase, interferon-inducible double stranded RNA dependent activator
qPCR	Real-time polymerase chain reaction
RasGRF	Ras guanine nucleotide exchange factor
RIM	Radiation-induced Morphea
RIPA	Radioimmunoprecipitation assay buffer
RT	Room temperature
SASP	Senescence-associated secretory phenotype
SDS-PAGE	Sodium dodecyl sulfate–polyacrylamide gel electrophoresis
SEM	Standard error of the mean
siRNA	Small interfering Ribonucleic acid
SR	Sinus rhythm
Tcf21	Transcription factor 21
TGF-β	Transforming growth factor beta
Vim	Vimentin
WT	Wild type
α-AR	Alpha adrenoceptor
αSMA	Alpha smooth muscle actin
β-AR	Beta adrenoceptor

1 Introduction

1.1 Fibroblasts

Fibroblasts are cells ubiquitously present in the human body (Doppler et al., 2017). Based on histological examinations of the heart, most authors agree that fibroblasts are the largest population of non-myocytes (Nag, 1980) making up 15 - 30 % of cardiac cells (Pinto et al., 2016). Morphologically, fibroblasts are small (< 50 µm) spindle shaped cells with multiple stellate processes; a flat, oval nucleus, extensive rough endoplasmic reticulum and plenty of cytoplasmic granules (Goldsmith et al., 2004; Camelliti et al., 2005; Baudino et al., 2006; Yue et al., 2011). To date, no exclusively cardiac-fibroblast-specific marker protein has been identified. Therefore, the co-expression of e.g. vimentin, human fibroblast surface protein, fibroblast activation protein (FAP), alpha smooth muscle actin (αSMA), collagen and discoidin domain receptor 2 (DDR2) is approved to identify a fibroblast in the heart (Ivey und Tallquist, 2016). The main fibroblast functions can be categorized in a) structural support and maintenance of the extracellular matrix (ECM), b) chemical and electrical signaling and c) wound healing (Kendall und Feghali-Bostwick, 2014; Künzel, 2014; Klesen et al., 2018).

Structural support and maintenance of the ECM

Fibroblasts are the principal source of ECM in the heart. By forming a scaffold of ground substance (e.g., glycosaminoglycanes like hyaluron), structural proteins comprising mainly collagen type 1 and 3 and adhesive proteins (e.g., laminin and fibronectin) (Kendall und Feghali-Bostwick, 2014), fibroblasts provide an orderly tissue architecture to embed cardiomyocytes and guarantee their proper function. The balance of ECM (mainly collagen) deposition and degradation is maintained by matrix metalloproteinases (MMPs), which break down interstitial collagen (Wynn, 2008; Baum und Duffy, 2011). Dysfunction of ECM homeostasis can result in fibrosis-related disease, eventually leading to failure of the affected organ (Kendall und Feghali-Bostwick, 2014).

Chemical and electrical signaling

Communication between different cell types is crucial for regular organ function. Fibroblasts are reported to secrete and respond to a plethora of proteins, cytokines and growth factors allowing them to communicate with neighboring cells (Wynn, 2008; Baum und Duffy, 2011; Kuenzel et al., 2018). Consequently, recent research has demonstrated that fibroblasts are substantially involved in angiogenesis and immune response by orchestrating the involved

(Jordana et al., 1994; Porter und Turner, 2009; Baum und Duffy, 2011; Kendall und Feghali-Bostwick, 2014). Besides chemical means of communication, fibroblasts have been shown to interact with other cardiac cells via electrical signals (Camelliti et al., 2005; Klesen et al., 2018). Fibroblasts can couple to myocytes via connexins 43 and 45 or nanotubes to propagate action potentials and exchange ions and cytosolic proteins (Camelliti et al., 2005; Dixon und Davies, 2011; Quinn et al., 2016). This finding however indicated that altered electrophysiological properties of fibroblasts might be a source of arrhythmia (Poulet et al., 2016; Klesen et al., 2018).

Wound healing

Fibroblasts are essential for wound healing. Upon injury fibroblasts proliferate, secrete new ECM as a scaffold for regenerative tissue and express αSMA filaments allowing them to manipulate the ECM fibers and surrounding cells to close the wound. Furthermore, activated fibroblasts recruit immune cells involved in the process of wound healing by chemotaxing (Gabbiani, 2003; Midwood et al., 2004; Bainbridge, 2013; Kendall und Feghali-Bostwick, 2014). A recently published study revealed that myofibroblasts contribute to engulfment of dead cells after myocardial infarction and thereby help to limit inflammation and further contribute to ordered wound healing (Nakaya et al., 2017).

1.2 Fibroblast activation – myofibroblast-differentiation

Exposure to adequate stimuli initiates transition of fibroblasts from activated fibroblasts into their myofibroblast phenotype (Figure 1). Under physiological conditions myofibroblasts are absent in the heart. Activating stimuli comprise, inter alia, loss of cell-cell contacts, mechanical stress (rapid beating frequencies of the heart), myocardial injury (infarction and tissue hypoxia e.g.), chemical mediators (foremost TGF-β) and epigenetic factors like DNA methylation, histone modification and siRNAs (see Fig. 1) (Masur et al., 1996; Baum und Duffy, 2011; Liu et al., 2012; Robinson et al., 2012; Hu und Phan, 2013). *In vitro* experiments have demonstrated that activation of the TGF-β receptor 1 and 2 induces phosphorylation of the transcription regulators SMAD2 and SMAD3 which form a complex with SMAD4 in the nucleus and gene expression of myofibroblast-differentiation genes like ACTA2 which is encoding for αSMA (Tallquist und Molkentin, 2017). During the process of transition, activated fibroblasts and especially myofibroblasts secrete excessive ECM (see 1.1 Fibroblasts) and a plethora of (inflammation) mediators like TGF-β, angiotensin 2, interleukins and osteopontin (Petrov et al., 2002; Liu et al., 2012; Tallquist und Molkentin, 2017). Furthermore, they develop a contractile apparatus by forming ordered bundles of αSMA micro filaments which enables myofibroblasts to exert contractile force on the surrounding ECM and neighboring cells (Baum und Duffy, 2011). Finally, myofibroblasts become resistant towards apoptosis guaranteeing their

presence until a wound is closed and repaired or activating stimuli are absent (Rog-Zielinska et al., 2016; Tallquist und Molkentin, 2017). Pathologically prolonged presence of myofibroblasts though, leads to local inflammation and excessive deposition of interstitial collagen, fostering a pathological condition called fibrosis (Rog-Zielinska et al., 2016; Tallquist und Molkentin, 2017).

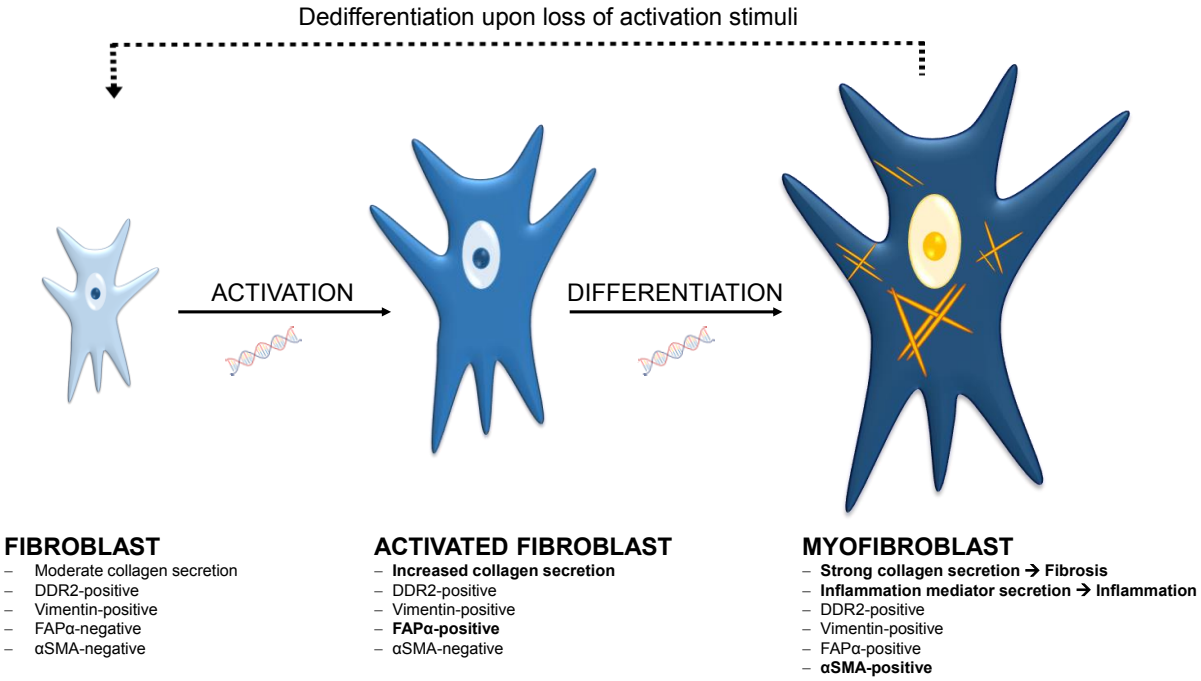

Figure 1. Schematic illustration of fibroblast activation and subsequent myofibroblast differentiation. The figure illustrates in a simplified manner the process of fibroblast-to-myofibroblast transition. Upon injury, chemical stimuli or epigenetic modification, fibroblasts become activated and secrete collagen and cytokines like TGF-β or osteopontin. As activation stimuli are present for a prolonged period, activated fibroblasts express contractile αSMA-microfilaments (orange bundles) and are referred to as myofibroblasts. (modified from *(Künzel, 2014; Tallquist und Molkentin, 2017)*

1.3 Fibrosis

In ancient Greek philosophy the ‘golden mean’ marked an optimality between the extremes of excess and deficiency. In the human organism, this optimality is called homeostasis and is required for proper function on organ-, tissue- and cell-level. Tissue homeostasis in the heart however, is mainly regulated by fibroblasts which secrete and degrade ECM proteins.

Cardiac fibrosis

A common hallmark of cardiovascular disease is the imbalance of ECM homeostasis with a shift towards synthesis, leading to excessive interstitial collagen deposition - fibrosis. In

the course of fibrosis, cardiac tissue stiffens and loses its ability to relax and contract orderly. Diminished elasticity causes diastolic (Burlew und Weber, 2002) and finally systolic dysfunction, resulting in reduced cardiac performance and lower life expectancy (Biernacka und Frangogiannis, 2011). Recent studies estimated that > 45 % of mortality is caused by fibrosis-associated disease in Western countries (Wynn, 2008; Rosenbloom et al., 2013).

Myofibroblasts are responsible for fibrosis development in the heart (Fan und Guan, 2016). With a rising proportion of myofibroblasts the disease progresses and aggravates. Due to fibrosis, diffusion distances increase continuously. As a result of this, tissue hypoxia occurs in the heart (Gramley et al., 2010). Hypoxia has been described to alter fibroblasts epigenetically on the level of DNA methylation (Robinson et al., 2012). Altered methylation patterns influence the transcription of genes. In primary human lung fibroblasts these epigenetic modifications were found to lead to fibroblast activation and fibrosis (Robinson et al., 2012). This mechanism could be applicable to cardiac fibroblasts as well.

Although cardiac fibrosis is a major health care issue, the currently available antifibrotic pharmacotherapy is insufficient. ACE or aldosterone inhibitors for example, which are known for their positive effects on fibrotic remodeling thus failed to prevent fibrosis progression in heart failure (Fang et al., 2017). Fibrotic remodeling of myocardium occurs in all chambers of the heart. In human atria, fibrosis becomes more prevalent with age and is a hallmark of remodeling due to atrial fibrillation.

(Non-cardiac) dermal fibrosis

Since fibroblasts are ubiquitously present in the human body their activation and the subsequent development of fibrosis can affect virtually all tissues and organs. There is evidence that localized e.g. fibrosis leads to an increase in systemic inflammation mediators such as TGF-β, osteopontin or interleukins (Wu et al., 2012; Wu und Assassi, 2013) which can then induce fibrosis in a different location. Especially dermal fibrosis is well-studied in this regard. An interesting but mechanistically poorly understood manifestation of skin fibrosis is the radiation-induced Morphea (RIM), which occurs in patients after successful treatment of breast cancer with chemo- and radiotherapy (Spalek et al., 2015). The dermatological term Morphea describes a circumscribed area of skin fibrosis which normally occurs in scleroderma. Although 1 in 500 breast cancer patients is affected by RIM (Spalek et al., 2015) the disease-relevant pathological mechanisms are only little understood. For this reason, the therapeutic options are confined to immunosuppression with only moderate success rates (Akay et al., 2010; Spalek et al., 2015). However, it is evident that fibroblast function must be altered in this

context and studying functional and molecular properties of primary fibroblasts from these patients could lead to novel treatment options.

1.4 Fibroblast function in sinus rhythm and atrial fibrillation

Sinus rhythm (SR) is characterized by the periodical excitation and contraction of the atria followed by the ventricles. This regular excitation is generated by specialized myocytes which are called pacemaker cells. Atrial fibrillation (AF) on the other hand is the result of uncoordinated high frequency excitation, leading to irregular contraction of the atria. AF is the most prevalent tachyarrhythmia in clinical practice with rising prevalence in the elderly (Miyasaka et al., 2006).

Sinus rhythm and atrial fibrillation

Physiological excitation of the heart is initiated in pacemaker cells located within the sinus node. The excitation wave front propagates through the atrial myocardium to the atrio-ventricular node from where it seizes both ventricles in an orderly manner. The autonomous nervous system modifies the intrinsic rhythm (sinus rhythm) for optimal adaptation of blood supply to the needs of the organism. AF constitutes a common arrhythmia with high-frequency, uncoordinated activation of the atrial myocardium and irregular conduction of the excitation wave to the ventricles. The tachyarrhythmia is a frequent cause of heart failure. Since the fibrillating atria do not contract efficiently, blood flow slows down and is prone to clot formation that may cause embolic stroke (Calvo et al., 2018). Many comorbidities are associated with AF, including diabetes, hypertension and heart failure (Calvo et al., 2018).

Epidemiological studies indicate that overall AF prevalence ranges from 1.9 – 2.9 % in European adults (Zoni-Berisso et al., 2014). Globally, AF incidence and prevalence increased drastically in the past decades which could result in an estimated number of over 50 million affected patients worldwide by 2030 (Colilla et al., 2013; Zoni-Berisso et al., 2014). Based on these numbers AF can be described as a major health care problem that yet has to be solved.

Paroxysmal, persistent and permanent AF

Atrial fibrillation exhibits a progressive time course. In the beginning of the manifestation of the disease, AF terminates within 7 days (paroxysmal AF) either spontaneously or upon pharmacological or electrical conversion to sinus rhythm (Kirchhof et al., 2014; Kirchhof et al., 2016; Calkins et al., 2017). On the other hand, there is] Persistent AF lasts beyond 7 days, whereas long standing persistent AF is characterized by a duration of greater than 12 months. Finally, in permanent AF the persistence of AF is accepted by both patient and physician and there will be no further attempts to restore SR (Calvo et al., 2018).

Pathophysiology of AF

Despite intensive research in AF during the past decades, the underlying mechanisms of AF maintenance remain incompletely understood. AF is initiated when a trigger hits a vulnerable substrate (Künzel, 2014). A trigger may consist of focal ectopic activity originating from sinoatrial-like pacemaker cells in the sleeves of atrial myocardium that extend into the pulmonary veins (Jones et al., 2008) or within diseased atrial cells exhibiting early or delayed afterdepolarizations which exacerbate into extra systoles (Antzelevitch und Burashnikov, 2011). Mechanical stress, cellular calcium overload, genetic defects are typical initiating insults. Propagation of ectopic electric signals leads to reentry when the excitation waves spread around a conduction obstacle like for instance a fibrotic area and finds its originating myocardium re-excitable. Thus a short effective refractory period and slowing of conduction will favor reentry (Ravens, 2014).

With regard to AF maintenance, there are two accepted theories explaining the drivers of AF. The first concept is based on the existence of so-called rotors which create self-sustaining spiral waves of electricity in the tissue. Those rotors are considered the engine of fibrillation since they can lead to high frequency excitation of the atria (Jalife et al., 2002). The second theory is explained by asynchronous electrical activation of the atrial endo-, and epicardial layer of muscle. High resolution mapping of the right atria of AF patients revealed that excitation of these layer can be highly asynchronous and eventually an excitation wave front can break through into the other layer and thereby consolidate fibrillation (de Groot et al., 2016).

Remodeling in AF

One hallmark of AF is electrical, structural and cellular remodeling of the atria (Calvo et al., 2018). The clinically most relevant component of remodeling is probably fibrosis leading deteriorating cardiac function and further arhythmogenesis in the course of AF. Most of the fibrotic remodeling is mediated by pathologically activated myofibroblasts (Nattel et al., 2008; Baum und Duffy, 2011; Nattel und Harada, 2014; Calvo et al., 2018). For this reason, we have previously studied functional differences between fibroblasts derived from SR or AF patients (Poulet et al., 2016). Our main findings included that AF leads to diminished fibroblast proliferation but increases basal differentiation into myofibroblasts indicating that AF leads to profibrotic fibroblast activation (Poulet et al., 2016). There is a great need for fibroblast-specific upstream antiremodeling therapies (Calvo et al., 2018). However, the mechanisms underlying the phenomena observed by Poulet and colleagues remain to be investigated in order to identify new therapeutic targets.

1.5 Polo-like kinase 2

Polo-like kinase 2 (PLK2), also referred to as serum inducible kinase (Snk), belongs to a family of conserved serine/threonine protein kinases (Burns et al., 2003a; Shen et al., 2012),which is characterized by the presence of the C-terminal “polo box” domain which is crucial for protein interactions (Park et al., 2010). The kinase domain is localized at the N-terminus (Archambault und Carmena, 2012). The PLK-family has so far been associated with cell proliferation, reactive oxygen species production in the mitochondria and apoptosis (Strebhardt, 2010; de Cárcer et al., 2011, S. 1; Archambault und Carmena, 2012). PLK2 regulates centriole duplication and is mainly expressed in G1 phase (Warnke et al., 2004; Cizmecioglu et al., 2008; Cizmecioglu et al., 2012) and is therefore crucial for mitosis and cell proliferation (Burns et al., 2003a; Warnke et al., 2004). Furthermore, PLK2 can induce a G2/M checkpoint of the cell cycle to induce cell cycle arrest (Clay et al., 1993; Glover et al., 1998; Ma et al., 2003). Consequently, PLK2 overexpression has been reported in malignant neoplasia going alongside with uncontrolled proliferation (Strebhardt, 2010; Ou et al., 2016). To date PLKs have been foremost the subject of neurological studies. In the brain, PLK2 is responsible for the regulation of synaptic plasticity by controlling Ras signaling. PLK2 phosphorylates RasGRF1 which is a guanidine exchange factor that stimulates downstream Ras activity. After phosphorylation, pRasGRF1 is degraded in the proteasome (Lee, Lee et al., 2011; Lee, Hoe et al., 2011). Taken together, PLK2 acts as a negative regulator of Ras activity. However, a potential involvement of PLK2 in cardiovascular pathophysiology remains to be elucidated. Recent research published by Mochizuki et al. proved that PLK2 expression of cardiac progenitor cells is higher as long as they remain in a proliferative state. Upon terminal differentiation though, PLK2 expression is drastically reduced. Instead of terminal differentiation though, cells can also enter a dormant non-proliferative state called senescence (Coppé et al., 2008). Experimental data revealed that loss of PLK2 function leads to induction of senescence (Deng et al., 2017). Cell senescence is linked to physiological cell aging but also marks a response to cellular stress. However, senescent cells are, although being dormant, metabolically active. The senescence-associated secretory phenotype (SASP) causes inflammation (Coppé et al., 2008) that favors fibrosis development (Boos et al., 2006; Boos und Lip, o. J.). The mechanisms regulating PLK2 expression and the physiological functions of PLK2 in the adult heart remain widely unknown. Although. PLK2 expression was shown to be regulated by p53, miR-126 and via promoter methylation (Burns et al., 2003b; Syed et al., 2006; Benetatos et al., 2011; Liu et al., 2014), further studies will be necessary to identify the mediators responsible for PLK2 regulation as well as the main PLK2 substrates in the heart.

1.6 Osteopontin

Osteopontin (OPN) is a secreted phosphoprotein of the extracellular matrix which is produced by various cardiac cell types including fibroblasts, myocytes, endothelial cells and macrophages (Trueblood et al., 2001; Singh et al., 2010; Collins et al., 2012; Zhao et al., 2016). OPN was identified to serve in signaling pathways beyond its originally considered function in bone mineralization (Noda, 1989). *In vitro* studies confirmed that OPN increases myofibroblast-differentiation, collagen secretion and inflammation thereby contributing to fibrosis development in the heart (Pardo et al., 2005; Singh et al., 2010). Clinical research confirmed that elevated plasma levels of OPN were present in patients with permanent AF (Güneş et al., 2017). With regard to the inflammatory component of AF, OPN seems to be a promising target in the center of inflammation processes. Supporting this hypothesis, inhibition or knockout (KO) of OPN clearly reduced fibrotic tissue remodeling in dilated cardiomyopathy and after myocardial infarction in mouse models (Trueblood et al., 2001; Zhao et al., 2016). Yet, an experimentally based molecular link between PLK2 and OPN has to be elucidated.

1.7 Aim of the study

The following study was designed to foster the understanding of PLK2 function in the healthy and diseased heart with particular emphasis on patients suffering from atrial fibrillation. Primary human, murine and rat cardiac fibroblasts were isolated and generally characterized with regard to PLK2 function. Echocardiography and surface ECG recordings were obtained from a specific PLK2 knockout mouse model to study the impact of PLK2 on cardiac function. Atrial tissue samples and peripheral blood from patients in SR and AF were studied for fibrosis markers, inflammation proteins and epigenetic modifications. In an approach for deep phenotyping, a secretome analysis of PLK2 KO and wildtype fibroblasts was performed at King's College London and expanded by an RNA sequencing. The following questions were addressed in this study:

a) *What is the physiological function of PLK2 in cardiac fibroblasts and how is it altered in atrial fibrillation?*

b) *Which molecular pathways are involved in the signaling of cardiac PLK2 and are there putative drug targets up- or downstream of PLK2?*

c) *Are there putative clinical implications by targeting PLK2 or its signaling cascade?*

d) *Is the PLK2-signaling axis generally relevant in (non-cardiac) fibrotic remodeling?*

Since our previous work revealed marked functional differences between fibroblasts from SR and AF patients, we need to clarify the underlying molecular mechanisms of these phenomena in order to expand our knowledge about atrial fibrillation pathophysiology. Greater knowledge will ultimately lead to new drug targets and complement existing therapeutic strategies to fibroblast specific antifibrotic pharmacotherapy.

2 Material and Methods

2.1 Material list

2.1.1 Devices and experimental hardware

Function	Product specification	Supplier
Analytical balance	MC BA 100	Sartorius, Göttingen, Germany
Human tissue preparation	Binocular S761	Olympus, Tokyo, Japan
Autoclave	Vakulab HP	Münchener Medizin Mechanik, Munich, Germany
Cell culture hood	HeraSafe KSP15	Thermo Fisher Scientific, Waltham, USA
Cell culture incubator	BBD 6220	Thermo Fisher Scientific, Waltham, USA
Cell culture suction	BVC professional suction	VACUUBRAND GMBH + CO KG, Wertheim, Germany
Echocardiography setup	Vevo3100	FUJIFILM VisualSonics, Amsterdam, The Netherlands
Hypoxia chamber	CB 60	BINDER GmbH, Tuttlingen, Germany
Automatic stainer for histology	Linear Stainer COT 20	Medite, Burgdorf, Germany
Digital fluorescence microscope	BZ-X710	Keyence, Osaka, Japan
Microplate reader	BioTek SynergyHTX multi-mode reader	BioTek Germany, Bad Friedrichshall, Germany
Western blot and PCR gel development device	Fusion FX	Vilber Lourmat, Eberhardzell, Germany
PCR gel casting chamber	40-1515	Peqlab, Erlangen, Germany
PCR electrophoresis chamber	41-2025	Peqlab, Erlangen, Germany

Western blot gel casting glass plates	1 mm, 1.5 mm, 2 mm	Bio-Rad Laboratories GmbH, Munich, Germany
Western blot gel casting frame	Mini-PROTEAN® Tetra Cell Casting Stand	Bio-Rad Laboratories GmbH, Munich, Germany
Western blot electrophoresis chamber	Mini-Protean 3	Bio-Rad Laboratories GmbH, Munich, Germany
Western blot power supply	PowerPack Basic	Bio-Rad Laboratories GmbH, Munich, Germany
Western blot table shaker	Gyro-rocker SSL3	Cole-Parmer, Stone, UK
Western blot roller mixer	Stuart roller mixer SRT9	Cole-Parmer, Stone, UK
Electric ball mill	TissueLyser LT	Qiagen, Hilden, Germany
Microscopes	Primo Star	Zeiss, Oberkochen, Germany
	LSM-510 confocal microscope	Zeiss, Oberkochen, Germany
	Olympus CK40	Olympus, Tokyo, Japan
Magnetic stirrer	RH Basic	IKA, Staufen im Breisgau, Germany
Microtome	RM 2235	Leica, Wetzlar, Germany
Microwave	HF 22023	Siemens, Munich, Germany
Paraffin embedding system	TES Valida	Medite, Burgdorf, Germany
Paraffin stretch bath	1052	Gesellschaft für Labortechnik, Burgwedel, Germany

PCR cycler	Mastercycler nexus (gradient)	Eppendorf, Hamburg, Germany
pH meter	pH Level 2	WTW Inolab, Weilheim, Germany
Cordless pipetting controller	Pipetus	Hirschmann, Eberstadt, Germany
Powersupply (gel electrophoresis)	PowerPac Basic	Bio-Rad Laboratories GmbH, Munich, Germany
qPCR cycler	CFX96 Touch Deep Well Real-Time PCR detection system	Bio-Rad Laboratories GmbH, Munich, Germany
Ultrapure water filtration system	Milli-Q Q-Pod	Merck Millipore, Burlington, USA
Spectrophotometer	Nanodrop 1000	Thermo Fisher Scientific, Waltham, USA
Thermomixer	Thermomixer compact	Eppendorf, Hamburg, Germany
Convection drying oven	UT 6760	Heraeus, Hanau, Germany
Vortex	Minishaker MS2	IKA, Staufen im Breisgau, Germany
Centrifuges	Microfuge 18	Beckmann Coulter, Brea, USA
	Megafuge 8R	Heraeus, Hanau, Germany
	3K30	Sigma-Aldrich, St. Louis, USA

2.1.2 Software

Function	**Product specification**	**Supplier**
PC operating system	Windows 10	Microsoft Corporation, Redmont, USA
Image editing	Paint.NET	dotPDN LLC

Office productivity software	Microsoft Office (MS Word, MS Powerpoint, MS Excel)	Microsoft Corporation, Redmont, USA
Spectrophotometer	Nanodrop 1000 v3.7	Thermo Fisher Scientific, Waltham, USA
Microplate reader operation	BioTek Gen5 data analysis software	BioTek Germany, Bad Friedrichshall, Germany
Statistical analysis	GraphPad Prism 5	GraphPad Software, San Diego, USA
Operating system western blot and PCR gel development device	Fusion-Capt	Vilber Lourmat, Eberhardzell, Germany
Digital fluorescence microscope	BZ-X Viewer	Keyence, Osaka, Japan
	BZ-X Analyzer	Keyence, Osaka, Japan
Operating and analysis of qPCR	CFX Manager	Bio-Rad Laboratories GmbH, Munich, Germany

2.1.3 Cell culture consumables

Function	**Product specification**	**Supplier**
Filtration of cell debris and tissue	100 µm nylon filter	BD Biosciences, San Jose, USA
Sterile plastic tubes	BD Falcon tubes (15 ml, 50 ml)	BD Biosciences, San Jose, USA
Petri dishes	Nunclon surface	Nunc, Roskilde, DK
Cell culture plates	6-, 12-, 24-wells Nunclon surface	Nunc, Roskilde, DK
Cell scraper	24 cm, 30 cm	TPP, Trasadingen, CH
Mesh	Cell strainer 40 µm	Corning, Tewksbury, USA
Disposable plastic pipettes	5 ml, 10 ml, 25 ml, 50 ml	Sigma-Aldrich, St. Louis, USA

Disposable pipette tips	SafeSeal tips for pipettes (10 µl, 20 µl, 100 µl, 200 µl, 1000 µl)	Sigma-Aldrich, St. Louis, USA
Disposable sterile scalpel	Techno cut	Myco Medical, Cary, USA
Eppendorf tubes	50 µl, 500 µl, 1.500µl, 2.000 µl	Eppendorf, Hamburg, Germany
Glass coverslips	1 cm diameter	Warner Instruments, Hamden, USA
Microscope glass slides	24 x 60 mm	Engelbrecht, Edermünde, Germany

2.1.4 Cell culture media, supplements and chemicals

Function	**Product specification**	**Supplier**
Fibroblast medium	Dulbeccos's Modified Eagle Medium (DMEM), high glucose	Gibco-Life Technologies, Carlsbad, USA
Wash buffer	Phosphate Buffered Saline (PBS)	Sigma-Aldrich, St. Louis, USA
Nutritive medium supplement	Fetal calf serum (FCS)	Sigma-Aldrich, St. Louis, USA
Antibiotics	Penicillin/ Streptomycin (10000 U/ml)	Gibco-Life Technologies, Carlsbad, USA
Cell detachment	0.25% Trypsin-EDTA	TPP, Trasadingen, CH
Cell viability staining	Trypan blue stain 0.4%	Thermo Fisher Scientific, Waltham, USA
Specific ERK1/2 inhibitor	SCH772984	Selleckchem, Munich, Germany
Specific PLK2 inhibitor	TC-S 7005	Tocris Bioscience, Bristol, UK
Osteopontininhibitor	Mesalazine (5-Asa)	Sigma-Aldrich, St. Louis, USA

Solvent for PLK2 inhibitor	Dimethyl sulfoxide (DMSO)	Sigma-Aldrich, St. Louis, USA
Fixation of cells/ tissue	Roti®-Histofix 4 %	Carl Roth GmbH + Co. KG, Karlsruhe, Germany
Permeabilization of cells	Triton-X 100	VWR International LLC, Radnor, USA
Mounting medium	Fluoromount-G	Sigma-Aldrich, St. Louis, USA
Chromatin staining of nuclei	4′,6-Diamidin-2-phenylindol (DAPI)	Sigma-Aldrich, St. Louis, USA

2.1.4 Kits and reagents

Function	**Product specification**	**Supplier**
RNA isolation	PeqLab total RNA mini	Peqlab Biotechnologie GmbH, Erlangen, Germany
cDNA synthesis	PeqGold cDNA synthesis kit	Peqlab Biotechnologie GmbH, Erlangen, Germany
gDNA isolation	PureLink Genomic DNA Extraction kit	Thermo Fisher Scientific, Waltham, USA
qPCR mastermix	SYBR green	Bio-Rad Laboratories GmbH, Munich, Germany
Bisulfite conversion	EZ DNA starter kit	Zymo Research, Irvine, USA
Assessment of cell migration	Cell migration kit	Cell Biolabs Inc., San Diego, USA
Senescence detection	Senescence Detection Kit (ab65351)	Abcam, Cambridge, UK
Histology staining	H&E fast staining kit	Carl Roth GmbH + Co. KG, Karlsruhe, Germany
	Trichrome Stain (Masson) Kit	Sigma-Aldrich, St. Louis, USA

	Picro Sirius Red Stain Kit (Connective Tissue Stain) (ab150681)	Abcam, Cambridge, UK
DNA ladder marker	GeneRuler™ 100bp	Thermo Fisher Scientific, Waltham, USA
Migration assay	Wound Healing Assay	Cell Biolabs, Inc., San Diego, USA
Protein concentration measurement assay	Pierce™ BCA Protein Assay Kit	Thermo Fisher Scientific, Waltham, USA
Western blot development substrate	Pierce™ ECL Western Blotting Substrate	Thermo Fisher Scientific, Waltham, USA

2.2 Cell isolation and cell culture conditions

2.2.1 Human sample acquisition

All patients enclosed in this study gave written informed consent according to the Declaration of Helsinki. Human cardiac tissue samples (right atrial appendages) were collected in collaboration with Herzzentrum Dresden GmbH from patients who underwent open heart surgery like bypass or valve replacement (official file number: EK 114082202). Only tissue specimen that accrued anyway in the course of an operation have been used for this study - no extra tissue was removed from patients. Peripheral blood samples from AF patients who would undergo ablation of pulmonary veins were collected prior to the intervention in EDTA-tubes (EK 465122013). Low voltage zones being electrophysiological indicators for fibrotic tissue areas were assessed by electrophysiological mapping of the left atrium and defined as bipolar voltage < 0.5 mV. The obtained blood samples were kept at 4° C for a maximum of 1 h. The tubes were subsequently centrifuged for 10 min at 1000 g at 4° C. Then, the plasma was transferred into 500 µl Eppendorf tubes and stored at -80° C until analysis. Detailed patient data can be found in supplemental tables 5 -7 (see: 6 Supplementary Data).

2.2.2 Human right atrial fibroblast isolation

Primary human right atrial fibroblasts were isolated via outgrowth method from cardiac biopsies (Poulet et al., 2016). Prior to fibroblast isolation, heart tissue was dissected carefully under a laminar flow. The epicardium and epicardial fat were removed to avoid the outgrowth of other cell types than fibroblasts (Figure 2 b). Myocardial tissue was subsequently cut into small pieces of approximately 1 mm3 with a sterile scalpel. Afterwards, the tissue pieces were placed on a 6 cm petri dish (Figure 2 c). Carefully, 1 ml of cell culture medium was added drop by drop to avoid dislocation of the tissue chunks. The primary cultures were then kept at 37° C and 5 % CO_2 for 21 days to allow outgrowth of fibroblasts in a more physiological way.

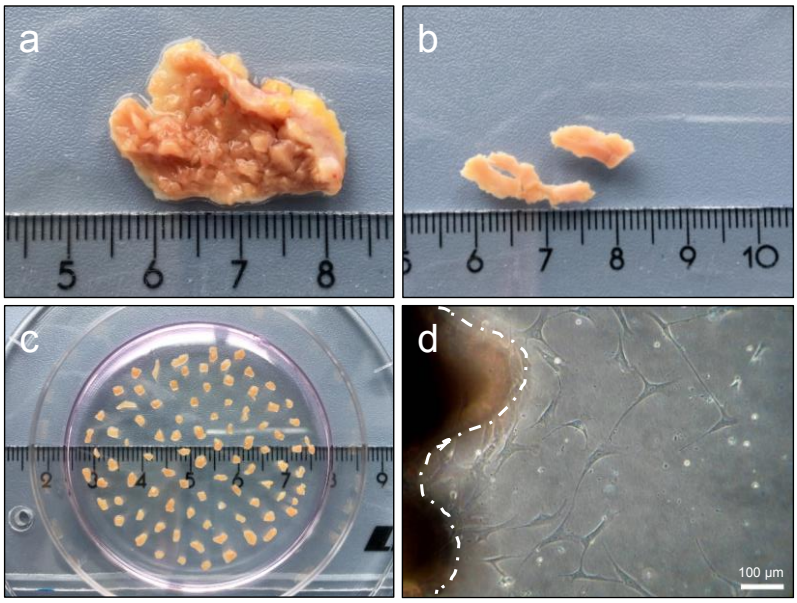

Figure 2. Human tissue preparation and fibroblast outgrowth. **a)** Typical human right atrial appendage. **b)** Isolated myocardial tissue. **c)** Primary culture after tissue dissection. **d)** Primary atrial fibroblasts growing out of the tissue (tissue borders are indicated by the white line).

2.2.3 Murine and rat cardiac fibroblast isolation

PLK2 WT and KO mice (Ma et al., 2003; Inglis et al., 2009) are commercially available via The Jackson Laboratory (129S.B6N-*Plk2*^{tm1Elan}/J, stock number: 017001 Plk2 KO) but these animals have not been characterized with regard to cardiac development and function, yet. Wild type Wistar rats were purchased from Charles River Laboratories. Primary murine and rat cardiac fibroblasts were isolated enzymatically via Langendorff-perfusion (El-Armouche et al., 2008). The supernatant was centrifuged for 1 min at 350 g to remove heavier components like cardiomyocytes and debris. The resulting supernatant was centrifuged a second time for 1 min at 750 g to sediment contained fibroblasts. The supernatant was removed and the resulting pellet was resuspended in cell culture medium and transferred into a t25 cell culture flask for primary culture. Cells were harvested for experiments when optical confluence was at around 90 %. The animal study was approved by the local bioethics committee (T 2014/5; TVA 25/2017, TVV 64/2018) and internationally accepted animal welfare guidelines (Guillen, 2012) were followed.

2.2.4 Immortalized human ventricular fibroblasts

Immortalized human ventricular fibroblasts were purchased from abm Inc. (Richmond, Canada) and adjusted to our cell culture conditions (see 2.2.7). The rationale to buy these cells was the opportunity to perform larger scaled experiments without the confounder of patients'

bio variability. Furthermore, immortalized fibroblasts are known to display higher proliferation rates which increases cell availability for experiments compared to human primary fibroblasts.

2.2.5 Human dermal fibroblasts

Primary human dermal fibroblasts were obtained from Prof. Claudia Günther's working group (Dermatology Department, University hospital Carl Gustav Carus, Dresden, Germany). These fibroblasts have either been isolated of healthy female breast skin (Control fibroblasts) or from RIM lesions (RIM fibroblasts).

2.2.6 Ultrasonic-augmented primary murine fibroblast isolation

In order to improve the enzymatic fibroblast isolation via Langendorff-perfusion, we generated a novel fibroblast isolation method using ultrasonic waves and enzymatic tissue digestion. This fast and cost-effective method delivered high-quality viable primary fibroblasts. The detailed protocol can be found in the supplemental data. The protocol is currently in revision at the Journal of Visualized Experiments (JoVE).

2.2.7 Cell culture conditions

Cells were cultured in Dulbecco modified eagle medium supplemented with 10% fetal calf serum and 1% penicillin/ streptomycin. Petri dishes and cell culture flasks did not require additional coating. Cells were kept in a humidified surrounding at 37° C and with 5 % CO_2.The cell culture medium was changed every other day. To expose the cells towards hypoxic conditions (1 % O_2) cells were cultured in a hypoxia incubator chamber for 24 up to 96 h depending on the experimental setup.

2.3 Cell culture based experiments

2.3.1 Immunocytochemistry

To perform immunocytochemical staining experiments, fibroblasts were seeded on 1 cm glass cover slips and cultivated for 7±1 days until they reached approximately 90% of optical confluence. Cells were then washed 3 times with cold PBS, fixed in 4% PFA for 15 min at RT, washed and subsequently permeabilised using Triton X. After blocking with FCS, the cover slips were incubated with primary antibody (DDR2, Vimentin, hFSP, αSMA, Col1, PLK2 (dilution 1:200)) and DAPI for 1 h in a dark, humidified surrounding at RT. After 10 times washing by gently dipping the cover slips into a beaker containing cold PBS, the secondary antibodies Alexa-Fluor 448 or Alexa Fluor 597 (Abcam, Cambridge, UK) were applied for 1 h under the same conditions as described for the primary antibody. The cover slips were washed 10 times again and mounted onto microscope glass slides using Fluoromount G. To avoid

dislocation, the cover slips were fixed with transparent nail polish. The samples were kept in the dark until fluorescence images were obtained with a Zeiss LSM-510 confocal microscope.

2.3.2 Proliferation

To determine fibroblast proliferation, cells were plated at densities of $1*10^4$/ well of a 12-well plate (Figure 3). To harvest and count cells, the wells were incubated with 1 ml 0.25 % trypsin for 5 min at 37° C. The reaction was stopped by adding the double amount of cell culture medium. Cells were detached using a cell scraper. The cell suspension was then centrifuged for 5 min at 350 g. The supernatant was removed and cells were resuspended in 1 ml cell culture medium. Finally, the cells were counted using a Bürker chamber.

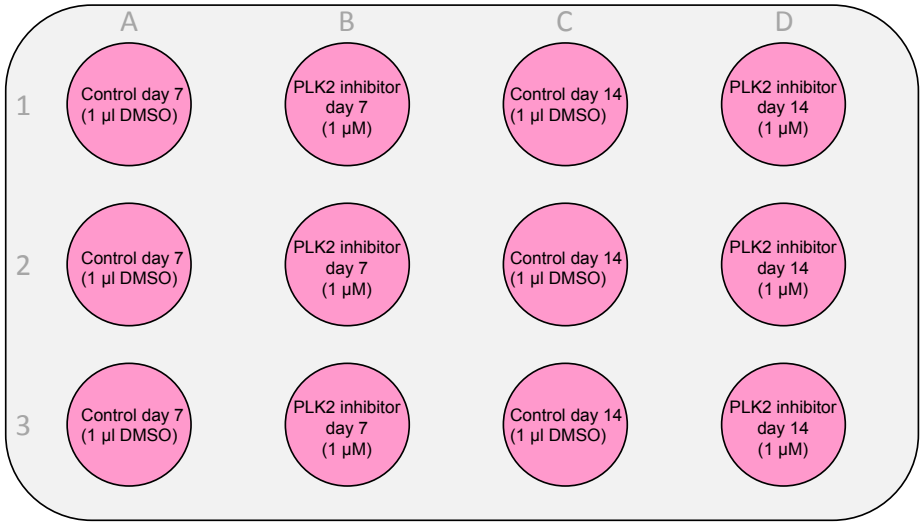

Figure 3. Example of plate layout for proliferation experiments. Cells were harvested after 7 (day 7) or 14 days (day 14), respectively. Control indicates solvent control (1 µl DMSO), PLK2 inhibitor indicates TC-S 7005 1 µM.

2.3.3 Migration

To explore the effect of PLK2 inhibition on migration capacity a commercially available wound healing assay was performed (Cell Biolabs). Plastic dividers which were included in the kit were placed into a 24-well plate ensuring a cell-free area in the middle of the well. Equal densities of $2.5*10^4$ cells were seeded on each side of the divider. After 24 hours the dividers were removed and cells were washed twice with PBS and images were obtained (Figure 4 a). Fresh medium containing drug (PLK2 inhibitor e.g.) or solvent control (1 µL DMSO) were added. Afterwards, a picture of the newly created cell free area (wound) was acquired (t = 0 h). After 24 hours the cells were washed with PBS three times and fixed with 4% formaldehyde for 15 min at RT. The nuclei were stained with DAPI. After DAPI staining a fluorescence image of the well was acquired in order to count the cells which migrated into the wound area (t = 24 h) (Figure 4 b).

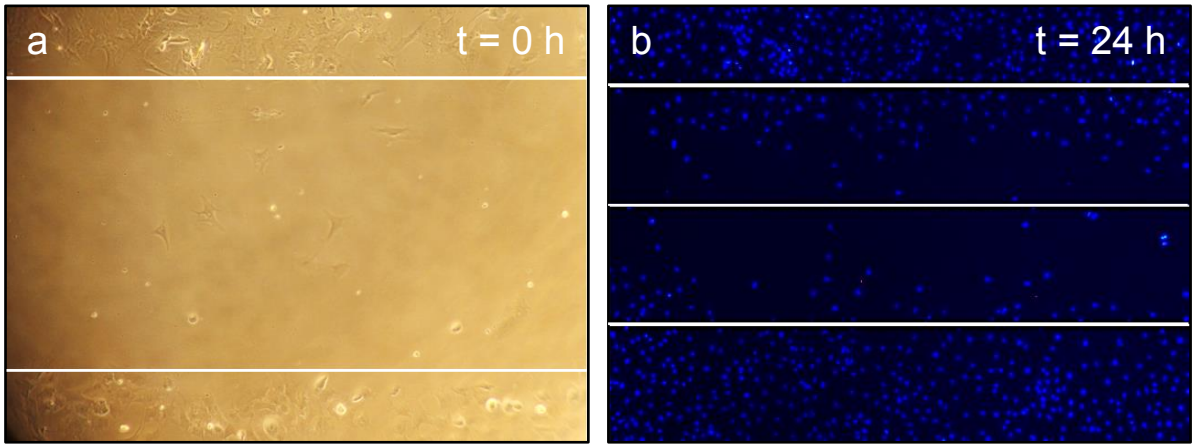

Figure 4. Migration assay. a) Example image of the cell-free area (wound) after seeding at t = 0 h. **b)** DAPI staining to count the number of migrated cells into the former wound area after 24 h.

2.3.4 β-galactosidase staining for senescent cells

Fibroblasts were plated on 6-well plates at densities of 2.5*104 cells/ well and kept in culture for 7 days. Afterwards cells were fixed with 4 % formaldehyde for 15 min at RT and the senescence staining was performed. Therefore, a commercially available senescence detection kit (β-galactosidase staining) was purchased and performed according to the manufacturer's instructions. Cells that were positive for β-galactosidase were considered senescent (Figure 5).

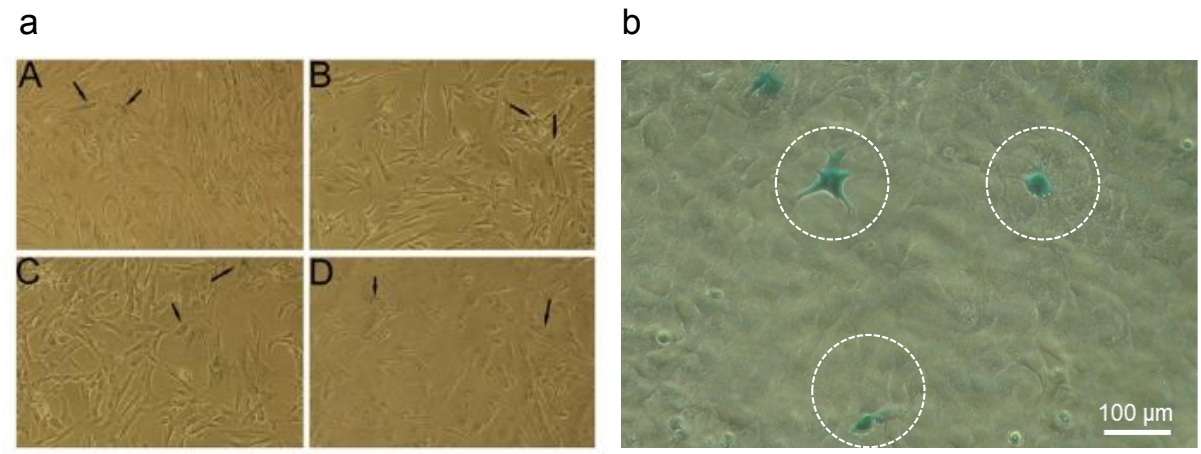

Figure 5. Detection of β-galactosidase positive cells. a) Example picture from the manufacturer (modified from abcam), the black arrows mark β-galactosidase positive cells. **b)** Example of senescent human cardiac fibroblasts, the white circle mark β-galactosidase positive cells.

2.3.5 Hypoxia cell culture

To evaluate the effects of chronic hypoxia (1 % O_2) on the methylation status of the PLK2 gene and subsequently it's expression on mRNA level, fibroblasts were seeded on 6-well plates at densities of $5*10^4$/ well. Plates were prepared in duplicate for hypoxia incubation and control. After 24 h the treatment plate was transferred into a hypoxia chamber for 24 and up to 72 h. RNA or genomic DNA (gDNA) were isolated afterwards to evaluate the effects of hypoxia on PLK2 gene expression.

2.4 Molecular biology

2.4.1 Western Blot

SDS-PAGE, western blotting and immunodetection. Protein was extracted from whole heart tissue with Kranias lysis buffer containing 10 % protease and phosphatase inhibitors. To isolate protein from cells, RIPA buffer containing 10 % protease and phosphatase inhibitors was used. Protein concentration was measured with a BCA kit (Pierce). For gel electrophoresis 8 - 15 % polyacrylamide gels were used. 30 µg of protein were loaded into each lane of a gel. Proteins were subsequently transferred to a 0.45 µm nitrocellulose membrane. Equal loading was proven with a ponceau red staining. Before blocking, the mebranes were cut to enable the application of several primary antibodies. The blocking step was done in 5 % milk for 1 hour at RT. After blocking, the membranes were washed 3 times with 0.1 % TBST for 3x 10 min. Membranes were incubated with primary antibodies overnight at 4° C. After 3 times washing with 0.1 % TBST for 3x 30 min, secondary antibodies (anti mouse or anti rabbit) were applied for 1 h at RT under constant gentle shaking. After a final washing step (3x 10 min with 0.1 % TBST), membranes were incubated with ECL development solution and placed in a Fusion FX device to acquire images. Standard housekeeping proteins, depending on the molecular weight of the proteins of interest, were glyceraldehyde 3-phosphate dehydrogenase (GAPDH), calsequestrin (CSQ) or eukaryotic elongation factor 2 (EEF2). Data analysis was done with the Fusion CaptAdvance software.

Table 1: Kranias lysis buffer

Chemical	Concentration
Tris	30 mM
EDTA	5 mM
NaF	30 mM
SDS	3 %
Glycerol	10 %
pH	Adjusted to 8.8

Table 2: RIPA lysis buffer

Chemical	Concentration
Tris	30 mM
EDTA	0.5 mM
NaCl	150 mM
NP-40	1 %
SDS 10 %	0.1 %

2.4.2 Quantitative polymerase chain reaction (qPCR)

RNA isolation. Total RNA from either cardiac tissue samples or cultured cardiac fibroblasts was isolated using the PeqLab total RNA mini kit according to the manufacturer's instructions. The optional on column DNAse1 digestion was performed for each RNA isolation. RNA concentration was measured using the nanodrop photometer.

Reverse transcription - cDNA synthesis. Reverse transcription of RNA into cDNA was performed with the PeqGold cDNA synthesis kit according to the manufacturer's instructions.

Quantitative real-time PCR (qPCR). Real-time PCR was used to measure the gene expression of PLK2. Specific exon-exon spanning primers for PLK2 were designed using the Primer Blast

software. GAPDH was used as standard housekeeping gene. For hypoxia experiments RPL32 was used as a hypoxia-stable housekeeper. PCR was performed in a CFX96 Touch Deep Well Real-Time PCR Detection System. Samples were amplified in duplicates or triplicates as indicated in the corresponding figures in the results part. Data analysis was done with the CFX manager software. Results were calculated and interpreted using relative quantification.

Table 3: RT mastermix

Component	**Volume per 20 µl reaction**
SsoAdvanced universal SYBR® Green supermix (2x)	10 µl
Forward primer	1 µl
Reverse primer	1 µl
Template	100 ng (volume variable)
Nuclease-free H_2O	variable
Total reaction mix volume	20 µl

2.4.3 Methylation specific polymerase chain reaction

The methylation-specific PCR was performed according to previously literature (Syed et al., 2006; Benetatos et al., 2011; Robinson et al., 2012). Genomic DNA (gDNA) was isolated using the PureLink Genomic DNA Extraction kit (Thermo Fisher). Purified gDNA was subsequently bisulfite converted using the EZ DNA starter kit according to the manufacturer's instructions. The following PCR protocol was designed according to the suggestions of ZYMO Research. For unmethylated samples 36 cycles were run and for detection of DNA methylation 40 runs, respectively. For electrophoresis, the PCR products were then applied to a 2% agarose gel containing HD green. Visualization of gel bands was achieved with a Fusion FX (peqlab) development device.

PLK2 *unmethylated for.: 5'-CACCCCACAACCAACCAAACACACA-3'*

PLK2 *unmethylated rev.: 5'-GGATGGTTTTGAAGGTTTTTTTGTGGTT-3' (product = 142 bp)*

PLK2 *methylated for.: 5'-CCCACGACCGACCGAACGCGCG-3'*

PLK2 *methylated rev.: 5'-ACGGTTTTGAAGGTTTTTTCGCGGTC-3' (product = 137 bp)*

2.4.4 Human osteopontin ELISA

To measure the osteopontin concentration in the peripheral blood of healthy SR control and AF patients with or without fibrosis, an enzyme linked immunosorbent assay (ELISA) was performed as previously published (Güneş et al., 2017). We purchased the human osteopontin ELISA kit from abcam and used it according to the manufacturer's instructions. To generate an appropriate standard curve, a four parameter logistic fit was done using the Graph Pad Prism software (version 5).

2.5 Secretome analysis

To evaluate the effect of PLK2 KO on the fibroblasts secretome, cell culture media were collected and studied. Fibroblasts were seeded on t25 cell culture flasks and grown until they reached 90 % of optical density. Cells were then washed 3 times with PBS, followed by a 10 min incubation with PBS at 37° C. PBS was gently removed and replaced by serum-free DMEM with 1% PS. Serum-free culture is crucial to avoid albumin "contamination". Cells were further cultivated for 72 h. Afterwards the cell medium was removed, filled into cryo tubes and frozen in liquid nitrogen. The samples were stored at -80° C until analysis. The secretome analysis of PLK2 WT and KO fibroblasts was then performed in the laboratory of our cooperation partner Prof. Manuel Mayr at King's College London. After purification the proteins from the cell culture media were loaded onto a commercially available electrophoresis gel and separated. A silver staining was performed (Figure 6) to visualize the protein band and allow cutting of the gel for further digestion which is required for the final MS run. The MS run and data analysis were performed as previously published by Prof. Mayr (Suna et al., 2018).

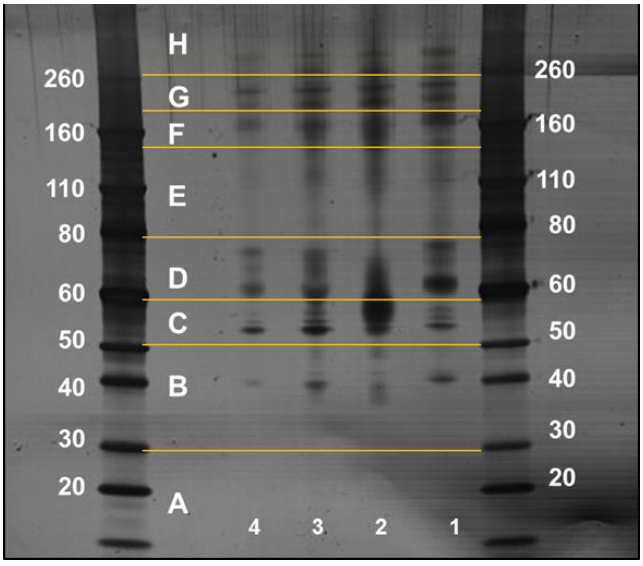

Figure 6. Representative silver stained electrophoresis gel. The gel was cut into lanes using a protein standard marker (right and left lanes). Lanes 2 C and 2 D are an example of remaining albumin that could not be washed off prior to serum-free culture.

2.6 Transcriptome analysis

The transcriptome analysis of 3 PLK2 WT vs 4 PLK2 KO fibroblast RNA samples was conducted in cooperation with the department of gynecology and the National Center for Tumor Diseases (NCT), Partner Site Dresden. RNA was isolated as described above. The sequencing and bioinformatic analysis were done as previously published (Schott et al., 2017; Kuenzel et al., 2018).

2.7 Echocardiography and surface ECG recording

PLK2 WT and KO mice were anesthetized with 2 - 4% isoflurane and subsequent ultrasound images were acquired in supine position using a Vevo 3100 Imaging System. Body temperature (core temperature) was measured using a rectal temperature probe. Core temperature was maintained at 37 °C. Surface ECG recordings were obtained using limb electrodes. A standard 2D echocardiographic study was performed in the parasternal long-axis and short-axis views for assessment of diastolic and systolic function.

2.8 Statistical analysis

For statistical analysis and graphic representation of the data, Graph Pad Prism software (version 5, San Diego, USA) was used. Data is presented as mean ± SEM. For comparisons between two groups student's t-test was used with Welsh's correction if appropriate. When comparing three groups, a one-way ANOVA with Newman-Keuls posttest was performed. P-values < 0.05 were considered statistically significant and indicated with asterisks (*) in the corresponding figures ($*p < 0.05$; $**p < 0.01$; $***p < 0.001$). In cases of clear trends but with short missing of the limit of significance p-values were given in the figure.

3 Results

3.1 Differentially regulated gene expression in SR and AF fibroblasts

3.1.1 Validation of the Affymetrix microarray

A previously published study from our laboratory revealed marked functional differences in fibroblasts derived from SR and AF patients. These differences comprised lower proliferation and migration rates but contrariwise elevated differentiation into myofibroblasts in AF derived fibroblasts compared to SR controls (Poulet et al., 2016). An Affymetrix® microarray for more than 10.000 genes was performed as a first attempt to reveal the underlying molecular mechanism responsible for these phenomena. Out of the genes which were regulated in fibroblasts from AF patients compared to SR controls, we put particular emphasis on target genes that have been associated with a) immune response, b) regulation of proliferation and apoptosis or c) cell migration/ invasion. These genes comprised CACNB4 (calcium channel, involved in proliferation, differentiation (Rima et al., 2017)), PDGFA (platelet-derived growth factor A, involved in proliferation (Bonner et al., 1990)), ANO1 (Ca^{2+}-activated Cl^- channel, involved in proliferation and migration (Jacobsen et al., 2013; Guan et al., 2016)), MMP1 (matrix metallo proteinase, involved in proliferation and migration (Das et al., 2017; He et al., 2017)) and PLK2 (polo-like kinase 2, involved in proliferation, apoptosis and oxidative stress (Ma et al., 2003; Mochizuki et al., 2017)). To validate the findings from the microarray, quantitative PCR was performed. The results did not reveal significant regulation of ANO1, CACNB4, PDGFA and MMP1, although there were clear trends for reduced PDGFA and MMP1 expression in AF samples (Figure 7 d). However, there was a significant 1.6-fold reduction of PLK2 mRNA expression in AF samples (Figure 8 a). This finding was further validated by western blot analysis revealing significantly lower PLK2 protein abundance in AF tissue samples (Figure 8 b and c).

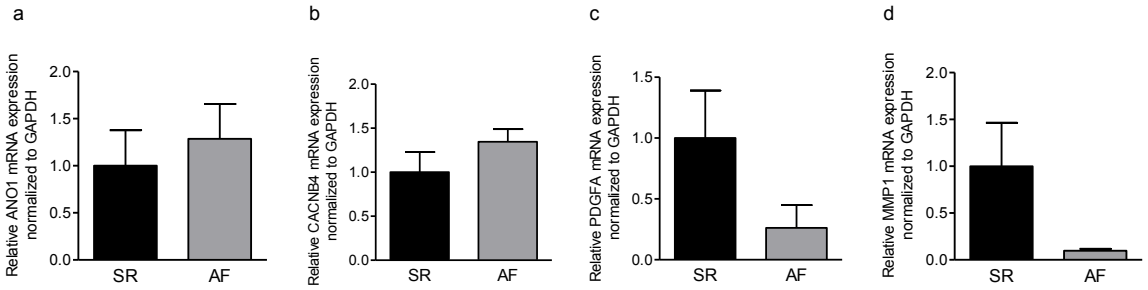

Figure 7. qPCR analysis of mRNA expression normalized to *GAPDH* for selected genes in SR and AF. a) Relative mRNA expression of *ANO1* in SR and AF fibroblasts. **b)** Relative mRNA expression of *CACNB4* in SR and AF fibroblasts. **c)** Relative mRNA expression of *PDGFA* in SR and AF fibroblasts. **d)** Relative mRNA expression of *MMP1* in SR and AF fibroblasts, (n_{SR} = 7; n_{AF} = 5). The results failed to reach the level of statistical significance.

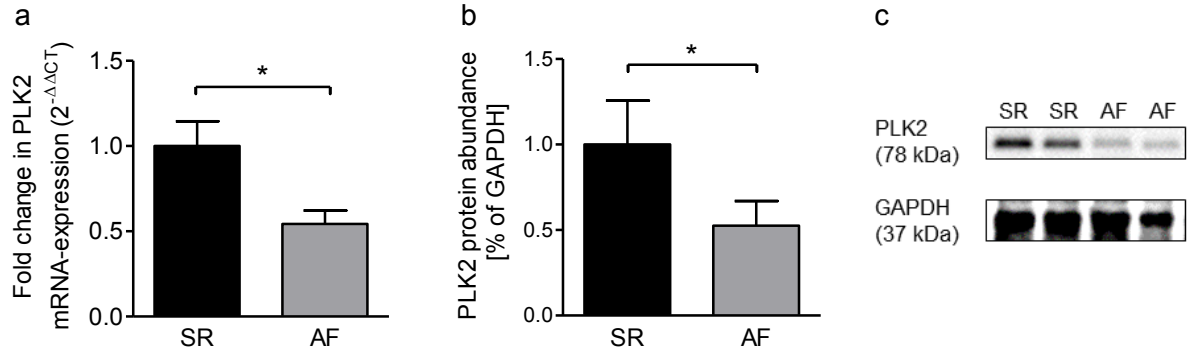

Figure 8. Analysis of PLK2 gene expression and protein abundance. **a)** Expression of *PLK2* mRNA normalized to GAPDH in primary human atrial fibroblasts from SR and AF patients, analyzed with qPCR (n = 7 vs. 5). **b)** Quantification of western blot for PLK2 protein abundance in SR and AF atrial tissue lysates (n = 9 per group). **c)** Example western blot. p-values < 0.05 were considered statistically significant.

3.1.2 Epigenetic modification of the *PLK2* promoter in AF

Recent studies focused on differential expression of polo-like kinase in malignant neoplasia. DNA methylation was described as one frequently occurring mechanism of *PLK* expression regulation (Syed et al., 2006; Benetatos et al., 2011; Coley et al., 2012b). DNA methylation is reported to occur in CpG-islands which are short segments of eukaryotic DNA ahead of promoter regions. Methylation of these islands results in blockade of gene transcription of the following gene region. In analogy to these studies we investigated the methylation status of the CpG-island of the *PLK2* promoter (Syed et al., 2006; Benetatos et al., 2011) in SR and AF atrial tissue samples and isolated fibroblasts with methylation specific PCR. Methylation was present in 6 out of 13 AF samples but in none of the analyzed SR (n = 11) samples suggesting a correlation of PLK2 downregulation and promoter methylation in AF (Figure 9).

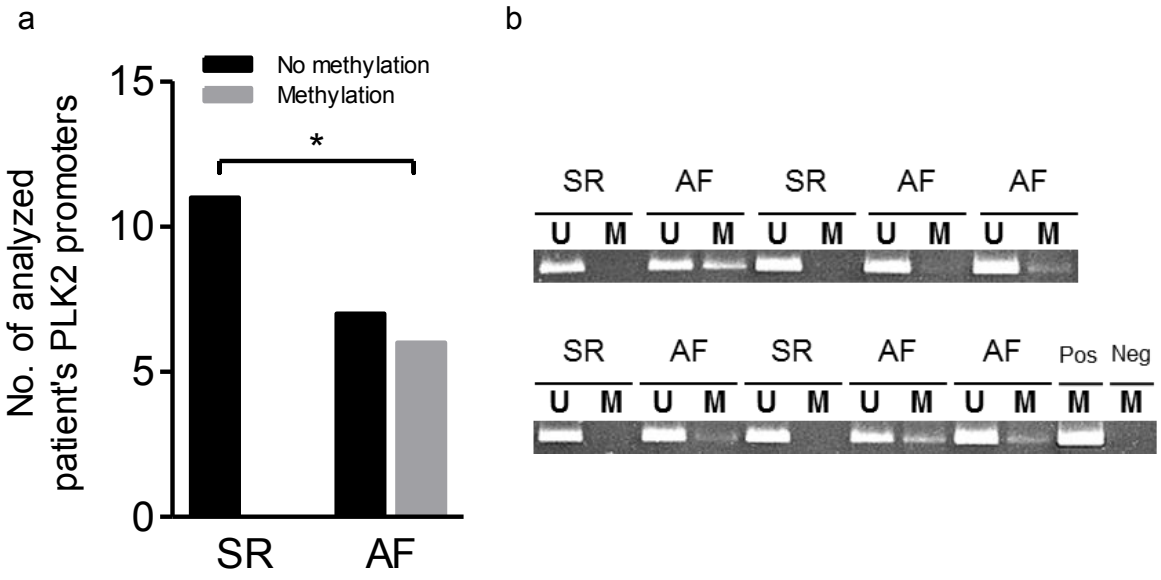

Figure 9. Analysis of the methylation status of the PLK2 gene promoter. a) Quantification of SR and AF heart tissue samples in which methylation was present or not. Statistical analysis was done with Fisher 's exact test. **b)** Methylation-specific PCR of the PLK2 promotor region (U: unmethylated, M: methylated, Pos = positive control (human universal methylated DNA standard), Neg = water control). p-values < 0.05 were considered statistically significant.

3.1.3 Effect of rapid ventricular pacing on PLK2 protein expression

To prove the assumption that AF is causal for PLK2 downregulation, we obtained protein lysates from a canine ventricular tachycardia pacing model (Hanna et al., 2004). The only variable in this model was whether or not the animals received pacing or a SHAM surgery. For this reason, confounding variables such as age, comorbidities, medication, etc. could be excluded. We found a reduction of PLK2 protein abundance by 48% after rapid ventricular pacing for 5 weeks. Due to the limited number of animals the result slightly failed to reach the level of statistical significance ($p = 0.056$).

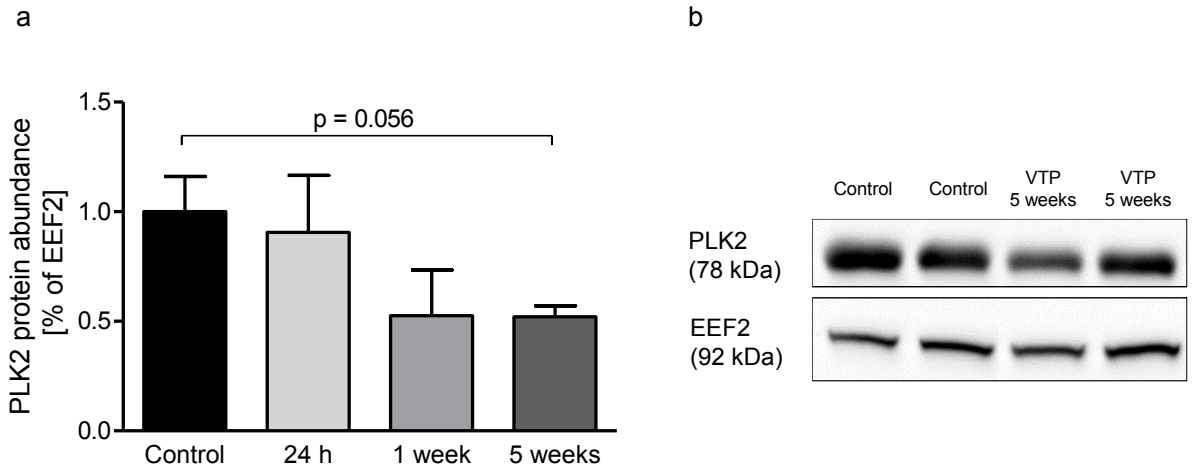

Figure 10. PLK2 protein abundance in ventricular tachy-pacing dog samples. **a)** Quantification of western blot for PLK2 protein abundance in VTP dog samples (n = 3 - 4 per group). **b)** Example western blot for a. p-values < 0.05 were considered statistically significant.

3.2 Effect of PLK2 inhibition or deficiency on fibroblast function *in vitro*

3.2.1 Fibroblast identification

Cells analyzed in this study were either isolated with the outgrowth method or via centrifugation of Langendorff supernatants (see 2.2). Stainings for vimentin (Vim), human fibroblast surface protein (hFSP) and DDR2 were done to identify the isolated cells as fibroblasts. Almost all cells (≈ 99%) were positive for those three markers. There was no contamination with other cell types like endothelial cells detectable. Figure 11 shows representative staining images for the marker proteins.

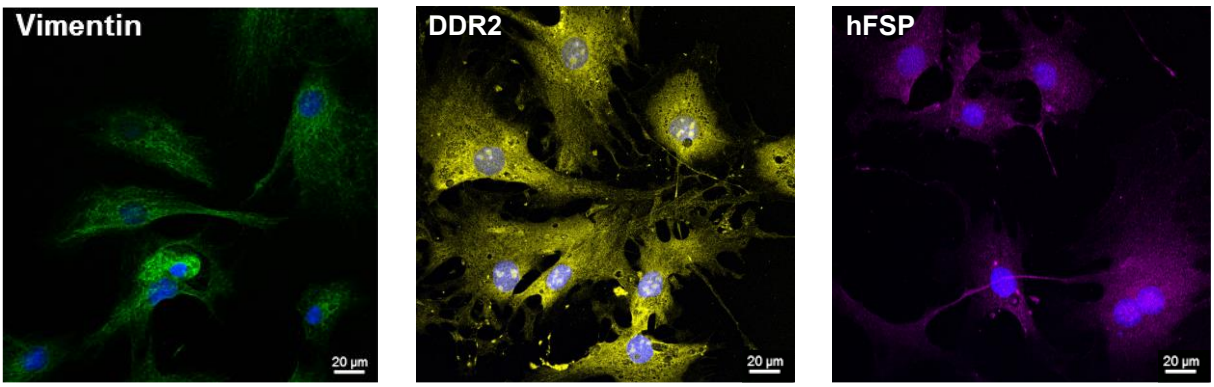

Figure 11. Immunocytochemical fibroblast identification. Representative staining images of primary fibroblasts for the fibroblast marker proteins vimentin DDR2 and hFSP, after P1. The nuclei were stained with DAPI (blue). The scale bar equals 20 µm. The original colour of the fluorescence signal (green) was altered for better visibility with the ZEN2.3 lite software for DDR2 and hFSP.

3.2.2 Effect of PLK2 inhibition on human atrial myofibroblast differentiation

There are several well-established factors stimulating fibroblasts to undergo phenotypic transition into myofibroblasts. These factors include amongst others: mechanical stress, missing cell-cell contacts, hypoxia, inflammatory cytokines or prolonged cell culture (Baum und Duffy, 2011; Tallquist und Molkentin, 2017). Despite the variety of appropriate stimuli, the common hallmark of fibroblast-to-myofibroblast differentiation is the expression of organized αSMA microfilaments (Figure 12).

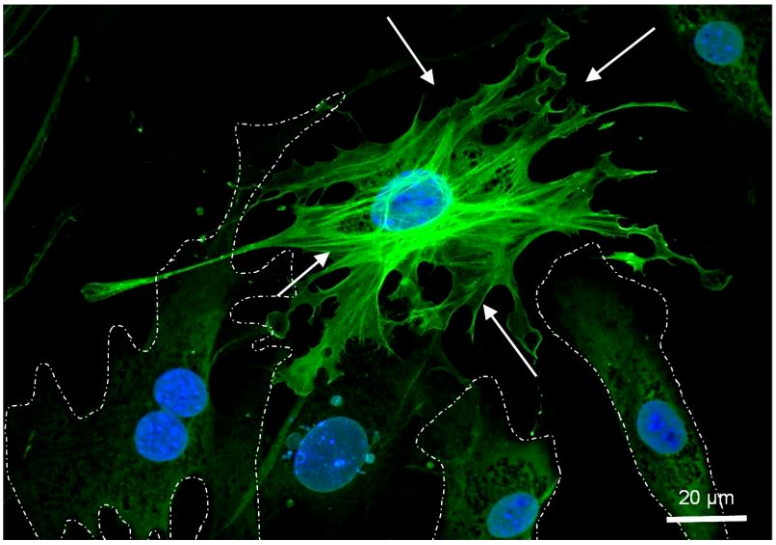

Figure 12. Immunofluorescence staining for αSMA in myofibroblasts. The white arrows indicate a myofibroblast displaying orderly arranged αSMA microfilaments. The dashed line indicates fibroblasts without αSMA microfilaments. The nuclei were stained with DAPI (blue). The scale bar equals 20 µm.

In this study we analyzed the effect of PLK2 inhibition with 1 µM TC-S 7005. Fibroblasts were grown on coverslips and incubated with PLK2 inhibitor for 7±1 days until they reached > 80 % of optical confluence. In parallel, control fibroblasts were grown in the presence of 1 µl DMSO/ml cell culture medium as solvent control. After immunological staining (described in 2.3.1) images of the cells were acquired with a confocal microscope. An overview image was obtained for further quantitative analysis. 50 cells at least were analyzed for each sample to determine the number of αSMA-positive cells. Inhibition of PLK2 led to increased myofibroblast differentiation. Compared to solvent control (18.1 % myofibroblasts), there was an increase of 26.8 % of myofibroblasts in the PLK2 inhibitor-treated samples (44.9 % myofibroblasts in total) (Figure 13 a to c).

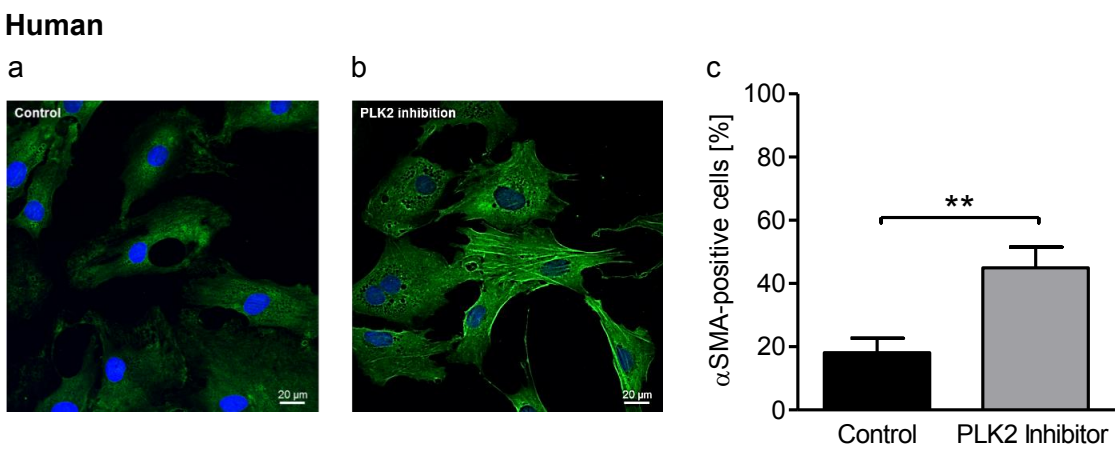

Figure 13. Analysis of PLK2 inhibition-dependent myofibroblast differentiation. a) Solvent control immunofluorescence staining image for αSMA. **b)** Immunofluorescence staining image for αSMA in the presence of PLK2 inhibitor, the nuclei were stained with DAPI (blue). **c)** Quantification of immunostaining experiments for αSMA protein abundance dependent on PLK2 inhibition (n = 6 in each group). Primary right atrial SR fibroblasts were incubated either with 1 µM TC-S 7005 (specific PLK2 inhibitor) or DMSO control (1 µl/ml of cell culture medium) for 7±1 days. p-values < 0.05 were considered statistically significant.

3.2.2.1 Effect of genetic knockout PLK2 on murine cardiac myofibroblast differentiation

To consolidate the observed effect that pharmacological inhibition of PLK2 increases differentiation of fibroblasts into myofibroblasts, PLK2-deficient cardiac fibroblasts were isolated from commercially available PLK2 knock-out (KO) mice and their wild type littermates. Similar results were observed in these murine fibroblasts. PLK2 KO fibroblast cultures displayed on average 35.6 % of myofibroblasts whereas only 13.1 % of the wildtype fibroblasts underwent phenotypic transition into myofibroblasts (Figure 14 a to c). On average, KO of PLK2 increased myofibroblast differentiation by 22.5 % which is comparable to the effect of pharmacological inhibition (+ 26.8 %).

Murine

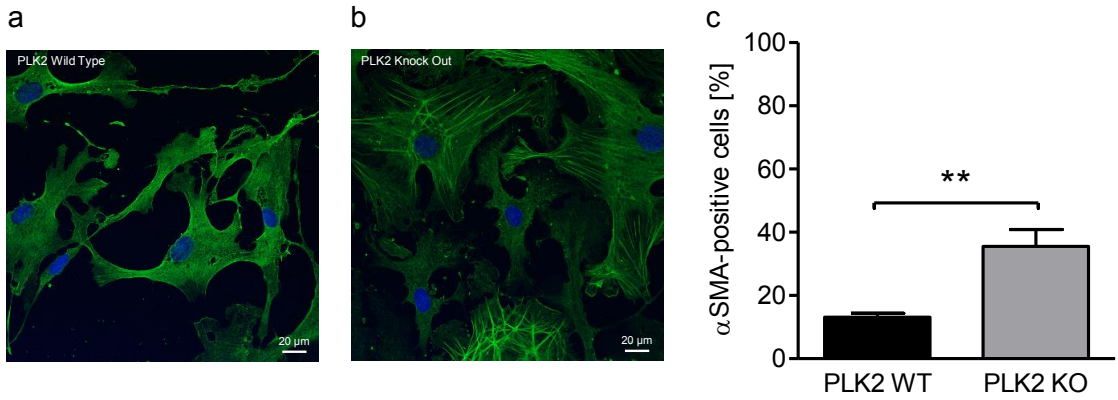

Figure 14. Analysis of PLK2 knockout-dependent myofibroblast differentiation. a) and **b)** Immunofluorescence staining images for αSMA, the nuclei were stained with DAPI (blue). **c)** Quantification of immunostaining experiments for αSMA protein abundance dependent on PLK2 knockout (n = 4 per group). Primary murine cardiac PLK2 wild type and knockout fibroblasts were grown on glass cover slips for 7±1 days. p-values < 0.05 were considered statistically significant.

3.2.2.2 Effect of pharmacological PLK2 inhibition on human atrial fibroblast proliferation

Since reduced PLK2 expression and lower fibroblast proliferation were present in AF (Poulet et al., 2016) we tried to reveal whether these findings are causally linked or merely epiphenomena. In order to answer this question, primary fibroblasts from SR patients were seeded into 12-well cell culture plates at densities of $1*10^4$ cells/ well and cultivated for 14 days in the presence of solvent control (1 µl DMSO/ml cell culture medium) or 1 µM TC-S 7005, respectively (see 2.3.2). Cells were counted after 7 and 14 days to extrapolate proliferation curves. Pharmacological inhibition of PLK2 significantly reduced fibroblast proliferation by 23 % after 7 and 31 % after 14 days (Figure 15).

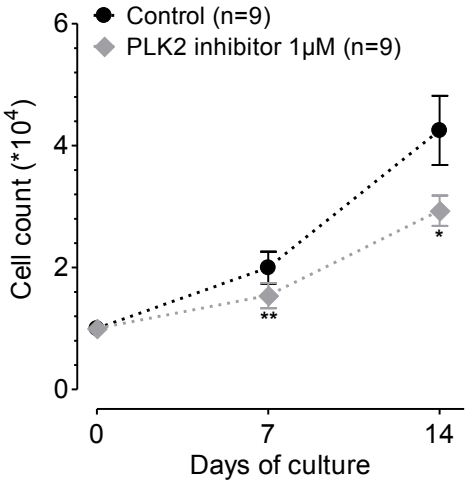

Figure 15. Effect of PLK2 inhibition on human atrial fibroblast proliferation. Proliferation curves of primary human SR fibroblasts. Cells were incubated either with 1 µM TC-S 7005 or DMSO control (1 µl/ ml of cell culture medium) (n = 9 per group). p-values < 0.05 were considered statistically significant.

3.2.2.3 Effect of genetic KO of the PLK2 gene on murine cardiac fibroblast proliferation

In analogy to increased myofibroblast differentiation caused by KO of PLK2 we also tested the effects of the KO on fibroblast proliferation. In this set of experiments cell proliferation was assessed after 5 and 10 days. Preliminary proliferation experiments were done with rat cardiac fibroblasts due to their good availability. We noticed very fast proliferation compared to human fibroblasts leading to excessive cell densities in the cell culture wells after 14 days (Figure 16 a). For this reason, the observation period was shortened to 10 days. Based on these preliminary experiments with rat cardiac fibroblasts, we also expected higher proliferation rates in murine fibroblasts. Surprisingly, basal murine fibroblast proliferation was significantly lower than observed in rat fibroblasts. However, the results were comparable to the human proliferation curves though proliferation was slightly lower in general. Similar to PLK2 inhibition, the genetic KO reduced proliferation by about 30% after 5 and 10 days (Figure 16 b).

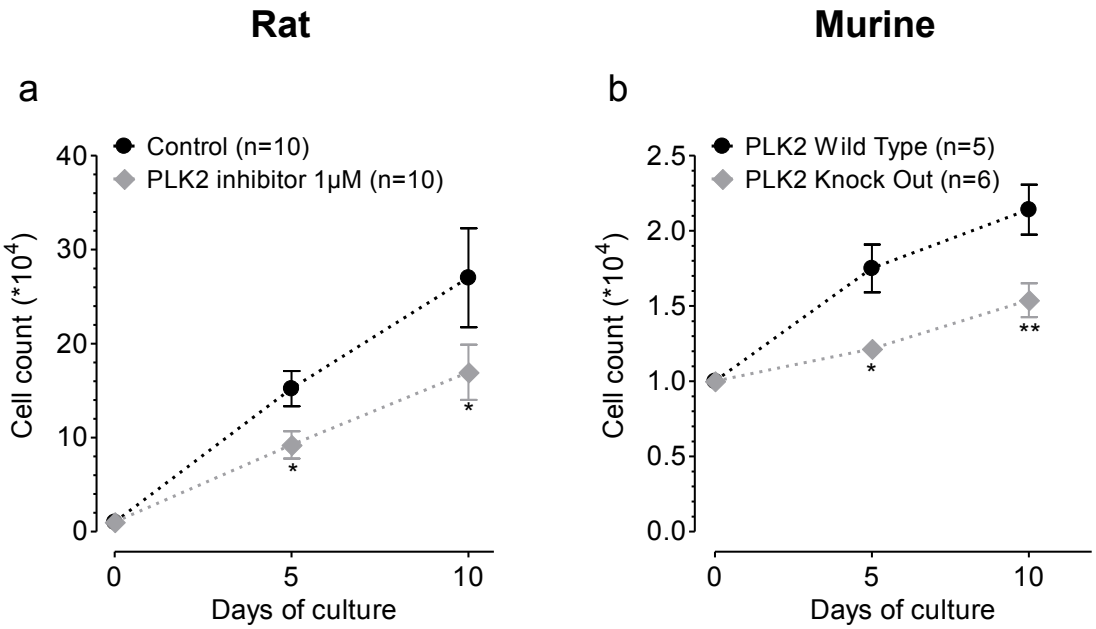

Figure 16. Rodent cardiac fibroblast proliferation. a) Preliminary proliferation experiments with rat cardiac fibroblasts, solvent control vs. 1 µM TC-S 7005, (n = 10 per group). **b)** Proliferation curves of primary PLK2 WT and KO mouse cardiac fibroblasts (n = 5 vs. 6). p-values < 0.05 were considered statistically significant.

3.2.2.4 Effect of pharmacological PLK2 inhibition on human atrial fibroblast migration

Since fibroblasts derived from SR and AF patients were shown to differ in terms of lower migration capacity in AF compared to SR, we tested whether PLK2 inhibition would result in the same observation. Human right atrial fibroblasts from SR patients were treated with solvent control or 1 µM TC-S 7005 (see 2.2.3). There was no significant difference between solvent control and PLK2 inhibitor group (Figure 17).

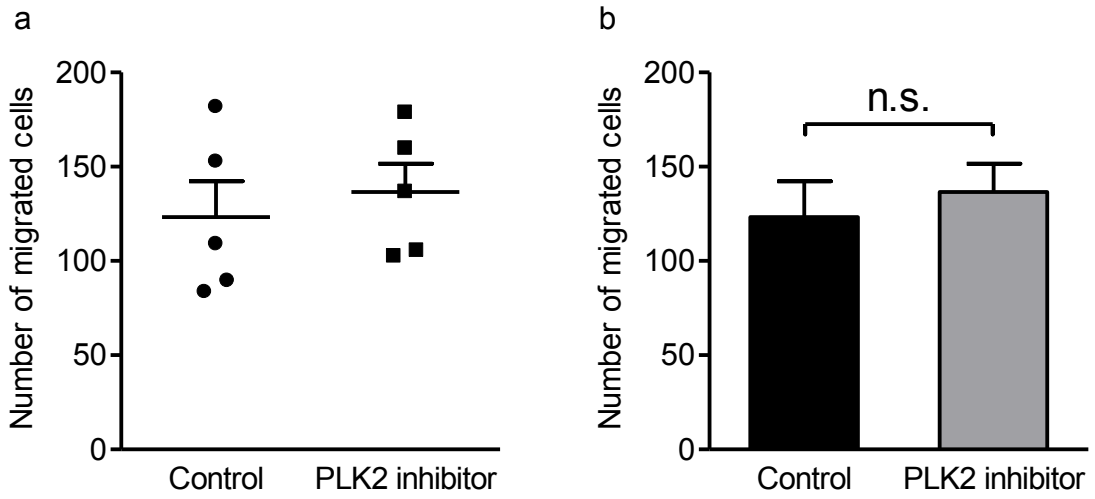

Figure 17. Effect of PLK2 inhibition on human atrial fibroblast migration. Migration capacity of primary human atrial fibroblasts was tested for DMSO control (1 µl/ ml of cell culture medium) or 1 µM TC-S 7005 (specific PLK2 inhibitor). **a)** Number of migrated cells depicted as scatter plot (n = 5 per group). **b)** Number of migrated cells from a) depicted as average values.

3.2.3 PLK2-dependent induction of cell senescence

In order to clarify the significance of PLK2 for senescence induction, a β-galactosidase staining was performed on cultured primary mouse PLK2 WT and KO fibroblasts (Figure 18 a). A trend towards increased senescence in PLK2 KO fibroblasts was found (Figure 18 b) although the results shortly failed to reach statistical significance ($p = 0.052$). Yet, pharmacological inhibition of PLK2 in primary human SR fibroblasts with 1 µM TC-S 7005 for 10 days resulted in significantly increased β-galactosidase activity compared to the vehicle-treated control group (Fig. 18 c).

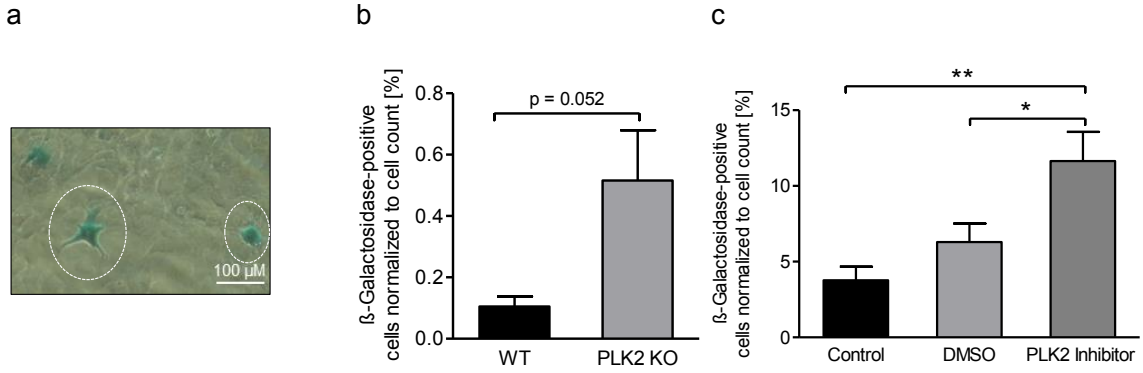

Figure 18. PLK2-dependent induction of cell senescence. a) Representative β-galactosidase-staining to detect cellular senescence. β-galactosidase-positive cells are stained green. The scale bar equals 100 µm. **b)** and **c)** Quantification of β-galactosidase-positive cells (senescent cells) depending on PLK2 expression/ function. Values are depicted as percentage of the total cell count/ well. **b)** Basal proportion of senescent fibroblasts in primary PLK2 WT and KO cell culture (n = 5 WT mice vs. 6 KO mice). c) Proportion of senescent fibroblasts in human primary SR fibroblast cell culture incubated with solvent control (1 µl DMSO/ ml medium) or 1 µM TC-S 7005 (PLK2 inhibitor) (n = 5 per group). p-values < 0.05 were considered statistically significant.

3.3 Effect of PLK2 deficiency on heart tissue and function

3.3.1 Fibrosis marker protein expression in SR and AF heart tissue

In vitro and clinical research have confirmed that AF is accompanied by and causes fibrotic tissue remodeling (Rudolph et al., 2010; Nattel und Harada, 2014; Heijman et al., 2018; Klesen et al., 2018). To identify dysregulated myofibroblast and fibrosis markers correlating with lower PLK2 expression in AF, we performed western blots for FAPα (Figure 19 a), αSMA (Figure 19 b) and vimentin (Figure 19 c). These markers indicate fibroblast activation (FAPα), myofibroblast differentiation (αSMA) and gain of cell size (vimentin). In line with the literature, all of them were significantly more abundant in AF samples compared to SR controls (Figure 19 a-c). The upregulation of FAPα in AF though (Figure 19 a) marks a novel finding indicating a general fibroblast activation in a pre-myofibroblast state.

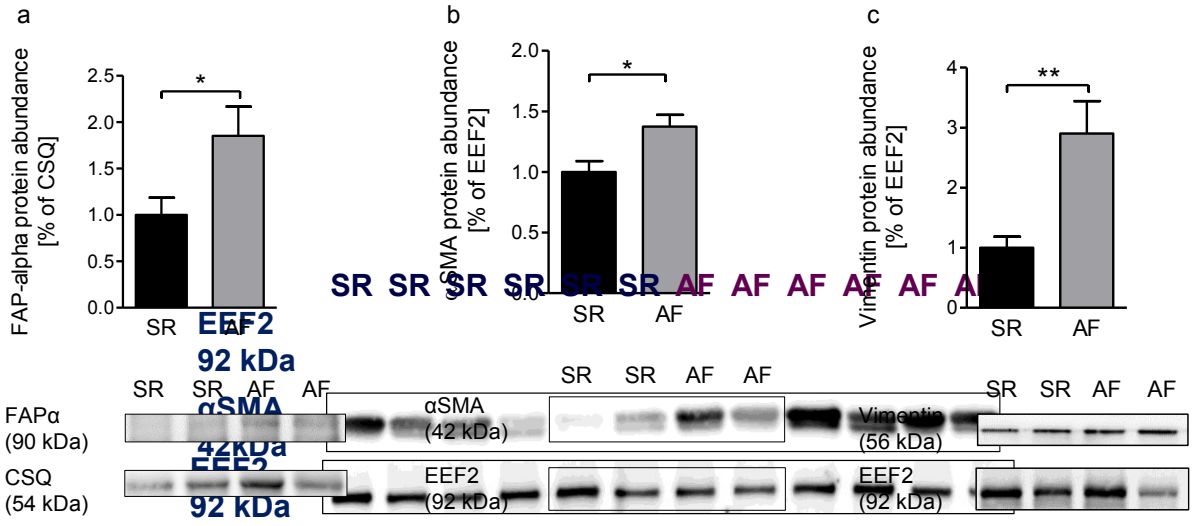

Figure 19. Analysis of myofibroblast and fibrosis markers in SR and AF atrial tissue. a) Protein abundance of fibroblast activation protein alpha (FAPα) normalized to the housekeeping protein calsequestrin (CSQ) (n = 12 vs. 13). The panel below shoes an original example western blot. **b)** Protein abundance of the myofibroblast marker protein alpha smooth muscle actin (αSMA) normalized to the housekeeping protein eukaryotic elongation factor 2 (EEF2) (n = 10 per group). The panel below shoes an original example western blot. **c)** Protein abundance of the fibroblast marker vimentin normalized to the housekeeping protein EEF2 (n = 10 per group). The lower panels show corresponding original western blots. p-values < 0.05 were considered statistically significant.

3.3.2 αSMA expression in PLK2 WT and PLK2 KO heart tissue

Based on the findings that PLK2 expression is significantly lower in AF compared to SR controls and that especially the most recognized myofibroblast marker αSMA is upregulated in AF, we made western blots for αSMA of mouse PLK2 WT and KO heart tissue to identify a correlation of PLK2 and αSMA expression. We found a 4-fold upregulation of αSMA in PLK2 KO samples (Figure 20 a and b).

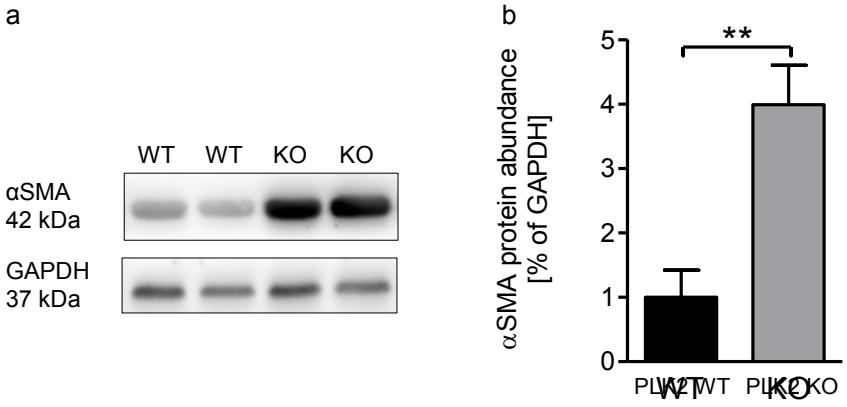

Figure 20. αSMA expression in PLK2 WT and PLK2 KO heart tissue. a) Original western blot for αSMA. **b)** Quantification of αSMA protein abundance (normalized to GAPDH) in heart tissue samples from PLK2 WT and KO mice analyzed by western blot (n = 6 vs. 10 animals). p-values < 0.05 were considered statistically significant.

3.3.3. Fibrotic tissue remodeling in PLK2 KO mouse hearts

Since myofibroblast and fibrosis markers were significantly elevated in PLK2 KO mouse hearts, we investigated the presence of contiguous interstitial fibrosis areas. Sirius red staining of 8 months old PLK2 WT and KO heart sections demarked vast interstitial fibrosis areas, especially in the left ventricle in PLK2 KO animals compared to their WT littermates (Figure 21 right panel). Quantification was omitted as there were no contiguous interstitial fibrosis areas present in the WT samples (Figure 21 left panel).

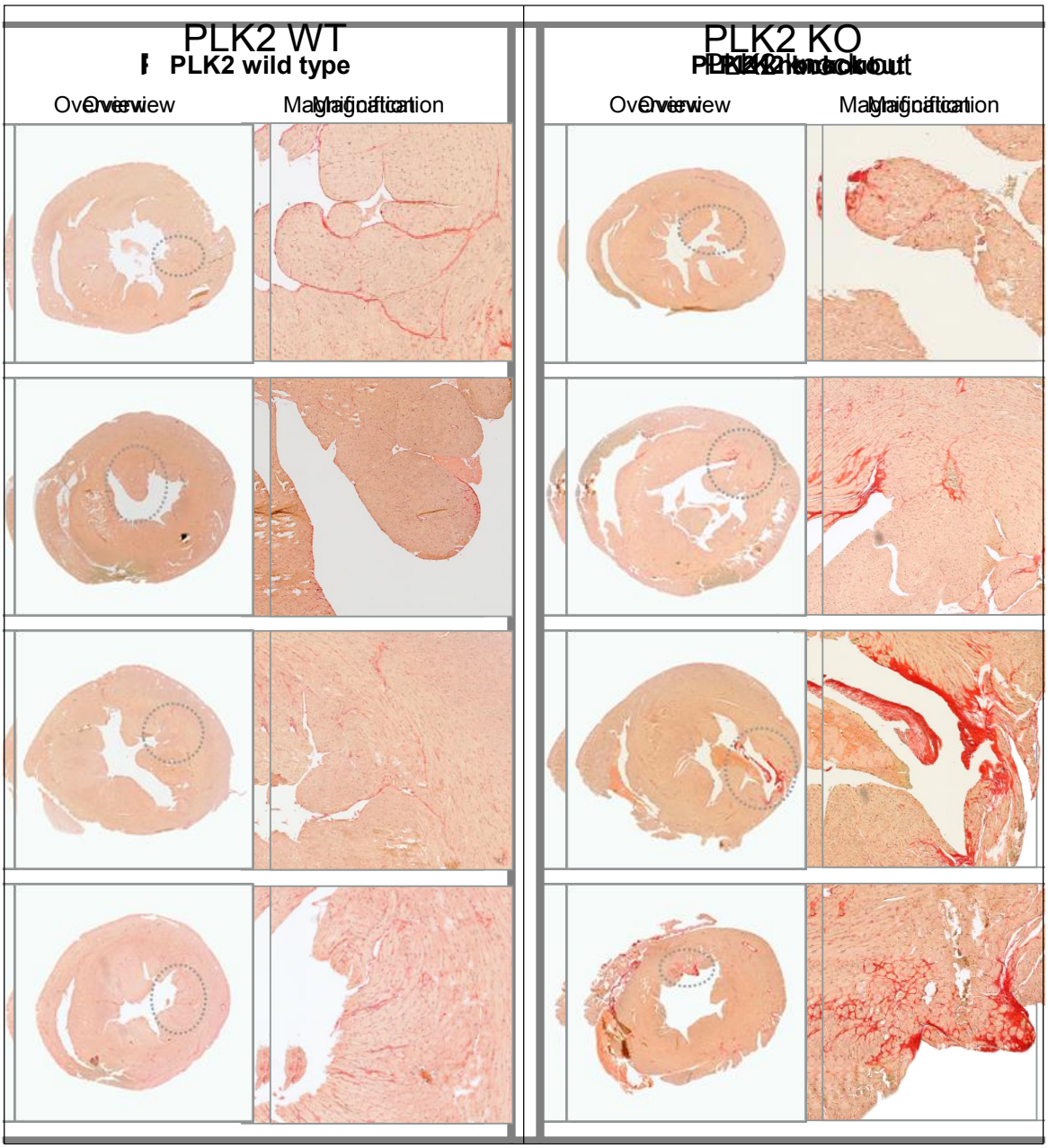

Figure 21. Sirius red staining of histological sections of PLK2 WT and KO hearts. Paraffin sections of murine hearts. Collagen was stained intensively red. The area displayed is located mid-ventricular (halfway between the cardiac valves and the apex cordis). **Left panel)** PLK2 wildtype samples displayed as overview and with a corresponding magnified area. **Right panel)** PLK2 knockout samples displayed as overview and with a corresponding magnified area.

3.3.4. Effects of fibrotic tissue remodeling on the heart and body development

The heart weight and corresponding tibia length of 4 months old PLK2 WT, heterozygous (HET) and KO animals were measured to assess to which extent the fibrotic remodeling affects heart development and potentially heart function. Although we did not find a shorter overall survival of PLK2 KO mice compared to their WT littermates, the PLK2 KO hearts were significantly lighter than WT hearts (-35.3 mg) (Figure 22). The heart weight was normalized to the corresponding tibia length as a body weight-independent reference (Yin et al., 1982). Using the tibia length was necessary since the PLK2 knockout significantly influenced the body weight development of the mice (Figure 23 a) but did not affect the tibia length (Figure 23 b). Heterozygous animals were significantly lighter than their WT littermates and there was a pronounced trend towards lighter body weight in the PLK2 KO mice.

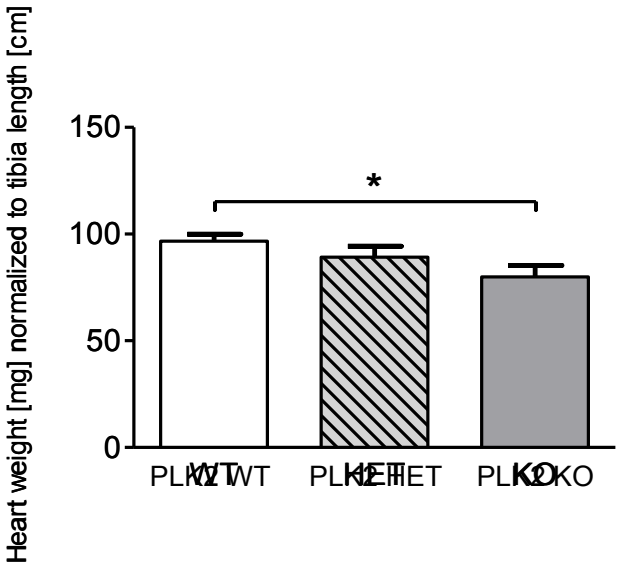

Figure 22. PLK2 mouse model heart weight normalized to tibia length at 4 months of age. (n_{WT} = 20, n_{HET} = 12, n_{KO} = 15). p-values < 0.05 were considered statistically significant.

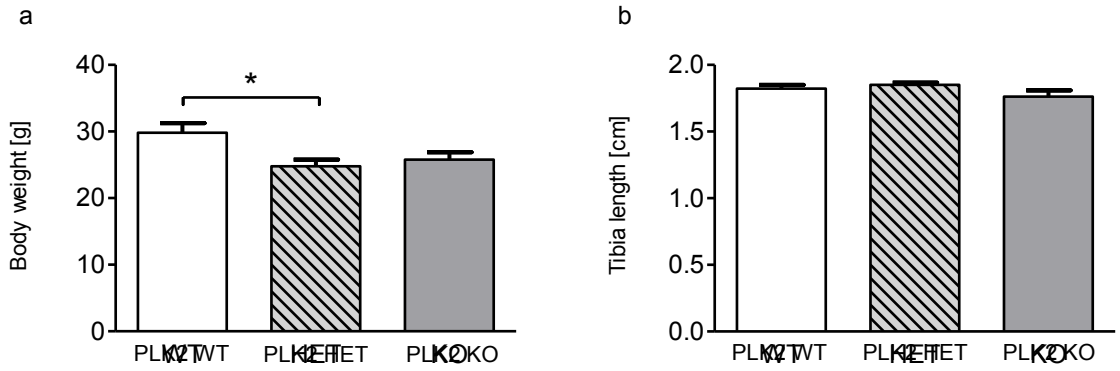

Figure 23. PLK2 mouse model body weight and tibia length at 4 months of age. a) Comparison of PLK2 WT, HET and KO mouse body weight at 4 months of age (n_{WT} = 9, n_{HET} = 10, n_{KO} = 4). **b)** Comparison of PLK2 WT, HET and KO mouse tibia length at 4 months of age (n_{WT} = 9, n_{HET} = 10, n_{KO} = 4). p-values < 0.05 were considered statistically significant.

3.3.5 PLK2 KO impairs the cardiac performance *in vivo*

Since lack of PLK2 expression and/ or function induced a marked myofibroblast phenotype *in vitro* and interstitial fibrosis in the mouse model, we further assessed the functional consequences of the genetic PLK2 KO using transthoracic echocardiography in 4 vs. 4 PLK2 WT and KO animals. Although the heart rate was not altered (Figure 24 a), we found a significant reduction in stroke volume, and end diastolic volume in the KO group (Figure 24 b and d). This finding was in line with a reduced cardiac output in the KO group (Figure24 f). Interestingly the ejection fraction was only minimally reduced (Figure 24 e).

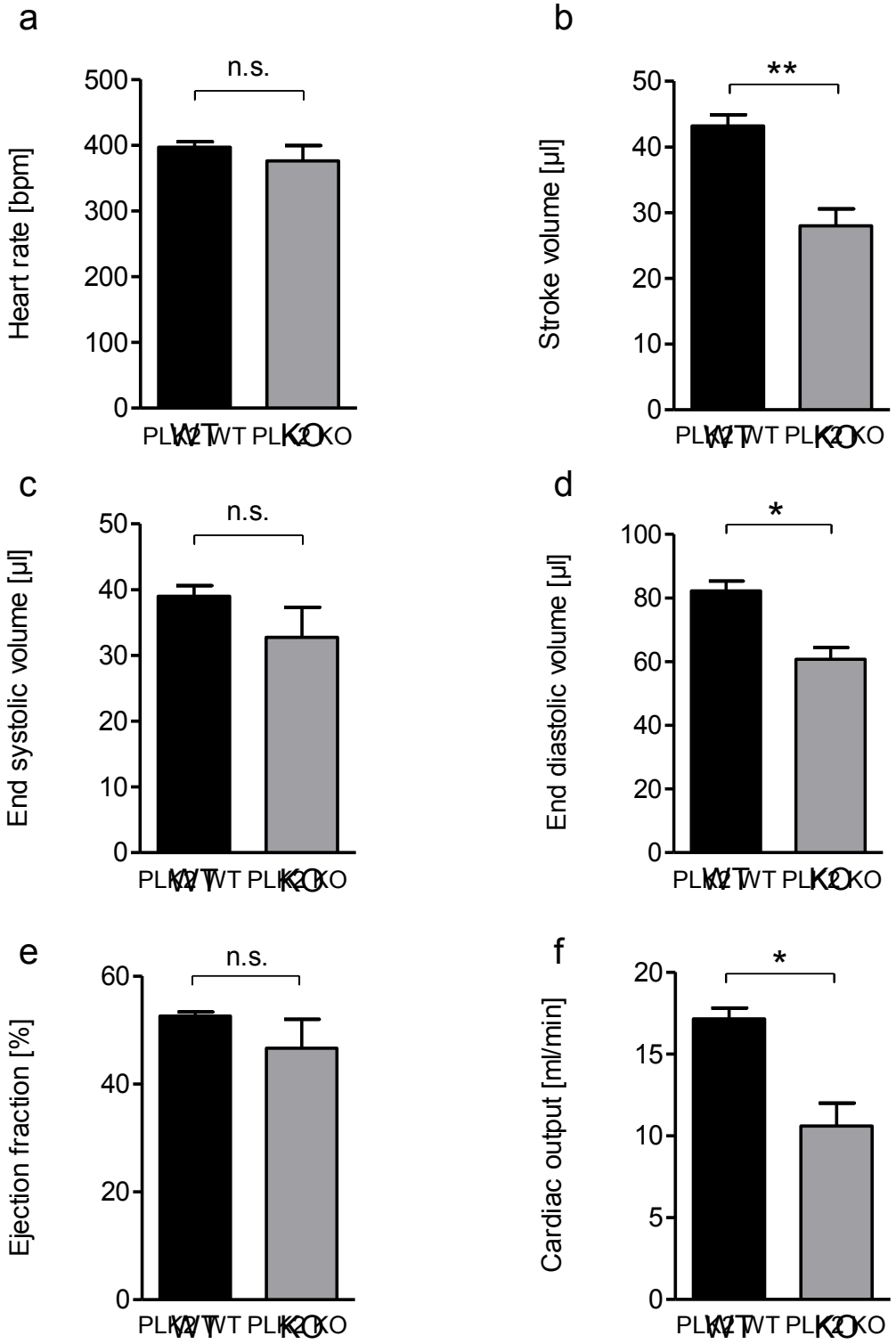

Figure 24. Echocardiographic comparison of PLK2 WT and KO mice. Transthoracic echocardiography was performed on anesthetized PLK2 WT and KO mice with a Vevo3100 small animal echocardiography device. **a)** Heart rate [beats per minute], **b)** Stroke volume [µl], **c)** End dystolic volume [µl], **d)** End diastolic volume [µl], **e)** Ejection fraction [%], **f)** Cardiac output [ml per minute]. (n = 4 animals per group). p-values < 0.05 were considered statistically significant.

3.3.6 Effects of PLK2 KO on selected surface ECG parameters

In human AF samples we found reduced PLK2 gene and protein expression. Using surface ECGs we intended to clarify if PLK2 KO could also induce AF-typical changes in the KO animals. Surface ECGs were obtained during echocardiography. Compared to their WT littermates the PLK2 KO mice displayed a prolonged PQ and QRS duration and a prolonged PR interval (Figure 25 b – d).

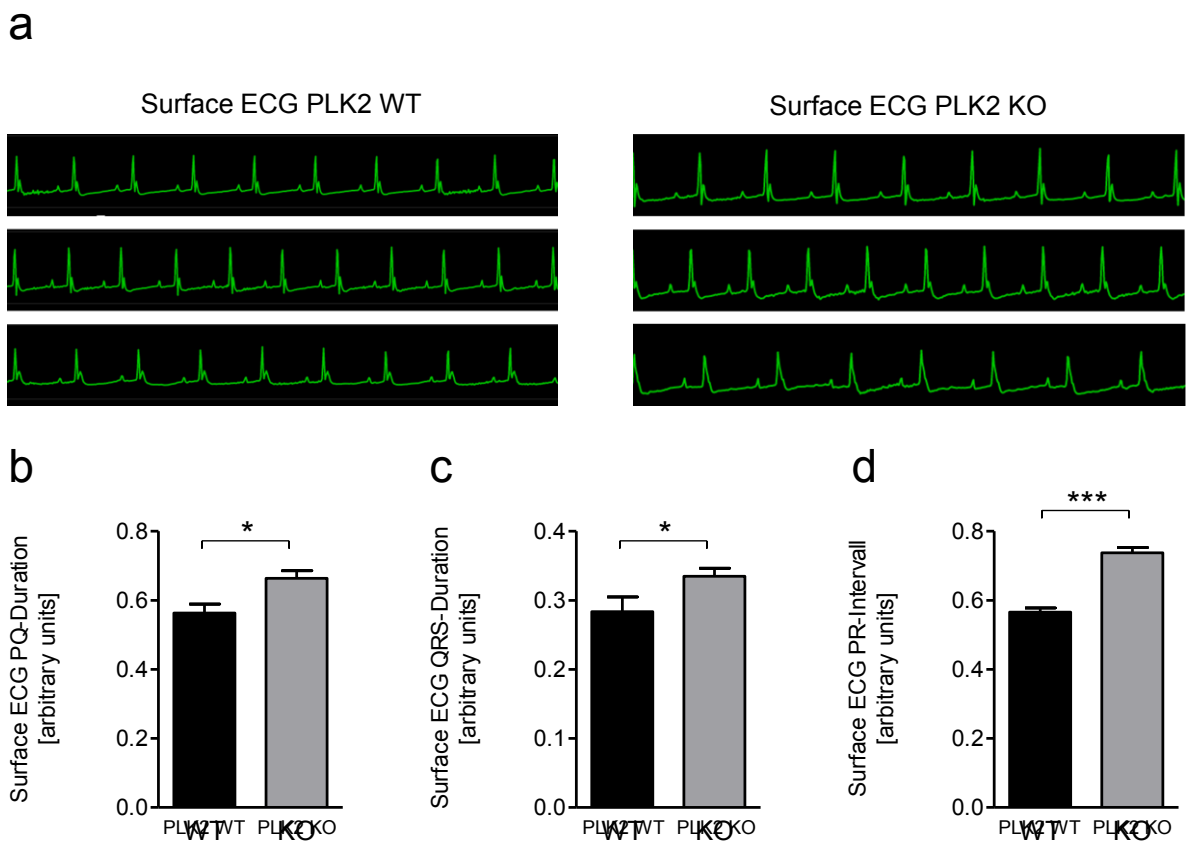

Figure 25. Surface ECG recordings from PLK2 WT and PLK2 KO mice. Surface ECGs were acquired during echocardiography. The data is presented in arbitrary units resulting from the measurement of specific ECG sections. **a)** Example ECG recordings. **b)** PQ duration. **c)** QRS duration. **d)** PR interval. (n = 4 animals per group). p-values < 0.05 were considered statistically significant.

3.4 Effects of PLK2 on the fibroblast secretome

3.4.1 Most regulated proteins in PLK2 KO fibroblast cell culture medium

PLK2 inhibition and genetic KO led to significantly increased myofibroblast differentiation and senescence induction. Based on these findings, we studied the senescence associated secretory phenotype (SASP) (Coppé et al., 2008) of PLK2 KO and WT mouse fibroblasts with mass spectrometry. The proteins secreted by fibroblasts (further referred to as "secretome") into the cell culture medium were analyzed with particular emphasis on inflammation mediators. The most highly regulated proteins (until p = 0.05) are assembled in Table 4.

3.4.2 PLK2 KO induces OPN *de novo* secretion

Among the significantly regulated proteins, we found de novo expression of 3 proteins in the PLK2 KO fibroblast media. Macrophage metalloelastase, OPN and Glycine-tRNA ligase were only abundant in the PLK2 KO group (Table 4, Figure 26 a). Since OPN has already been associated with cardiovascular inflammation and heart failure (Zhao et al., 2016),we further focused on this mediator. Consistent with our finding in the mass spectrometry, OPN protein abundance was similarly elevated in right atrial tissue samples from AF patients compared to SR controls (Figure 26 b.).

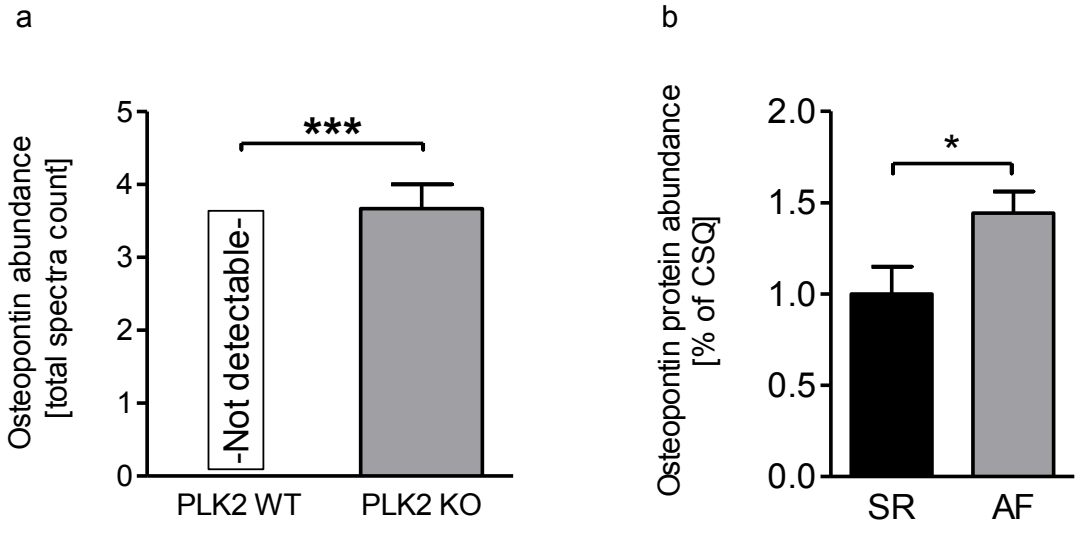

Figure 26. PLK2-dependent osteopontin expression. a) Osteopontin protein abundance in PLK2 WT or KO fibroblast cell culture medium analyzed by mass spectrometry. PLK2 KO fibroblasts secrete osteopontin *de novo* (n = 3 mice per group). **b)** Quantification of western blots for osteopontin protein abundance in SR and AF right atrial tissue lysates (n = 10 per group). p-values < 0.05 were considered statistically significant.

Table 4 Significantly differentially expressed proteins of the secretome analysis

#	Protein name	UniProt Accession No.	Molecular Weight	p-Value	Number of identified spectra					
					KO 1	KO 2	KO 3	WT 1	WT 2	WT 3
1	Macrophage metalloelastase	MMP12_MOUSE	55 kDa	0.00016	9	8	7	0	0	0
2	**Osteopontin**	**OSTP_MOUSE**	**66 kDa**	**0.00039**	**4**	**4**	**3**	**0**	**0**	**0**
3	Glycine-tRNA ligase	SYG_MOUSE	82 kDa	0.0022	3	2	2	0	0	0
4	Transcription elongation factor B polypeptide 1	ELOC_MOUSE	12 kDa	0.0022	0	0	0	3	2	2
5	Properdin	PROP_MOUSE	50 kDa	0.0022	3	2	2	0	0	0
6	A disintegrin and metalloproteinase with thrombospondin motifs 5	ATS5_MOUSE	102 kDa	0.0061	7	9	8	12	12	14
7	40S ribosomal protein S3	RS3_MOUSE	27 kDa	0.0078	5	4	5	3	2	2
8	Protein disulfide-isomerase A6	PDIA6_MOUSE	48 kDa	0.011	17	17	15	10	11	13
9	Glutaminyl-peptide cyclotransferase	QPCT_MOUSE	41 kDa	0.013	4	3	4	6	6	5
10	Lysosomal acid lipase/cholesteryl ester hydrolase	LICH_MOUSE	45 kDa	0.016	5	4	4	0	2	2
11	Calsyntenin-1	CSTN1_MOUSE	109 kDa	0.025	20	19	20	17	13	16
12	Ribonuclease T2	RNT2_MOUSE	30 kDa	0.025	4	2	3	5	5	6
13	Disintegrin and metalloproteinase domain-containing protein 9	ADAM9_MOUSE	92 kDa	0.029	6	4	3	2	0	0
14	Lysosomal alpha-glucosidase	LYAG_MOUSE	106 kDa	0.033	9	5	6	10	11	11
15	Serotransferrin	TRFE_MOUSE	77 kDa	0.036	58	59	45	43	29	33
16	Putative phospholipase B-like 2	PLBL2_MOUSE	66 kDa	0.038	19	15	17	13	13	14
17	Cathepsin S	CATS_MOUSE	38 kDa	0.041	10	5	8	3	2	4
18	Cathepsin D	CATD_MOUSE	45 kDa	0.045	55	48	59	47	42	41

3.4.3 OPN levels in the peripheral blood of patients

The relationship of atrial fibrillation and plasma OPN levels has been subject of clinical research recently (Güneş et al., 2017). OPN was proven to be an independent predictor of AF recurrence after cryoballoon ablation and could therefore predict the long term success rate of invasive AF treatments (Güneş et al., 2017). Since OPN is associated with inflammation, fibrosis and atherosclerosis, high systemic levels of this mediator could be detrimental to patients. For this reason, we aimed to identify a positive correlation of electrophysiologically detected fibrosis and OPN levels in the peripheral blood of AF patients.

Patients undergoing pulmonary vein catheter ablation were enclosed in this study. 2.7 ml of venous blood were taken and stored in EDTA tubes in analogy to the procedure of Güneş and colleagues (Güneş et al., 2017). After centrifugation at 1000 g for 10 min, cell-depleted plasma was stored at -80° C for further analysis. The samples were matched according to the patients' age, sex, comorbidities and drugs. Control samples were donated by healthy volunteers without cardiac comorbidities. The ELISA analysis revealed a 1.7-fold increase of OPN in AF blood samples without fibrosis (16.78 ng/ml) and a 2.7-fold increase in samples from patients with fibrosis (25.99 ng/ml) compared to healthy SR controls (9.66 ng/ml) (Figure 27 a). We expected lower levels of OPN in the SR control group because of the significantly younger age of the healthy volunteers. To ascertain this hypothesis patient age and OPN plasma levels were correlated. The R^2 coefficient of 0.022 indicates no significant correlation of patient age and plasma OPN (Figure 27 b).

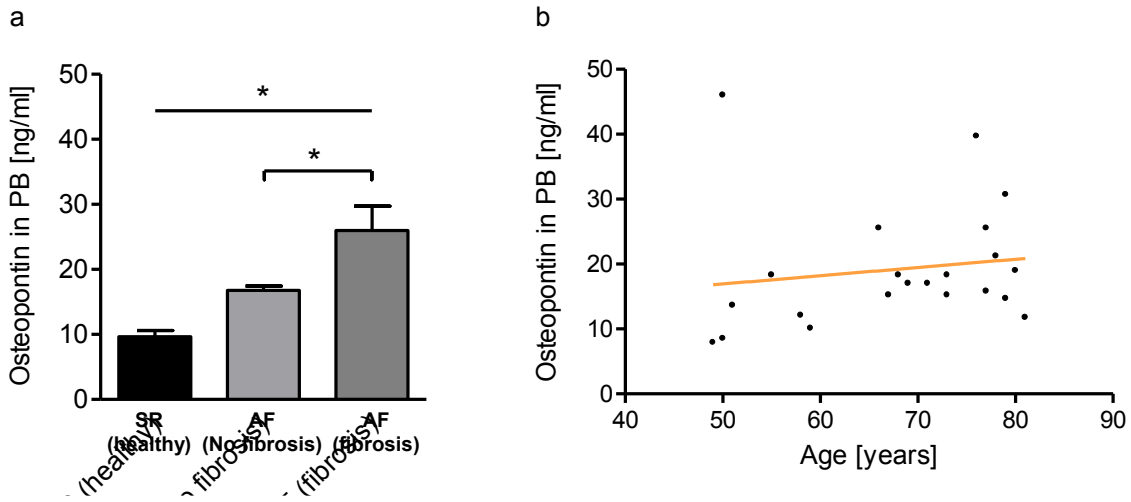

Figure 27. Systemic OPN protein expression in patients. a) Osteopontin concentration in patients' peripheral blood. Osteopontin concentration was measured with ELISA ($n_{SR(healthy)}$ = 4, $n_{AF(no\ fibrosis)}$ = 8, $n_{AF(fibrosis)}$ = 9). **b)** Correlation of osteopontin concentration in the peripheral blood and the patients' age. p-values < 0.05 were considered statistically significant.

3.5. Mechanistic link between PLK2 and OPN secretion

3.5.1 Identification of signaling pathways involved in OPN secretion

The work of Beck et al (Beck und Knecht, 2003) and Xie et al (Xie et al., 2004) provided evidence that p42/44 MAPK (ERK1/2) mediates OPN secretion. For this reason, we performed a western blot to confirm the expected higher abundance of p42/44 MAPK (ERK1) in PLK2 KO mice. We found a significant 1.25-fold higher p42 MAPK protein abundance in PLK2 KO mouse heart samples compared to PLK2 WT controls (Figure 28 a and b).

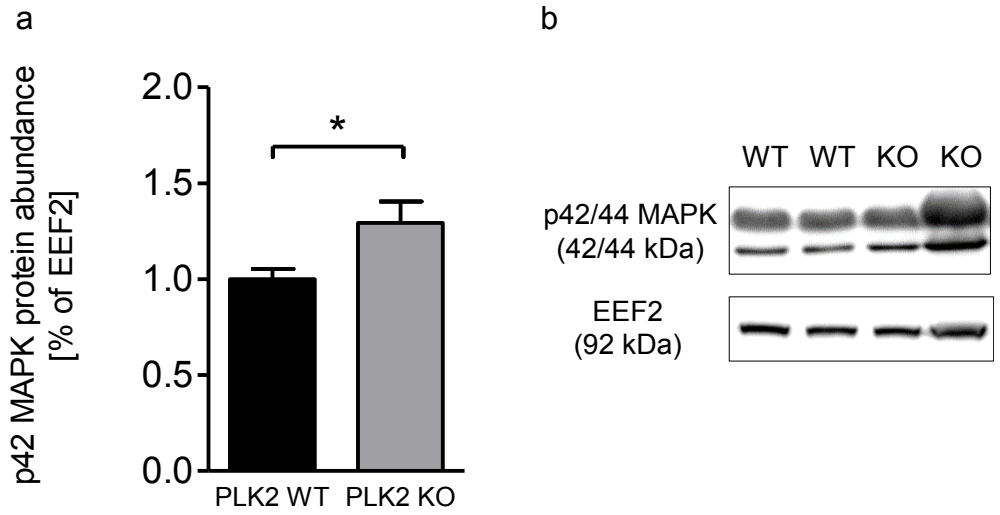

Figure 28. p42 MAPK expression in PLK2 WT and KO hearts. a) Quantification of western blots for p42/44 MAPK (n = 4 vs. 5 mice). **b)** Representative western blot experiment for a. p-values < 0.05 were considered statistically significant.

3.5.2 Identification of cardiac PLK2 substrates linked to the p42/44 MAPK pathway

We focused on the Ras pathway which was shown to be a downstream signaling cascade of PLK2 (Lee, Hoe et al., 2011). Especially RasGRF1, a guanidine exchange factor that stimulates Ras signaling was shown to be negatively regulated via PLK2-dependent phosphorylation. First, we analyzed protein expression of RasGRF which was described in the literature (Lee, Hoe et al., 2011). Western blot analysis revealed no expression of RasGRF1 in cardiac fibroblasts (Figure 29). Subsequent mRNA analysis revealed expression of RasGRF2 in cardiac fibroblasts (data not shown). Western blotting proved RasGRF2 upregulation in cardiac fibroblasts when PLK2 was inhibited with 1 µM TC-S 7005 for 72h compared to DMSO solvent control (Figure 30 a and b).

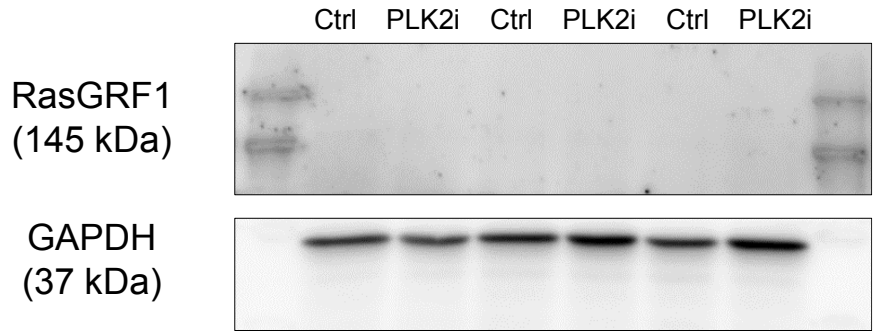

Figure 29. Original western blot for RasGRF1 protein abundance in human cardiac fibroblast. PLK2-dependence of RasGRF1 protein abundance was tested abundance in human ventricular fibroblasts which were treated with solvent control (1 µl DMSO/ ml cell culture medium) or 1 µM of a specific PLK2 inhibitor (TC-S 7005) for 72 hours (n = 3 per group.

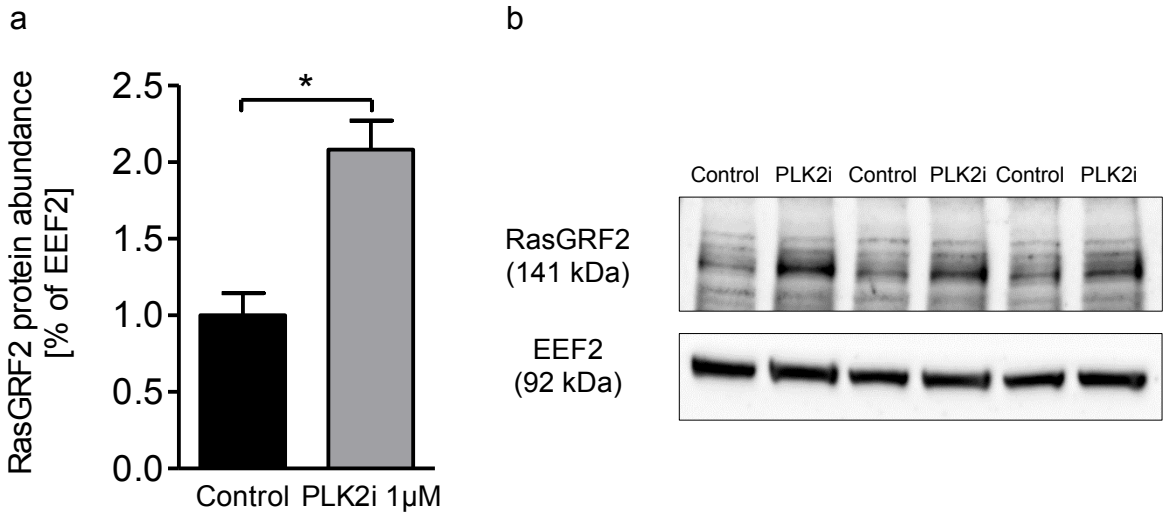

Figure 30. PLK2-dependent RasGRF2 protein abundance in human cardiac fibroblasts. a) Quantification of western blots for RasGRF2 protein abundance in human ventricular fibroblasts which were treated with solvent control (1 µl DMSO/ ml cell culture medium) or 1 µM of a specific PLK2 inhibitor (TC-S 7005) for 72 hours (n = 3 per group. **b)** The original western blot for a). p-values < 0.05 were considered statistically significant.

3.5.3. Pharmacological PLK2 inhibition increases MAPK expression

We tested whether pharmacological PLK2 inhibition with 1 µM TC-S 7005 would increase MAPK expression in a similar way like PLK2 KO did in the mouse model. We found comparable results in TC-S 7005 treated cells compared to DMSO control. There was a 1.63-fold increase of p42 MAPK (ERK2) and a 1.28-fold increase in p44 MAPK (ERK1) protein

abundance in the TC-S-treated group compared to control (Figure 31 a and b). Thus, we provide evidence that reduced PLK2 expression or function attenuates RasGRF2 degradation resulting in enhanced expression of p42/44 MAPK which can stimulate OPN transcription and secretion.

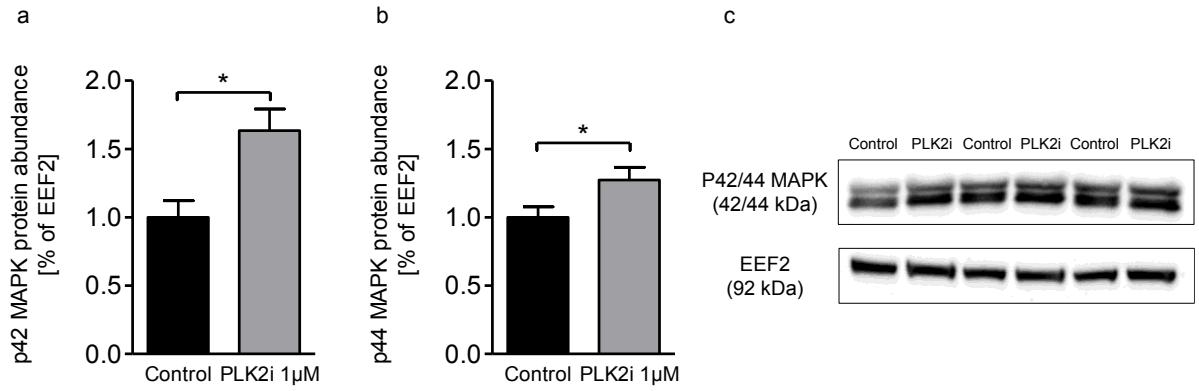

Figure 31. PLK2-dependent p42/44 MAPK expression in human cardiac fibroblasts. a) Quantification of western blots for p42 MAPK protein abundance in human ventricular fibroblasts which were treated with solvent control (1 µl DMSO/ ml cell culture medium) or 1 µM of a specific PLK2 inhibitor (TC-S 7005) for 72 hours (n = 3 per group). The results were normalized to EEF2. **b)** Quantification of western blots for p44 MAPK protein abundance in human ventricular fibroblasts which were treated with solvent control (1 µl DMSO/ ml cell culture medium) or 1 µM of a specific PLK2 inhibitor (TC-S 7005) for 72 hours (n = 3 per group). The results were normalized to EEF2. **c)** The original western blot for a) and b). p-values < 0.05 were considered statistically significant.

3.5.4 Suggested mechanism of PLK2-OPN interaction

In figure 32 the working hypothesis for the PLK2-OPN-axis is presented (Figure 32 a). We found that PLK2 inhibition led to increased RasGRF2 (Figure 32 b) protein abundance. Based on literature research we connected these results via the Ras pathway (Thomas et al., 1992). Inhibition of PLK2 in human ventricular fibroblasts led to enhanced p42 MAPK phosphorylation and subsequently to an increase in OPN protein abundance (Figure 32 c and d).

In order to verify these findings, PLK2 WT and KO fibroblasts were analyzed with regard to RasGRF2 protein abundance, p42 phosphorylation and OPN expression (Figure 33 a – c). Furthermore, the specific p42/44 MAPK inhibitor SCH772984 was used in these experiments. Primary PLK2 KO fibroblasts were cultured in the presence of 10 nM SCH772984 after P1 for 48 h. These experiments confirmed an elevated RasGRF2 protein abundance, increased p42 MAPK phosphorylation and increased OPN protein abundance (Figure 33 a – c). Additionally, inhibition of p42/44 MAPK decreased RasGRF2 and OPN protein abundance significantly (Figure 33 a and c).

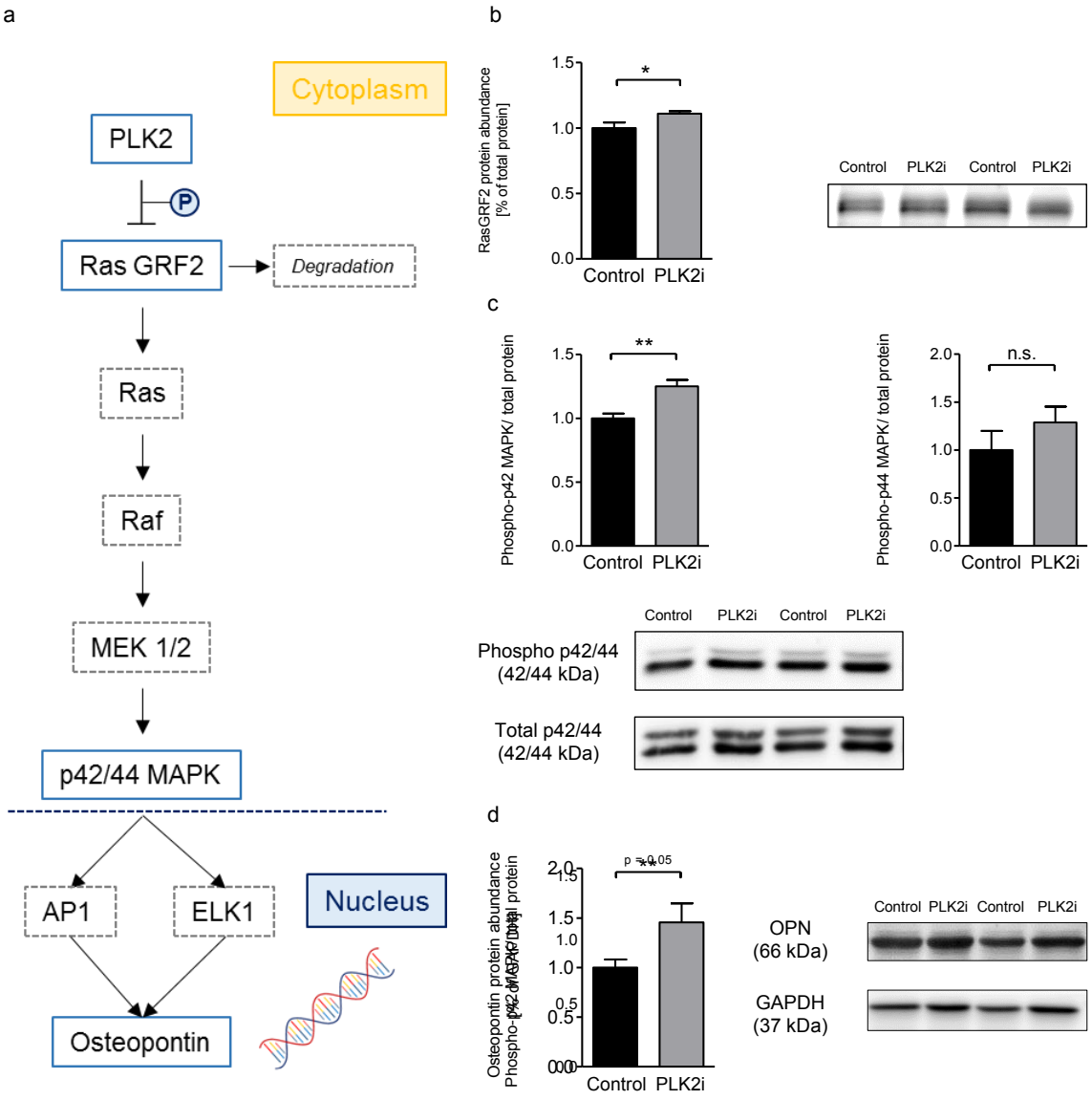

Figure 32. Suggested mechanism of PLK2-OPN interaction. Cells were either treated with solvent control (1 µl DMSO/ ml cell culture medium) or 1 µM of a specific PLK2 inhibitor (TC-S 7005) for 72 hours (n = 3 per group). **a)** PLK2 phosphorylates RasGRF2 and leads thereby to its proteasomal degradation. In Absence of PLK2 RasGRF2 is not degraded and stimulates the Ras pathway. Ras phosphorylates and thereby activates p42/44 MAPK which induces OPN transcription via AP1 and ELK1. The blue boxes in the scheme were experimentally proven, the grey boxes are assumptions based on literature research. **b)** Quantification and representative western blot for RasGRF2 protein abundance in human ventricular fibroblasts **c)** Quantification and representative western blot for total and phosphorylated (Thr202/Tyr204) p42/44 protein abundance in human ventricular fibroblasts. **d)** Quantification and representative western blot for OPN protein abundance in human ventricular fibroblasts. p-values < 0.05 were considered statistically significant.

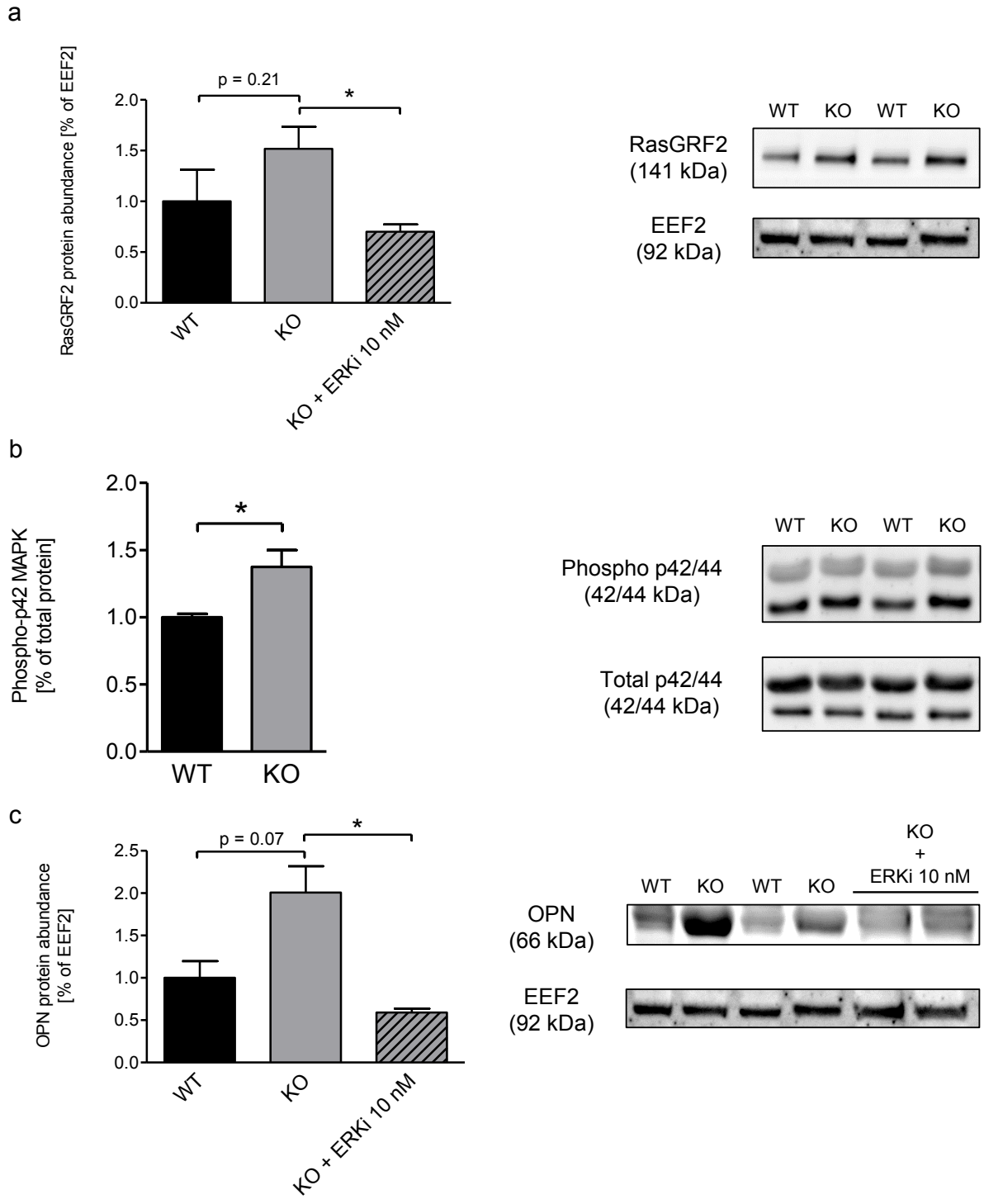

Figure 33. Effect of pharmacological p42/44 MAPK inhibition on PLK2 KO fibroblasts. Primary murine PLK2 WT and KO fibroblasts were used. Cells were either treated with solvent control (1 µl DMSO/ ml cell culture medium) or 10 nM of a specific ERK1/2 inhibitor ("ERKi", SCH772984) for 48 hours (n = 4 per group). a) Quantification and representative western blot for RasGRF2 protein abundance. **b)** Quantification and representative western blot for phosphorylated (Thr202/Tyr204) p42 protein abundance. **d)** Quantification and representative western blot for OPN protein abundance. p-values < 0.05 were considered statistically significant.

3.5.5 Comparison of the PLK2 wild type and knockout fibroblast transcriptome

In order to gain further mechanistic insight of possible PLK2 downstream interactions, we performed a transcriptome analysis of the very same wildtype and PLK2 KO fibroblasts that were used in the proteome analysis. The objective was to systemically characterize the effects of PLK2 KO on cardiac fibroblast mRNA expression. Surprisingly, there were no significant differences in mRNA expression between the wild type control and the PLK2 KO group. However, the obtained data clearly verified the knockout of PLK2 in comparison to the wild type animals (Table 5).

Table 5. Top 20 differentially expressed genes in the transcriptome analysis

Gene symbol	WT 1	WT 2	WT 3	KO 1	KO 2	KO 3	KO 4	p-value	Adjusted p-value (multiple testing)
Plk2	**690**	**951**	**541**	**1**	**0**	**0**	**0**	**4,127E-86**	**9,415E-82**
Xlr3b	28	23	23	3	4	7	1	3,599E-06	4,105E-02
Cnn1	497	105	23	16	10	29	4	2,952E-05	2,245E-01
Laptm5	5	6	1	12	22	33	50	1,624E-04	9,263E-01
Myh11	537	143	38	43	21	95	38	1,141E-03	9,999E-01
Ramp1	19	26	3	1	4	1	0	2,281E-03	9,999E-01
C1qb	1	12	1	14	38	30	108	2,567E-03	9,999E-01
Myl9	639	783	91	105	140	149	220	2,799E-03	9,999E-01
Bmf	20	71	25	3	7	19	17	3,721E-03	9,999E-01
Acta1	46	39	3	5	0	5	0	4,299E-03	9,999E-01
Ctss	1	9	1	7	46	17	59	4,725E-03	9,999E-01
Lhx9	9	27	8	4	4	2	0	6,445E-03	9,999E-01
C1qc	1	13	3	12	29	24	44	7,548E-03	9,999E-01
Gm27786	0	1	0	4	12	3	27	7,572E-03	9,999E-01
Sema6b	5	16	10	27	35	19	62	7,885E-03	9,999E-01
Tyrobp	2	2	2	2	17	11	36	9,252E-03	9,999E-01
Skiv2l2	377	391	270	421	631	603	565	9,289E-03	9,999E-01
Lmod1	143	130	26	44	15	55	16	9,611E-03	9,999E-01
Lmo2	9	13	10	13	69	15	82	1,168E-02	9,999E-01
Lyz2	476	196	188	274	681	805	1206	1,172E-02	9,999E-01

3.6. Upstream mechanism triggering PLK2 downregulation in AF

3.6.1 Hypoxia induced PLK2 downregulation

Recent studies in non-cardiac tissues (Syed et al., 2006; Benetatos et al., 2011) have demonstrated that PLK2 gene expression can be regulated by promoter methylation. Since we were able to proof promoter methylation in several AF heart tissue samples, it was our aim to induce methylation in primary human atrial SR fibroblasts to downregulate PLK2 expression. A common stimulus known to induce genome wide promoter methylation is chronic hypoxia (Robinson et al., 2012). After 24h of hypoxia treatment we found a significant downregulation of PLK2 mRNA expression (Figure 34). However, we did not find promoter methylation in the corresponding gDNA samples after 24 h (Figure 35). Since epigenetic modifications need to be passed to daughter cells to be broadly detectable we increased the time of hypoxia treatment to 72 h and 96 h that fibroblasts can pass through several cell cycles. Furthermore, we chose human ventricular fibroblasts for the prolonged experiments, since their proliferation rate is higher than that of primary atrial fibroblasts. Anyway, after 72 h there was no promoter methylation present (Figure 35). A recently published study by Robinson et al found that human fibroblasts have to be exposed to hypoxia for 8 days to develop robust genome wide DNA hypermethylation whereas 4 days can be sufficient to identify slight levels of methylation (Robinson et al., 2012). After 96 h of hypoxia treatment we detected methylation of the *PLK2 promoter* (Figure 35). To proof the concept of hypoxia-mediated promoter methylation we further used 0.25 mM Dimethyloxaloylglycine (DMOG), an inhibitor of PHD finger protein (PHF) and factor inhibiting HIF (FIH-1) mimicking hypoxia by upregulation of hypoxia-inducible factor (HIF-1α) (Ayrapetov et al., 2011). 96 h DMOG added further evidence that *PLK2* promoter methylation is hypoxia-sensitive (Figure 35).

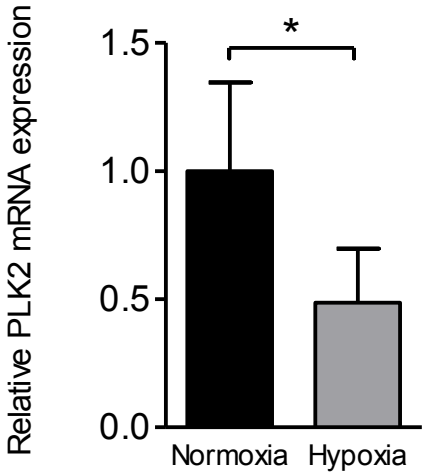

Figure 34. Effect of chronic hypoxia treatment on PLK2 mRNA expression. Primary human atrial SR fibroblasts were cultured either in a normoxic (20% O_2) or hypoxic (1% O_2) environment for 24 h (n= 6 per group). Relative mRNA expression was calculated with RPL32 as housekeeping gene. p-values < 0.05 were considered statistically significant.

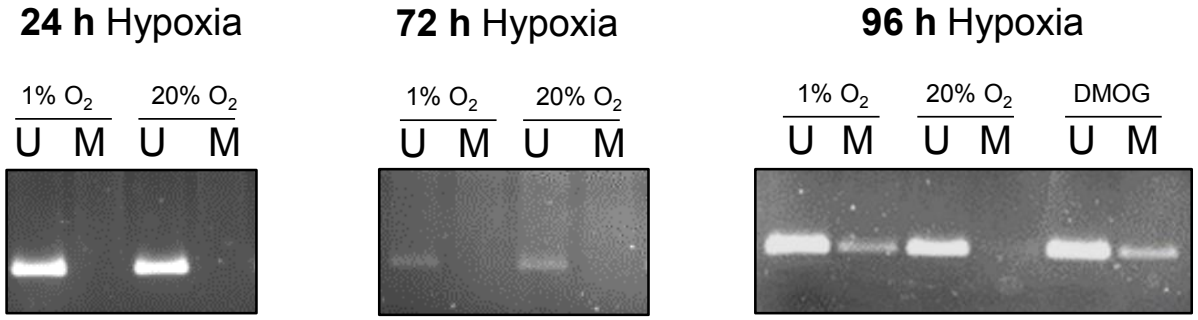

Figure 35. Methylation-specific PCR gel images of the *PLK2* promoter region. Methylation-specific PCR of the PLK2 promotor region. Primary human atrial fibroblasts were cultured either in a normoxic (20% O_2) or hypoxic (1% O_2) environment for 24 h, 72 h or 96 h. (U: unmethylated, M: methylated, Pos = positive control (human universal methylated DNA standard), H_2O = water control).

3.6.2 PRKRA-p53-dependent PLK2 downregulation

Since promoter methylation is not the only way of reducing gene expression, we further focused on direct regulators of PLK2 expression. Previous research on this topic has identified direct induction of PLK2 in a p53-dependent manner (Burns et al., 2003b). In the Affymetrix microarray data we found a significant mRNA up-regulation of the negative p53 regulator *PRKRA* (Li et al., 2007) in AF fibroblasts compared to SR (Figure 36 a). Consequently, *p53* mRNA expression was diminished in the AF group (Figure 36 b).

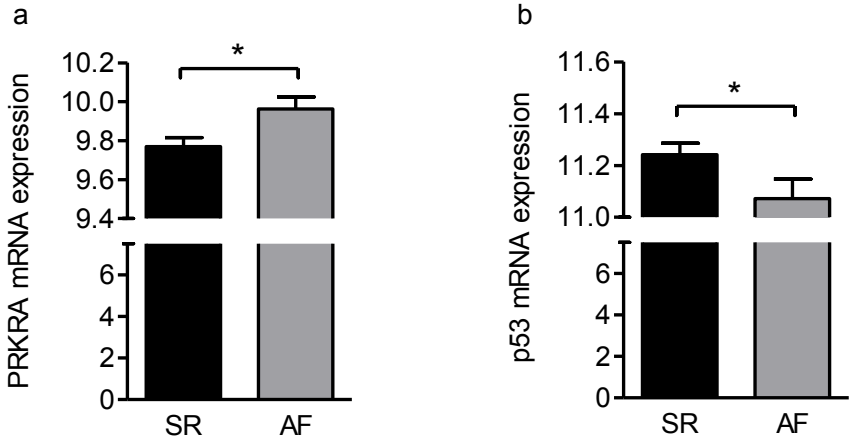

Figure 36. Upstream regulation of PLK2. a) mRNA expression of the negative p53 regulator PRKRA in primary human atrial fibroblasts from SR (n = 8) and AF (n = 6) patients analyzed with an Affymetrix chip microarray. **b)** mRNA expression of p53 in primary human atrial fibroblasts from SR (n = 8) and AF (n = 6) patients analyzed with an Affymetrix chip microarray. p-values < 0.05 were considered statistically significant. * = $p < 0.05$

3.7 Validation of the PLK2-p42/44MAPK-axis as a universally applicable fibrotic pathway

Our experiments identified a clear relevance of the PLK2-p42/44MAPK-signaling axis for myofibroblast differentiation and OPN secretion in cardiac fibroblasts during permanent AF. To prove whether the observed phenomena and mechanisms are generally valid in non-cardiac fibrosis, we used primary dermal fibroblasts from female control patients and patients suffering from radiation-induced Morphea (RIM) after breast cancer treatment.

3.7.1 Dermal fibroblast identification

As described in 3.2.1 cells were identified as fibroblasts by immunofluorescence staining for accepted fibroblast marker proteins. Here we used hFSP, DDR2 and Col1. All cells (≈ 99%) were positive for these marker proteins. Figure 37 displays representative staining results.

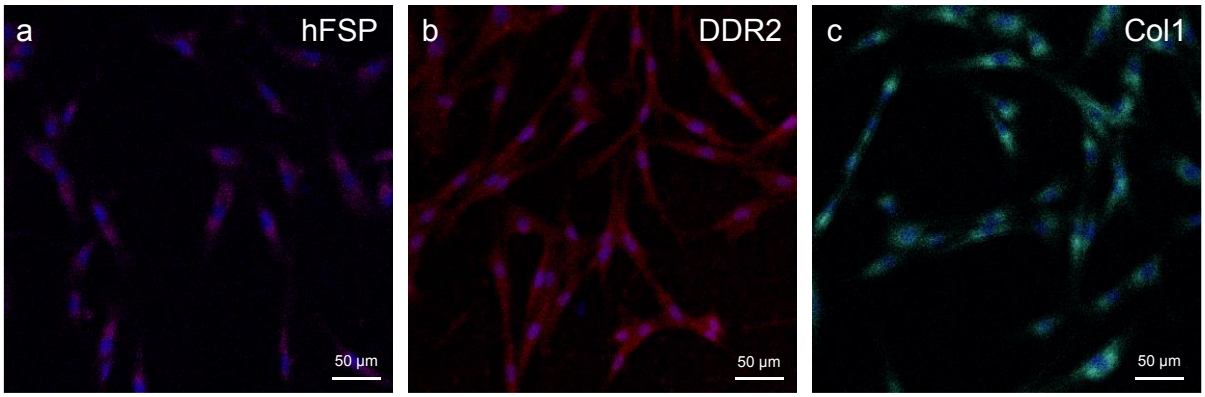

Figure 37. Immunocytochemical dermal fibroblast identification. Representative staining images of primary dermal fibroblasts for hFSP, DDR2 and Col1. The nuclei were stained with DAPI (blue). The scale bars equal 50 µm. The original colour of the fluorescence signal (far red) was altered for better visibility with the ZEN2.3 lite software for hFSP AND Col1.

3.7.2 PLK2 expression is altered in RIM fibroblasts

Comparably to AF fibroblasts, we found a clear trend towards reduced *PLK2* mRNA expression in dermal RIM fibroblasts (Figure 38 a). However, western blot experiments also revealed distinctly altered PLK2 protein abundance in RIM fibroblasts compared to control (Figure 38 b). Whereas control samples displayed clear and sharp PLK2 bands, the RIM samples displayed blurred bands which were merely above background noise. The trend towards altered or reduced PLK2 expression was further supported by immunofluorescence staining experiments which indicated a weaker PLK2 fluorescence signal in RIM fibroblasts compared to control (Figure 39).

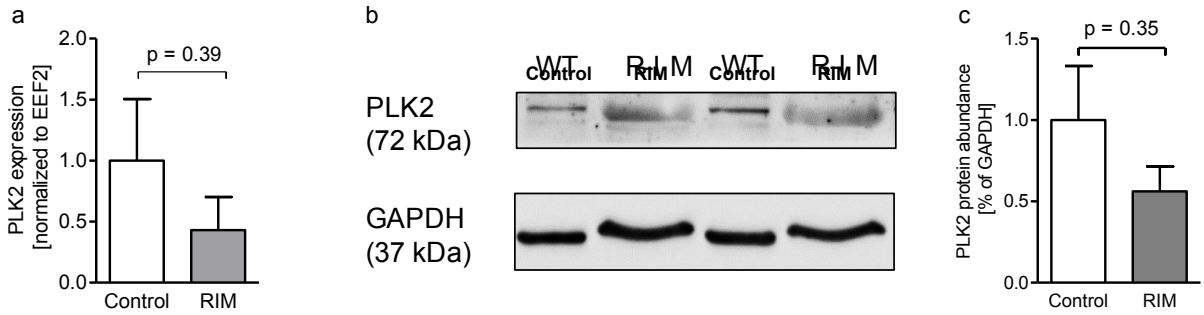

Figure 38. PLK2 mRNA and protein expression is altered in RIM fibroblasts. a) Expression of *PLK2* mRNA normalized to *EEF2* in primary human dermal fibroblasts from control and RIM patients, analyzed with qPCR (n = 3 per group). **b)** Representative western blot for PLK2 protein abundance in control and RIM fibroblasts. **c)** Quantification of western blot for PLK2 protein abundance in control and RIM fibroblasts (n = 3 per group). The results failed to reach the level of statistical significance.

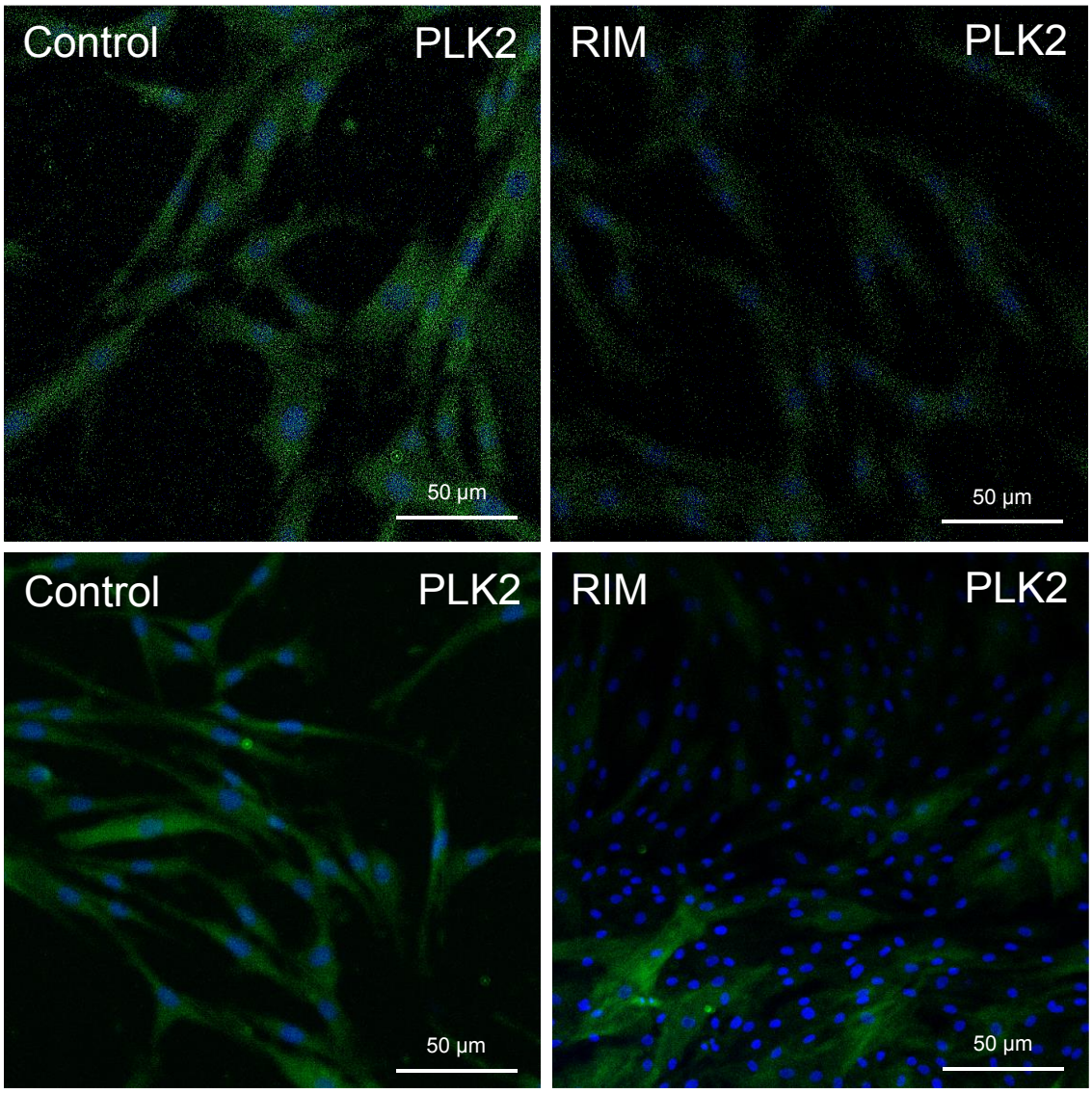

Figure 39. Immunocytochemical PLK2 detection in dermal fibroblasts. Representative staining images of primary dermal fibroblasts for PLK2. The nuclei were stained with DAPI (blue). The scale bars equal 50 µm.

3.7.3 Functional characterization of RIM fibroblasts

In order to understand whether the cardiac fibroblast dysfunction which was initially observed in AF fibroblasts (Poulet et al., 2016) and confirmed in PLK2-deficient cardiac fibroblasts in this study, represents a general principle of fibroblast adaptation to certain pathological stimuli, such as rapid pacing, chemical stimulation or irradiation, we characterized dermal control and RIM fibroblasts with particular emphasis on proliferation, migration and myofibroblast differentiation.

Proliferation

Dermal fibroblasts displayed higher proliferation rates than cardiac fibroblasts. However, in accordance to our prior observations, RIM fibroblasts proliferated significantly lower compared to control fibroblasts after 5 and 10 days of culture (Figure 40). In RIM fibroblasts, we found a reduction in cell count of 24.17% at day 5 and 48.11% at day 10 compared to Control fibroblasts.

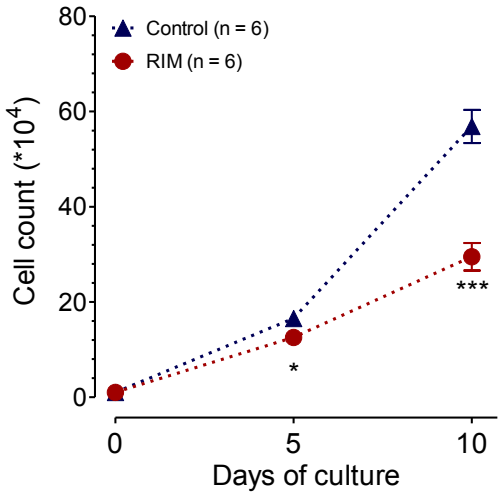

Fig. 40. Proliferative capacity of dermal Control and RIM fibroblasts. Proliferation curves of primary Control and RIM fibroblasts under basal (n = 6 experiments per group, Cells were isolated from N = 3 patients). p-values < 0.05 were considered statistically significant.

Migration

Comparably to AF fibroblasts, RIM fibroblasts displayed a significantly reduced migratory capacity. The number of migrated cells was 43% lower in RIM compared to Control (Figure 41).

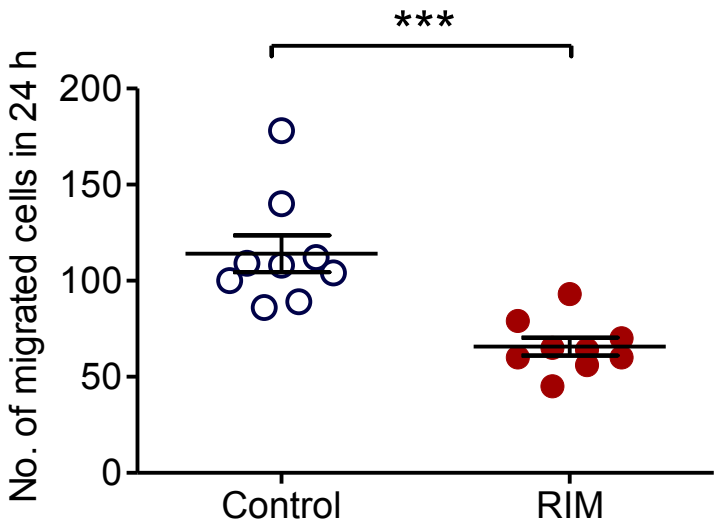

Fig. 41. Migratory capacity of dermal Control and RIM fibroblasts. Number of migrated primary Control and RIM fibroblasts in 24 h. (n = 9 experiments per group, Cells were isolated from N = 3 patients). p-values < 0.05 were considered statistically significant.

Differentiation

Finally, the basal differentiation into myofibroblasts was assessed. A cell was considered myofibroblast when orderly arranged αSMA microfilaments were present (Figure 42 a and b, cell in the center). Under basal conditions, 7.3% of Control fibroblasts were considered myofibroblasts whereas 23.5% of RIM fibroblasts were considered myofibroblasts (Figure 42 c).

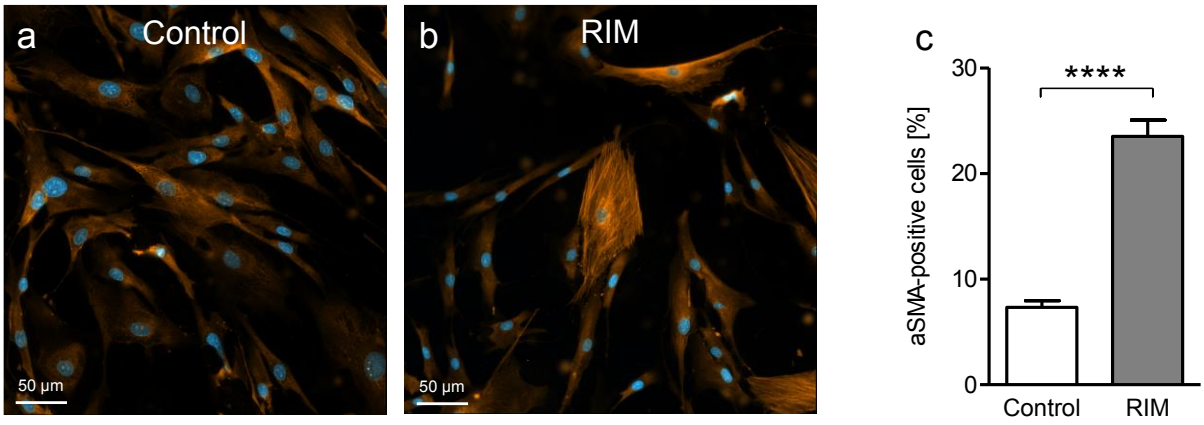

Figure 42. Analysis of myofibroblast differentiation in dermal fibroblasts. a) and **b)** Immunofluorescence staining images for αSMA, the nuclei were stained with DAPI (blue). **c)** Quantification of immunostaining experiments for αSMA protein abundance (n = 3 patients per group). Primary dermal fibroblasts were grown on glass cover slips for 4±1 days. p-values < 0.05 were considered statistically significant.

3.7.4 Effect of Mesalazine (5-aminosalicylic acid) on dermal fibroblasts

Mesalazine belongs to the group of an aminosalicylate anti-inflammatory drugs and is commonly used for the treatment of inflammatory bowel disease. However, recent studies on liver fibrosis identified Mesalazine as a potent osteopontin inhibitor with a long history of clinical use (Ramadan et al., 2018). Furthermore, there is evidence for the beneficial effects of aminosalicylate drugs in inflammatory skin disease such as psoriasis (Mastrofrancesco et al., 2014). In this respect, the effects of Mesalazine on dermal fibroblasts were tested *in vitro* with particular emphasis on functional properties and fibrosis-relevant protein abundance.

Fibrosis-relevant protein expression

To assess the effects of Mesalazine on fibrosis-relevant protein expression, RIM fibroblasts were treated with low-dose Mesalazine (1 µM or 1 mM) for 72 h. Based on literature information Mesalazine is used at higher concentrations (> 10 mM) *in vitro* (Schwab et al., 2008). Here we wanted to titrate an optimal dose for fibroblast treatment. There was trend towards an increase in PLK2 expression in the presence of 1 mM Mesalazine and a dose-dependent reduction in RasGRF2 protein abundance (Figure 43 a and b). The same effect was observed for OPN and αSMA (Figure 43 c and d). However, the results failed to reach the level of statistical significance. For this reason, Control and RIM cells were treated with 10 mM Mesalazine for 72h in the subsequent set of experiments. Compared to control fibroblasts, RIM fibroblasts expressed significantly more OPN and αSMA. We found a significant reduction of RasGRF2 protein abundance in RIM fibroblasts (Figure 44 a) after Mesalazine treatment. Accordingly, OPN and αSMA were also significantly reduced in RIM fibroblasts by 10 mM Mesalazine (Figure 44 b and c). In Control cells however, we found trends towards reduced expression of RasGRF2, OPN and αSMA (Figure 44 a – c).

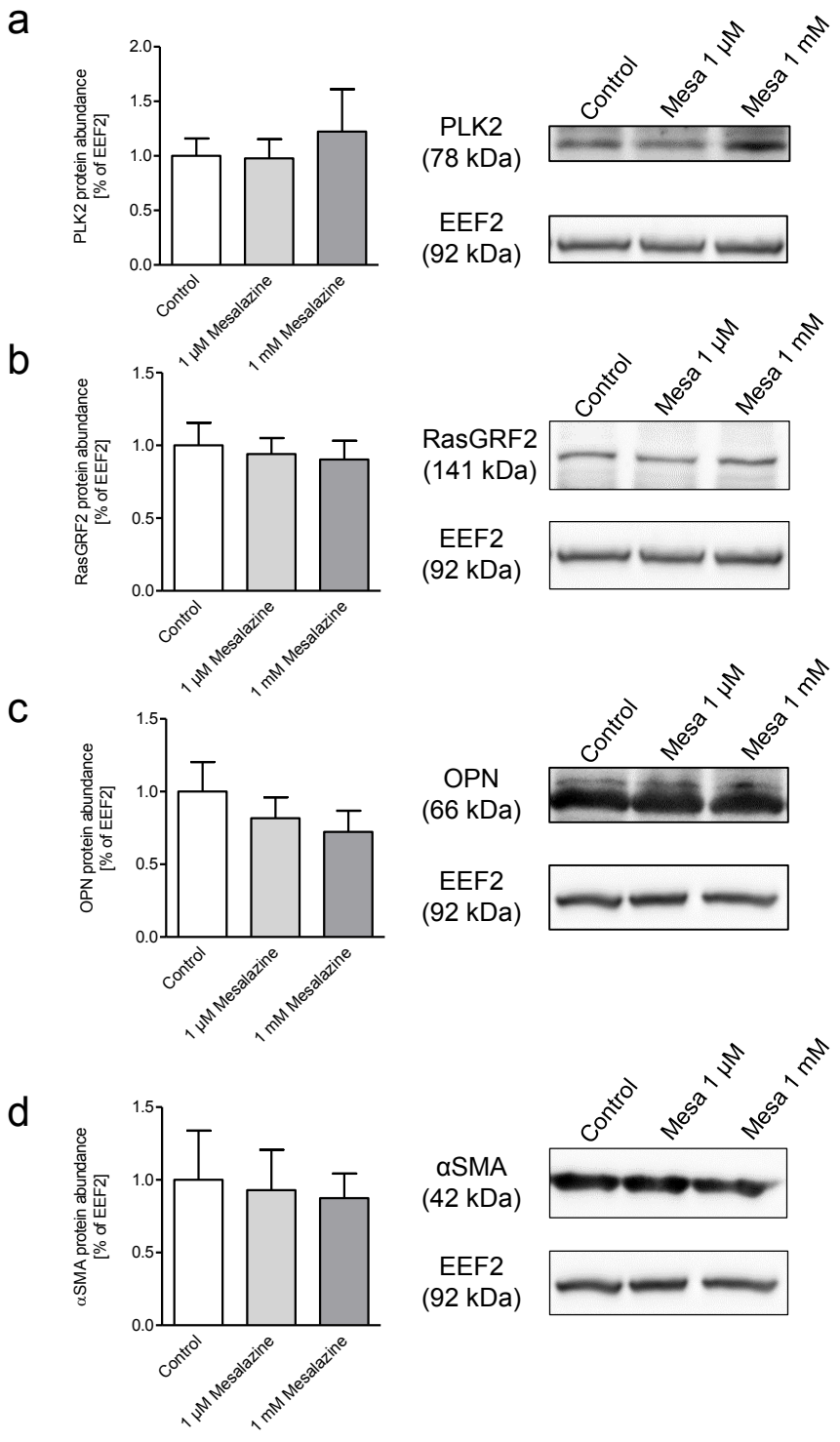

Figure 43. Effects of low-dose Mesalazine on fibrosis-relevant protein abundance. RIM fibroblasts were treated with solvent control (water, pH = 5.1) or Mesalazine at the concentrations stated above. For 72 h **a)** Protein abundance of PLK2. **b)** Protein abundance of RasGRF2. *c)* Protein abundance of OPN. **d)** Protein abundance of αSMA. The results failed to reach the level of statistical significance. (n = 3 per group).

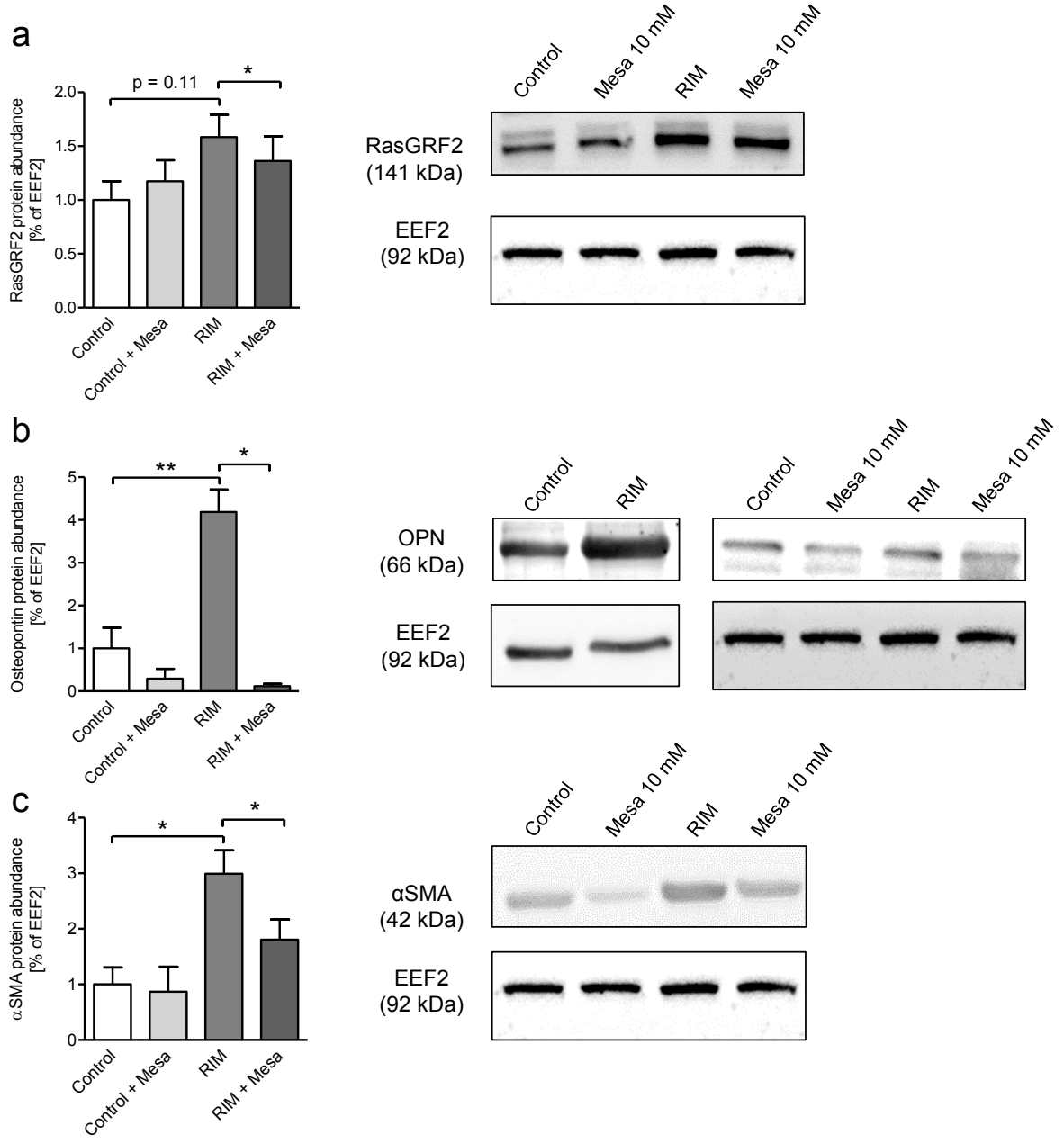

Figure 44. Effects of high-dose Mesalazine on fibrosis-relevant protein abundance. Control and RIM fibroblasts were treated with solvent control (water, pH = 5.1) or 10 mM for 72 h (n = 3 per group). **a)** Protein abundance of RasGRF2. **b)** Protein abundance of OPN. *c)* Protein abundance of αSMA. **d)** Protein abundance of αSMA. p-values < 0.05 were considered statistically significant.

Cell morphology and polarization

Cell morphology and polarization are important parameters to determine cell viability and their differentiation into myofibroblasts (Omelchenko et al., 2002). Here we tested if administration of Mesalazine to RIM fibroblasts which appeared less polarized, could improve cell morphology and polarization. We found that 10 mM Mesalazine applied for 72 h increased polarization and led to an overall more regular cell morphology (Figure 45 right panel).

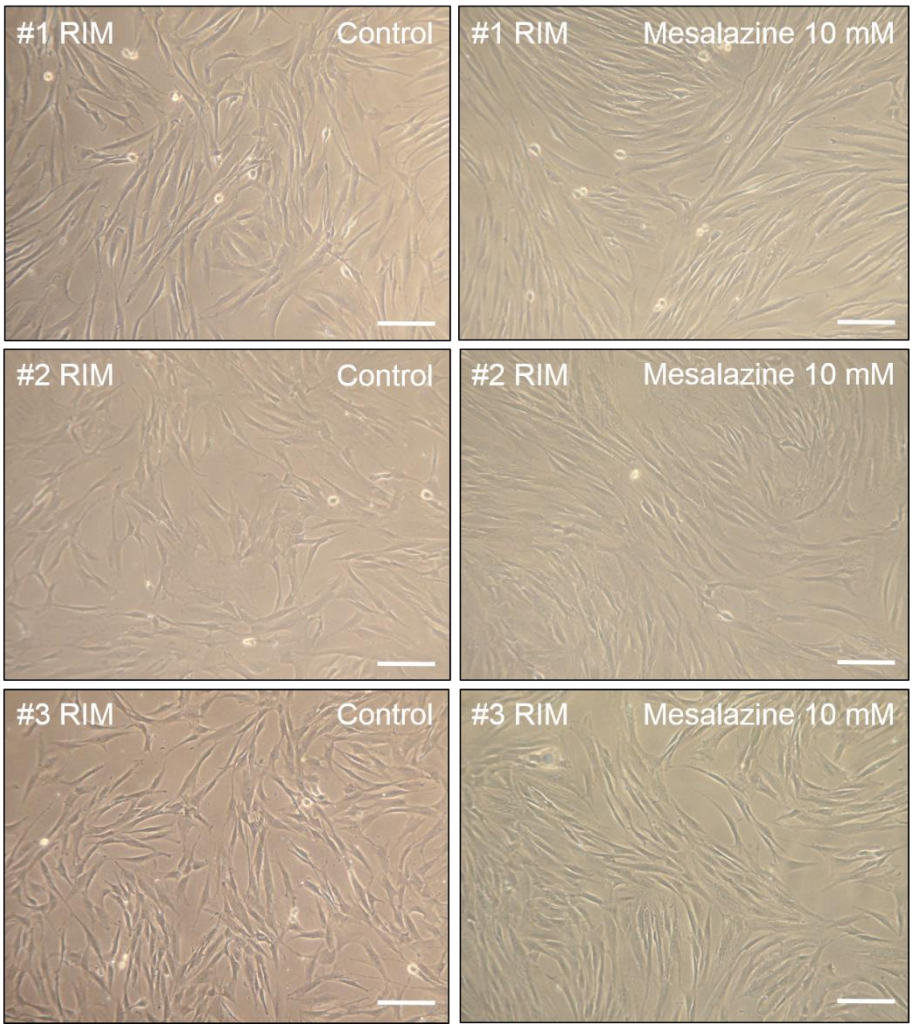

Figure 45. Influence of 10 mM Mesalazine on fibroblast morphology and polarization. Primary fibroblasts from RIM patients were exposed either to solvent control (water, pH = 5.1) or 10 mM Mesalazine for 72 h. The scale bar equals 200 µm.

Proliferation

In analogy to the experiments in 3.2.2.3 the effect of 10 mM Mesalazine on proliferation was tested. Cells between P5 and P10 were used for these experiments. Cells were seeded at initial densities of $1x10^4$ cells/ well and counted after 5 and 10 days. Mesalazine significantly reduced fibroblast proliferation in Control and RIM fibroblasts (Figure 46 a and b).

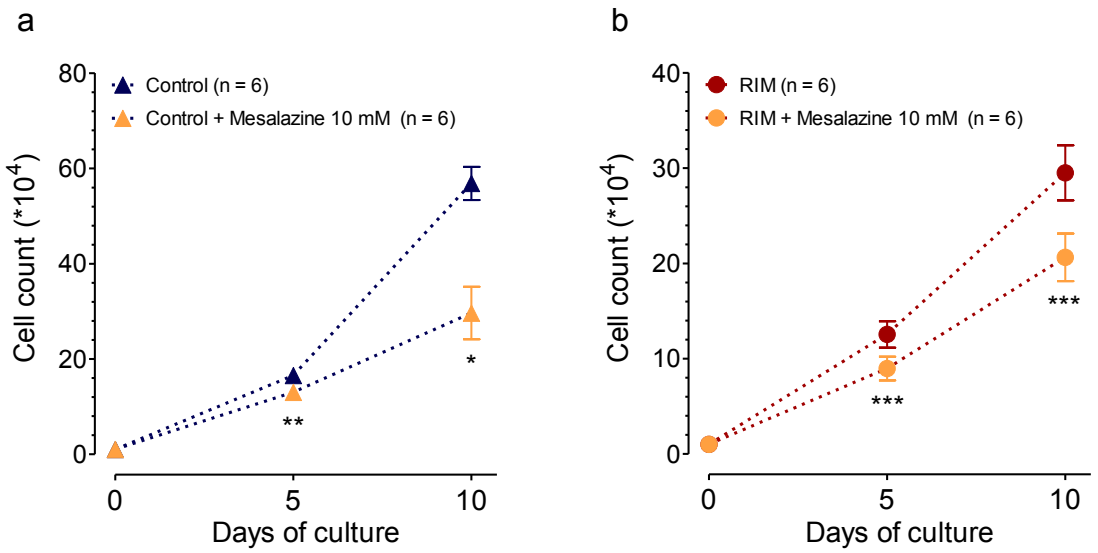

Figure 46. Influence of 10 mM Mesalazine on dermal fibroblast proliferation. a) Proliferation curves of primary Control fibroblasts in the presence of solvent control (water, pH = 5.1) or 10 mM Mesalazine (n = 6 experiments per group, Cells were isolated from N = 3 patients). b) Proliferation curves of primary RIM fibroblasts in the presence of solvent control (water, pH = 5.1) or 10 mM Mesalazine (n = 6 experiments per group, Cells were isolated from N = 3 patients). p-values < 0.05 were considered statistically significant.

Migration

Finally, the effects of 10 mM Mesalazine on dermal fibroblast migration were tested. Interestingly the effects of Mesalazine were adverse in Control and RIM cells. In Control fibroblasts 10 mM Mesalazine reduced cell migration. In RIM fibroblasts, however migration was elevated to the same migration rates that Control cells displayed in the presence of Mesalazine (Figure 47).

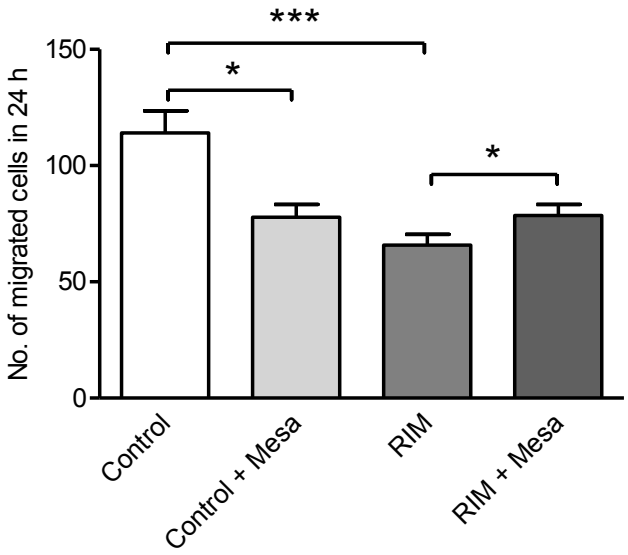

Figure 47. Effects of 10 mM Mesalazine on dermal fibroblast Migration. Cells were either treated with solvent control (water, pH = 5.1) or 10 mM Mesalazine for 24 h and subsequently counted. (n = 9 experiments per group, cells in both groups were isolated from N = 3 patients). p-values < 0.05 were considered statistically significant.

3.7.5 Molecular mechanisms involved in RIM

In order to clarify a general validity of the PLK2-OPN axis in myofibroblast differentiation and fibrosis, p42/44 MAPK phosphorylation was investigated. Due to reduced PLK2 and increased RasGRF2 protein abundance in RIM fibroblasts, we hypothesized an increase in p42/44 MAPK phosphorylation. P42 phosphorylation was 1.6 fold elevated in RIM fibroblasts compared to Control cells (Figure 48 a). There is evidence that activated (phosphorylated) p42 can phosphorylate SMAD2/3 (Yoon et al., 2015) which subsequently induces gene expression of collagens and αSMA (March et al., 2018). We found a trend towards more SMAD2/3 phosphorylation in RIM compared to Control fibroblasts (Figure 48 b). Thus SMAD phosphorylation was reduced by Mesalazine (Figure 46 b). Finally, we investigated the basal and Mesalazine-stimulated protein abundance of PPARγ in Control and RIM fibroblasts because Mesalazine was shown to induce PPARγ in non-dermal cells (Schwab et al., 2008). Studies focusing on liver fibrosis found that Mesalazine reduced αSMA and OPN protein abundance (Ramadan et al., 2018) without clarification of the molecular basis of these observation. We found a generally lower expression of PPARγ in RIM cells than in Control cells (Figure 48 c left panel). Pooled (Control and RIM) Mesalazine-treated fibroblasts expressed significantly more PPARγ compared to untreated cells (Figure 48 c right panel).

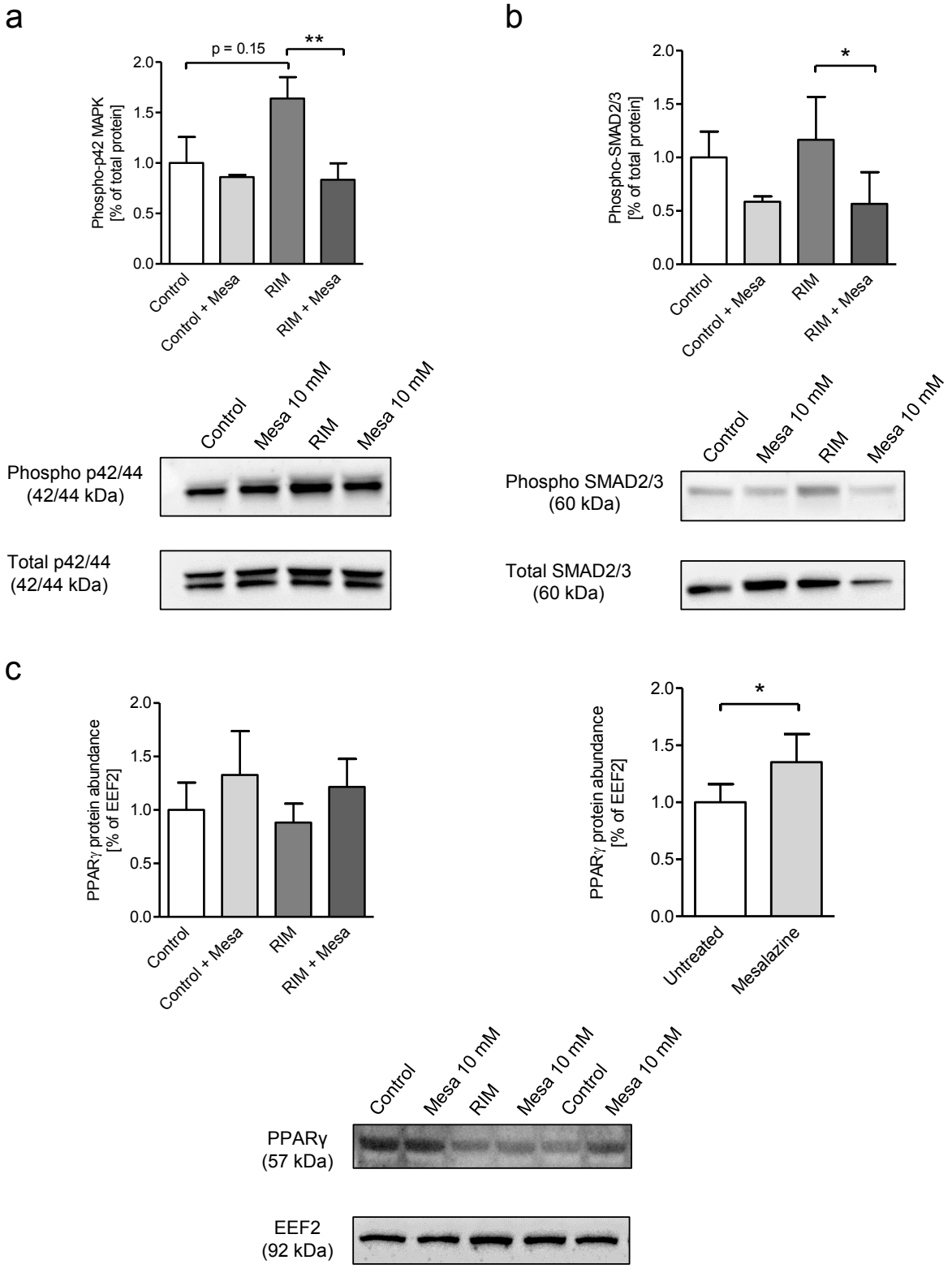

Figure 48. The role of p42/44 MAPK, SMAD2/3 and PPARγ in RIM fibroblasts. Cells were either treated with solvent control (water, pH = 5.1) or 10 mM Mesalazine for 72 h (n = 3 per group). **a)** Quantification and representative western blot of phosphorylated p42 MAPK in Control and RIM fibroblasts. **b)** Quantification and representative western blot of phosphorylated SMAD2/3 in Control and RIM fibroblasts. **c)** Quantification and representative western blot PPARγ in Control and RIM fibroblasts. The right panel displays the overall effect of Mesalazine on PPARγ protein abundance in Control and RIM fibroblasts. p-values < 0.05 were considered statistically significant.

4 Discussion

Over the last decade, considerable effort was put into identifying fibrosis mechanisms and putative therapeutic targets for innovative antifibrotic pharmacotherapy. Fibrosis was and continues to be a major determinant of clinical outcome in cardiovascular burdened patients. Stiffening of the myocardial walls and proarrhythmogenic remodeling of the atria are leading to deteriorating cardiac performance resulting in end stage heart failure and life threatening arrhythmia. However, available drugs and therapeutic approaches are still insufficient to prevent either fibrosis development or aggravation. Recent research has focused on novel molecular mediators that control fibroblast activation and differentiation in terms of cell-specific targeted pharmacotherapy. The family of polo-like kinases turned out to be a highly promising, as it is involved in these processes mentioned above, at least in non-cardiac tissue.

4.1 Summary of the main findings

Primary and commercially available human and murine cardiac fibroblasts, heart tissue and human peripheral venous blood were analyzed in the present study to gain insight in the (patho)physiological function of cardiac PLK2. The following main results were obtained:

1. We found a novel role for PLK2 in AF pathophysiology and cardiac fibrosis. Gene expression analysis revealed a significant 1.9-fold *PLK2* downregulation in primary human right fibroblasts derived from AF patients compared to SR control cells. This finding was validated on protein level in right atrial appendages with western blot and supported by samples of an AF dog model. Analysis of the methylation status of the *PLK2* promoter in SR and AF patients and a hypoxia cell culture model revealed hypoxia-induced promoter hypermethylation to be the likely cause of the observed PLK2 downregultion in AF patients.
2. Pharmacological inhibition of PLK2 with the specific PLK2 inhibitor TC-S 7005 and genetic KO in murine fibroblasts led to reduced cell proliferation but vice versa increased myofibroblast differentiation. PLK2 inhibition induced cell senescence in a considerable portion of fibroblasts. Cell migration however, was not affected by diminished PLK2 function.
3. In a broad secretome analysis of PLK2 WT and KO fibroblasts we found 20 significantly regulated secreted proteins in the two groups. The most promising finding was *a de*

novo secretion of the inflammatory cytokine-like phosphoprotein OPN. Consequently, OPN was elevated in AF heart tissue and the peripheral blood of AF patients.

4. We were able to decipher parts of the cardiac PLK2 signaling mechanism. We found that RasGRF2 is a substrate of cardiac PLK2, which accumulates in the absence of PLK2 leading to an increase in p42 MAPK phosphorylation and subsequent OPN and αSMA protein expression. Pharmacological inhibition of p42 MAPK thus reduced OPN protein expression below control values.
5. The functional and molecular characterization of dermal fibroblasts isolated from patients with radiation induced Morphea (a severe form of dermal fibrosis) implied a general validity and importance of the PLK2-p42MAPK-OPN-axis in (non-cardiac) fibrosis.

4.2 The function of PLK2 in the heart

4.2.1 Regulation of PLK2 gene expression

Regulation of eukaryotic gene expression is a complex and well-regulated process which basically focuses on controlling the initiation of gene transcription. Transcription is controlled by 2 major mechanisms: 1) proteins which modulate RNA polymerase and 2) modifications of the DNA in terms of chromatin density or methylation patterns (Cooper, 2000). Studies in non-cardiac tissue have pointed out that PLK2 gene expression is most likely target of DNA promoter methylation which leads to reduced PLK2 expression if present (Syed et al., 2006; Benetatos et al., 2011; Coley et al., 2012b). Yet, only little is known about PLK2 expression in the heart. Cardiac PLK2 expression was hitherto only described in human iPSC-derived cardiac progenitor cells (CPCs), which displayed an inverse correlation of PLK2 expression and increasing cell maturity (Mochizuki et al., 2017). Mochizuki and colleagues were able to show that downregulation of PLK2 increased the expression of lineage genes without further addition of differentiation medium (Mochizuki et al., 2017) indicating that downregulation of PLK2 in heart could be a physiological initiator of cell differentiation. This finding is consistent with the 1.9-fold downregulation of PLK2 mRNA expression in AF derived fibroblasts compared to SR controls. Based on our results and on the assumption that differentiated cells generally express less PLK2, it can be hypothesized that AF samples which have been shown to contain a larger proportion of differentiated myofibroblasts (Poulet et al., 2016) should also express less PLK2 overall. In order to derive therapeutic strategies from this finding, it is important to investigate and understand the underlying control mechanism(s) of PLK2 expression. In order to validate that the observed PLK2 downregulation is caused by AF, we analyzed western blot samples of control and rapidly paced dog heart tissue and found a

clear trend towards reduced PLK2 expression which slightly failed to reach the level of statistical significance ($p = 0.056$). However, this finding nonetheless strongly suggests that PLK2 downregulation in patient cells is caused by AF since confounding variables such as patient age, sex, comorbidities and medication were not present in the dog model. To understand the mechanism that reduces PLK2 expression during AF, the methylation status of the PLK2 promoter was analyzed in SR and AF patient samples, since methylation is a common epigenetic mechanism to silence gene expression (Lim und Maher, 2010). In 6 out of 13 AF atrial tissue samples we found methylation of the *PLK2* promoter in contrast to the SR controls ($n = 11$) in which methylation was absent. This finding is strengthened by previous studies that focused on PLK2 expression in hematological neoplasia. *PLK2* promoter methylation was frequently found in B-cell malignancies and acute myeloid leukemia, both neoplasia in which PLK2 expression was shown to be reduced (Syed et al., 2006; Benetatos et al., 2011). Anyway, it must be noted that the analysis in this study was performed in a small cohort of patient samples and that more extensive analysis is needed in order to draw a firm conclusion about general pathomechanisms from these results. The initiating trigger of promoter methylation also needs to be identified. There is convincing clinical and experimental data that AF and structural remodeling go alongside with tissue hypoxia and ischemic stress (Thijssen et al., 2002; Gramley et al., 2010; Stevenson et al., 2010; Lu et al., 2013; Opacic et al., 2016; Marulanda-Londoño und Chaturvedi, 2017). To date it is unclear whether hypoxia is the cause or the consequence of AF but effects of hypoxia on fibroblasts have been described in terms of higher myofibroblast differentiation (Robinson et al., 2012; Gao et al., 2014). Furthermore, Robinson and colleagues demonstrated elegantly that chronic hypoxia treatment of primary human lung fibroblasts induces genome wide DNA methylation (Robinson et al., 2012). Based on these evidences we exposed primary human right atrial and commercially available immortalized human ventricular fibroblasts to chronic hypoxia for 24 h, 72 h and 96 h (see 3.6.1). Although we found a significant PLK2 downregulation after 24 h of hypoxia treatment (Figure 34), there was no methylation present in the methylation-specific PCR at this time point (Figure 35 a). This result is in line with previous studies which determined 4 to 8 days of chronic hypoxia as the critical duration to induce DNA methylation (Robinson et al., 2012). For a prolonged hypoxia cell culture, special equipment, foremost a hypoxia cell culture bench, is necessary since short periods of normoxia e.g. for a medium change can be sufficient to remove hypoxia-induced effects (Wenger et al., 2015). Since our laboratory is not specialized in hypoxia, we were unable to perform an 8-days chronic hypoxia equipment for technical reasons. However, we performed hypoxia experiments without medium change for 72 h and 96 h. In accordance with Robinson *et al.* there was no methylation detectable after 72 h but slightly methylated bands occurred after 96 h (Figure 35 b and c). As a positive control we additionally exposed the cells to 0.25 mM dimethyloxaylglycine (DMOG). DMOG is known

to inhibit PHD finger protein (PHF) and factor inhibiting HIF (FIH-1) and thereby mimics maximal cellular hypoxia via accumulation of hypoxia inducible factor 1 alpha (HIF-1α) (Ayrapetov et al., 2011). Exposure to DMOG for 96 h clearly induced DNA methylation of the *PLK2* promoter and proofed that *PLK2* promoter methylation is sensitive to hypoxia (Figure 35 c). Despite of this, we were able to shed led on an additional negative upstream regulation mechanism of PLK2 via PRKRA and p53. P53 is reported to positively regulate PLK2 expression (Burns et al., 2003b, S. 2). This finding led us to the hypothesis that reduced p53 expression could additionally contribute to reduced PLK2 expression. We found enhanced expression of the negative p53 regulator PRKRA in AF fibroblasts compared to SR in the Affymetrix® microarray (Figure 36 a). Little is known about the regulation of PRKRA. However, endoplasmic reticulum stress (ER stress) was shown to induce PRKRA (Singh et al., 2009). ER stress in turn was also reported to be present in AF (Wiersma et al., 2017). For this reason, we hypothesize that the elevated PRKRA expression might be attributed to chronic ER stress in AF. Therefore, p53 expression is reduced in AF fibroblasts resulting in lower PLK2 expression in total. Taken together we provided experimental evidence for 2 upstream regulation mechanisms of PLK2 in AF which have to be addressed in future studies for better comprehension of AF pathophysiology.

4.2.2 *In vitro* effects of PLK2 modulation on cardiac fibroblasts

Since fibrosis is a crucial yet unmet complication in cardiovascular disease, the identification of novel fibroblast-specific targets is of high clinical relevance. The common aim of fibroblast studies is to identify mechanisms leading to fibroblast activation and subsequent myofibroblast differentiation (Figure 1). The expression of αSMA has been approved to be a reliable surrogate marker for myofibroblast differentiation. For this reason, the success or failure of a novel intervention on fibroblasts is usually measured by changes in αSMA expression. AF has been shown to be associated with fibroblast activation, myofibroblast differentiation and subsequent fibrosis (Nattel et al., 2008; Poulet et al., 2016; Lugenbiel et al., 2017). In this context, the need for fibroblast-specific antifibrotic therapy is evident. In the current study we put particular emphasis on the influence of lower PLK2 expression or inhibition respectively, on cardiac fibroblasts.

Myofibroblast differentiation

Fibroblasts from AF patients differentiate more into myofibroblasts compared to SR controls (Poulet et al., 2016). To explore whether this circumstance and our finding that AF fibroblasts express less PLK2 are mere coincidence or correlate, we studied the effect of the specific PLK2 inhibitor TC-S 7005 on fibroblast differentiation. We found a nearly 27 %

increase in myofibroblasts (fibroblasts with organized bundles of αSMA (Figure 12)) after PLK2 inhibition (see 3.2.2). To date there are no studies that explored the effect of PLK2 inhibition on cardiac myofibroblast differentiation. However, in CPCs that were later on differentiated into endothelial cells, maturation went alongside with lower PLK2 expression and loss of PLK2 induced terminal differentiation respectively (Mochizuki et al., 2017). Furthermore, downregulation of the PLK gene (not further specified) was proved to accompany the loss of proliferation ability in cardiomyocytes (Georgescu et al., 1997). Taken together, downregulation or reduced function of PLK2 appears to be a physiological mechanism linked to cell maturation or differentiation in the heart. This hypothesis is supported by the consistent results we obtained in PLK2 KO fibroblasts compared to WT controls. PLK2 KO led comparably to increased myofibroblast differentiation (+ 22.5 % myofibroblasts in KO compared to WT). Comparing basal myofibroblast differentiation in human and murine cells, it is evident that the basal fraction of myofibroblasts is higher in human cells. Various factors like patient age, comorbidities and administered drugs can influence the basal myofibroblast differentiation. The mice however do not have confounding comorbidities or have drug intake. The question why there are not even more myofibroblasts upon loss of PLK2 function remains to be clarified. A plausible explanation could be a certain redundancy with other PLK isoforms. PLK1 for example was shown to exert similar cellular functions like PLK2 in terms of proliferation (Jeong et al., 2018). A compensatory upregulation of other PLK isoforms could prevent myofibroblast differentiation to a greater extent. In addition, a complex process such as cell differentiation is usually not only controlled by one single mechanism.

Fibroblast proliferation

The second major cellular function studied in fibroblasts is proliferation. A higher proliferation rate is considered to contribute to fibrosis besides fibroblast activation and differentiation (Travers et al., 2016). AF has been shown to reduce fibroblast proliferation by a so far unknown mechanism (Poulet et al., 2016). Here we explored the possible contribution of PLK2 to reduced fibroblast proliferation in AF. We found reduced proliferation as well in experiments with pharmacological PLK2 inhibition as in experiments performed with PLK2 KO fibroblasts. In general, this finding is consistent with previously published data indicating that inhibition of PLK2 reduced cell proliferation (Liu, 2015; Mochizuki et al., 2017). Additionally, reduced proliferation is also a hallmark of terminally differentiated cells. In combination with our results from the differentiation experiments it is not surprising that inhibition or KO of PLK2 reduced proliferation as they enhanced myofibroblast differentiation. The therapeutic potential of this finding is arguable. In malignant neoplasia, reduced proliferation is clearly an advantage. Basically patients with fibrosis could also benefit from reduced fibroblast proliferation but the

increased differentiation of resident fibroblasts into myofibroblasts on the other hand could be negative for the clinical outcome of the patients.

Senescence induction

AF is increasingly regarded as an inflammatory disorder with a local and systemic component (Chung et al., 2001; Watanabe et al., 2005; Boos et al., 2006). Several inflammation mediators have been identified to be involved either in AF induction or maintenance such as TGF-β, TNFα, MMP1, Interleukin 1,2 and 6 and others (Hadi et al., 2010). Besides myofibroblasts which are known to secrete a plethora of cytokines (Calvo et al., 2018) there is a second considerable group of non-immune cells that secrete inflammatory mediators – senescent cells (Coppé et al., 2008; Rodier und Campisi, 2011). We investigated senescence induction depending on PLK2 function and found a trend towards increased cell senescence in PLK2 KO fibroblasts and significantly more senescent fibroblasts after pharmacological PLK2 inhibition (see 3.2.3). In the aging heart the fraction of senescent fibroblasts increases physiologically (Cowling, 2015). However, upon pathological stimuli, the fraction of senescent fibroblasts increases. Senescent cardiac fibroblasts are known to contribute fibrosis because their secretome shifts towards a more inflammatory phenotype (SASP) (Coppé et al., 2008; Zhu et al., 2013; Cowling, 2015). We found that PLK2 is a novel mediator of cardiac fibroblast senescence. Further investigations are thus required to elucidate the druggability of cardiac fibroblast senescence with special emphasis on a potential reversibility of once induced senescence as a tool to fight fibrosis.

4.2.3 *Ex vivo* effects of PLK2 KO

Cellular dysfunctions like fibroblast activation or senescence do not necessarily cause clinical symptoms or impair the patient' s quality of life. Tissue remodeling however bears a greater risk of causing debilitation. Fibrosis leads to wall stiffening and impairs the diastolic fillability of the ventricles and leads to heart failure on long term (Nihoyannopoulos und Dawson, 2009). Here, we wanted to clarify whether fibroblast activation and senescence induction which we found has tissue-level effects on PLK2 KO mice in terms of interstitial fibrosis development. Histological examination of explanted PLK2 WT and KO hearts revealed vast interstitial fibrosis areas (see 3.3.3, Figure 21) in the KOs whereas contiguous fibrosis areas were absent in WT. This finding indicates that PLK2 KO not only alters fibroblast function but has tangible impact on the organ structure and presumably the organ function. AF patients frequently suffer from heart failure with preserved ejection fraction (HFpEF) (Kotecha et al., 2016) which is characterized by elevated left ventricular filling resistance caused by fibrosis. Anyway, HFpEF patients do not display reduced ejection fraction or reduced cardiac output

because contraction force and heart rate are compensatory elevated (Mandinov et al., 2000). After a certain time, compensation fails and symptoms exacerbate. The molecular mechanisms leading to diastolic dysfunction or HFpEF are only little understood. Combining the facts that AF patients suffer from fibrosis and display PLK2 downregulation in cardiac fibroblasts which we prove to induce fibrosis at least in the PLK2 KO mouse model, we conclude that PLK2 downregulation could be a novel pathomechanism in AF leading to fibrosis and subsequent diastolic dysfunction.

4.2.4 *In vivo* effects of PLK2 KO

The genetic KO and pharmacological inhibition of PLK2 led to significantly altered fibroblast function. A pronounced myofibroblast phenotype was observed in vitro and accordingly PLK2 KO mice developed myocardial fibrosis. To test if PLK2 KO contributes to a HFpEF or HFpEF-like phenotype, we assessed the functional implications of the above described “myofibrosis phenotype” using transthoracic echocardiography and surface ECG recordings. In comparison to their WT littermates, 4 months old PLK2 KO mice showed significant systolic and diastolic dysfunction with lower stroke volume (WT: 43 ± 1.7 µl; PLK2 KO: 28 ± 2.6 µl) and lower enddiastolic volume (WT: 82 ± 3.1 µl; PLK2 KO: 60.7 ± 3.7 µl), respectively. Thus the cardiac output was also significantly reduced in the KO animals (WT: 17.1 ± 0.66 ml/min; PLK2 KO 10.6 ± ml/min). However, the ejection fraction and heart rate remained unaltered. These result are in line with the hypothesis that PLK2 KO leads to fibrosis which contributes to cardiac wall stiffening and thereby impairs the diastolic fillability. This hypothesis is supported by clinical investigations on patients with magnetic resonance proven cardiac fibrosis which revealed a strong correlation between the degree of fibrosis and the left ventricular diastolic dysfunction (Moreo Antonella et al., 2009). Surface ECG recordings revealed a prolongation of the PQ interval and of the QRS duration in PLK2 KO mice compared to their WT littermates. In patients, PQ prolongation indicating first degree atrioventricular block increases the risk of AF development significantly (Cheng et al., 2009; Tekkeşin et al., 2017). There is also clinical evidence that QRS prolongation can contribute to AF development and to increased mortality in patients (Whitbeck et al., 2014; Gigliotti et al., 2017). Taken together, genetic KO of PLK2 causes diastolic dysfunction and ECG abnormalities which are either typically found in AF or can contribute to AF development in patients. These results strengthen the hypothesis that cardiac PLK2 could be a valuable target in fighting cardiac fibrosis and subsequent heart failure and AF development. Since the animals tested so far were relatively young and AF as well as heart failure are generally present in elderly patients (Kazemian et al., 2012), follow-up experiments have to clarify whether heart rate and ejection fraction will deteriorate with age indicating a HFpEF phenotype.

4.2.5 PLK2 KO induces an inflammatory fibroblast secretome

The secretome analysis of PLK2 WT and KO fibroblasts revealed marked differences in the secreted proteins. Among the 3 most regulated proteins (see 3.4.1) macrophage metalloelastase (also known as MMP12) and OPN are known as mediators of atherosclerosis, inflammation and fibrosis (Goncalves et al., 2015; Zhao et al., 2016). We further focused on OPN since there are published associations of OPN with heart failure and most interesting with AF (Zhao et al., 2016; Güneş et al., 2017). To rule out the chance that elevated OPN is a cell culture artifact we confirmed the finding in human right atrial tissue lysates from AF patients compared to SR and thus found elevated OPN protein in AF tissue (Figure 26 b). This finding further supports the current opinion that AF is an inflammatory process (Hadi et al., 2010; Hu et al., 2015) plus it offers a potential therapeutic target in AF therapy.

4.2.6 PLK2 KO affects protein expression on the posttranscriptional level

The transcriptome analysis surprisingly revealed no significant differences in mRNA expression between PLK2 WT and KO fibroblasts except for the absence of PLK2 mRNA in the KOs. This finding suggests that PLK2 exerts its physiological functions predominantly on a posttranscriptional level e.g. RasGRF2 phosphorylation.

4.3 From bench to bedside – OPN in the peripheral blood

4.3.1 Selection of the study population

In previous studies we compared SR and AF patients concerning their fibroblast properties (Poulet). For electrophysiological experiments this criterion is reasonable and applicable. However, studying fibrosis mechanisms it has to be considered that AF is not the only stimulus leading to fibroblast activation and fibrosis. Although treated as control group SR patients are by no mean healthy. Our samples were obtained from patients who had to undergo open-heart surgery usually with the indication coronary artery disease. SR patients also suffer from hypertension and/ or diabetes and are equally treated with drugs like ACE inhibitors which are known for their antifibrotic effects (Pfeffer et al., 1995). For this reason, it is evident that SR and AF are no optimal criteria to distinguish patient groups to study fibrosis. For the analysis of OPN in the peripheral blood we chose to introduce new patient groups. Since we wanted to elucidate the extent to which activated fibroblasts contribute to OPN secretion into the peripheral blood, we compared AF patients without fibrosis and AF patients that displayed atrial fibrosis in electrophysiological mapping examinations (Piorkowski et al., 2018). This grouping is based on the assumption that fibrosis is the correlate of fibroblast activation. The SR control group was recruited from healthy volunteers who did not suffer from relevant disease.

4.3.2 OPN is elevated in the blood of AF patients with fibrosis

With a quantitative ELISA analysis, we were able to proof our hypothesis that AF with fibrosis goes alongside with elevated plasma OPN. We further found that age and plasma OPN do not correlate. Normalization of OPN to the fibrotic area would be very interesting to determine whether there is a direct correlation of fibrotic area size representing pathological fibroblast activation and the measured OPN. Right now these clinical data are not available for all patients so we cannot draw a conclusion yet. Although we hypothesize that the observed increase in OPN is mediated by myofibroblasts or senescent fibroblasts because of PLK2 downregulation that we found in other AF patients, we can only speculate about this mechanism in the OPN patients. Since these patients underwent minimal invasive ablation of the pulmonary veins, no tissue samples could be collected to determine PLK2 expression. A possibility would be a long-term follow-up to monitor these patients and acquire samples if they have to undergo cardiac surgery. Despite of these limitations, this novel finding demonstrates that AF patients with fibrosis might carry a higher risk for systemic complications like atherosclerosis (Zhao et al., 2016), fibrosis in other organs (Pardo et al., 2005) or even cancer (Rittling und Chambers, 2004; Zhao et al., 2018). Yet, beside those potentially increased risks, the finding also offers a new therapeutic target in AF patients with elevated plasma OPN.

4.4 A proposed mechanism of PLK2-OPN interaction

We intended to clarify the mechanistic link between loss of PLK2 function (either due to inhibition or genetic downregulation/ KO) and enhanced OPN secretion that was observed in PLK2 KO fibroblasts and AF patients whose tissue and fibroblast samples were shown to express less PLK2 than SR controls. We identified RasGRF2 as a novel substrate of PLK2 and that inhibition of PLK2 increased the expression of the RasGRF2 downstream target p42/44 MAPK (ERK1/2). So far, there is no experimental data focusing on the mechanisms of cardiac PLK2 function and protein interaction. It has been experimentally shown that PLK2 phosphorylates RasGRF1 leading to its degradation in the proteasome. Thereby the subsequent Ras-pathway is inhibited because RasGRF1 is an intrinsic activator of Ras (Lee, Lee et al., 2011; Lee, Hoe et al., 2011). Anyway, there is evidence supporting the claim that the Ras-pathway and p42/44 MAPK are important mediators of OPN transcription (Hickey et al., 2005; El-Tanani et al., 2006). Our study provides the first experimental data in favor of the claim, that inhibition of PLK2 increases RasGRF2 presence presumably due to diminished phosphorylation-dependent degradation of RasGRF2. RasGRF2 like RasGRF1 is known to stimulate the Ras pathway (Ruiz et al., 2007) resulting in higher expression of p42/44 MAPK (Alberola-Ila und Hernández-Hoyos, 2003) and increased phosphorylation of p42 MAPK which then stimulates OPN expression and secretion. A proof-of concept experiment using 10 nM of

the specific p42/44 MAPK inhibitor SCH772984 confirmed this theory with a significant reduction of OPN protein abundance (Figure 33). Additional experiments with phospho-specific RasGFR2 antibodies might help to further clarify this mechanism in future experiments.

4.5 Study limitations

4.5.1 The influence of fibroblast subpopulations

The embryonic origin of fibroblast populations within the organs of the human body is diverse. Current state-of-the-art lineage-tracing techniques allow to follow the cells traces throughout processes like tissue repair after myocardial infarction (Kanisicak et al., 2016). Kanisicak and colleagues elegantly revealed that myofibroblasts involved in post myocardial infarction processes originate from resident cardiac fibroblasts (Tcf21 lineage) and not from either endothelial, immune/myeloid or smooth muscle cells(Kanisicak et al., 2016). This is the argument in favor of a discussion which goes on for decades, that fibroblasts from different organs differ distinctly in their functions and cultural behavior. Still a distinct cardiac fibroblast marker protein is missing but there is experimental evidence that e.g. skin- and heart-derived fibroblasts are not as comparable as previously assumed since they differ in terms of morphology and cultural behavior (Conrad et al., 1977). In previous studies we found marked differences in proliferation, differentiation and migration between SR and AF right atrial fibroblasts (Poulet). There is even further evidence that the localization of a cell within the same organ can already influence it' s properties. Recent research focused on the molecular identities of atrial and ventricular iPS-cardiomyocytes revealing chamber-specific differences in e.g. ion channel expression or ECM production (Cyganek et al., 2018). Based on these findings it can be assumed that similar concepts apply for fibroblasts as well. Therefore, the choice of fibroblast subtype should be considered when comparing recent research to previous or when developing fibroblast-specific therapeutic approaches. In the present study we used only fibroblasts of cardiac origin. In human we preferably used primary right atrial fibroblasts but due to their limited availability and relatively long primary culture duration of about 3 weeks we also had to use human immortalized ventricular fibroblasts. We are aware that the results obtained in those ventricular fibroblasts have to be verified in primary atrial fibroblasts for best comparability. The experiments on the influence of PLK2 KO were performed on whole heart cardiac fibroblasts. These cells were isolated from the supernatant after the heart was digested enzymatically via Langendorff perfusion (El-Armouche et al., 2008). With this method it is not possible to obtain exclusively right atrial fibroblast in sufficiently large numbers to perform experiments.

4.5.2 Patient-based confounding variables

There is general consent about the confounding potential of patient demographics when doing research on human specimen. Factors like age, sex, race, comorbidities and medication can influence the obtained results considerably. Common disease like arterial hypertension, diabetes, hyperlipidemia or obstructive sleep apnea (OSAS) can have direct influence on e.g. epigenetic modifications, immune response or fibroblast function (Shamhart et al., 2014; Keating et al., 2016). Detailed patient data can be found in Table 5, 6 and 7. Due to the limited availability of patient samples a matching process as performed in clinical trials could not be applied to every set of experiments. Limited availability is also the reason for relatively small n-numbers in some experiments. We are aware of the fact that larger numbers of patients need to be tested to draw firm conclusions about clinical implications. Anyway, for the analysis of OPN in the peripheral blood a strict matching algorithm was applied since blood samples were easier to obtain than heart tissue. The patients were matched according to age, sex and comorbidities (Table 5). Matching for medication was not possible and matching for race was omitted because all patients were of Caucasian origin.

4.6 Clinical relevance – putative therapeutic targets

4.6.1 PLK2 modulation as therapeutic target

Over the past couple of years, the PLK family drew attention to itself as novel treatment target. The main focus of research has been in the oncological or neurodegenerative field (Burns et al., 2003a; Syed et al., 2006; Shen et al., 2012; Liu, 2015). The best described and analyzed PLK family member is PLK1 which has been identified as potential oncogene and drug target in several neoplasia (Cholewa et al., 2013; Liu, 2015; Jeong et al., 2018). PLK overexpression has been associated with excessive cell proliferation and resistance to chemotherapy. Volasertib, a promising specific PLK1 inhibitor was tested until phase 2 of clinical trials. However, the hoped-for translation of the extremely promising *in vitro* results failed (Rudolph et al., 2009; Gutteridge et al., 2016). In the heart there are currently no approaches to target PLKs. Based on our data we can state that cardiac PLK2 downregulation plays a critical role in fibroblast activation and therefore it could be a useful target to develop novel antifibrotic therapies. The results we obtained thus mimicked the pathophysiological finding of PLK2 downregulation in AF. We were able to reproduce the AF-specific fibroblast properties of reduced proliferation and increased myofibroblast differentiation (Poulet et al., 2016). For this reason, PLK2 inhibition in order to prevent fibrosis is no reasonable treatment option. In contrast our data suggest that stimulation, upregulation or overexpression of PLK2 could be able to reverse fibroblast dysfunction. Anyway, there are obstacles which must be overcome before treatment options can emerge. First, there are currently no specific PLK2

activators available. Upregulation of PLK2 was noticed when breast cancer cells were exposed to celastrol, a flavonoid found in different plants (Kim et al., 2013). We also performed experiments with celastrol on ventricular fibroblasts (data not shown). We noticed a trend towards PLK2 upregulation accompanied by substantial cytotoxicity. Further research is needed to assess the therapeutic value of celastrol to fight fibrosis. Second, PLK2 activation or upregulation has to be cardio-fibroblast-specific to be applied therapeutically. Unspecific upregulation which could be caused by celastrol administration, can potentially be dangerous for the patient since various neoplasia have been shown to express excessive PLK2 (Coley et al., 2012a). The novel findings that Tcf21 determines cardiac fibroblast fate during embryonic development and that cardiac myofibroblasts were found to express specifically periostin (Kanisicak et al., 2016) could serve as attack points to deliver a PLK2 activator directly to cardiac fibroblasts. The last therapeutic option we can suggest is the restoration of the physiological methylation state of the *PLK2* promoter. Since promoter methylation was absent in SR control samples, we conclude that methylation is related to pathological remodeling in AF. For this reason, the application of de- or hypomethylating agents like the DNMT inhibitor 5-azacytidine could be a treatment option (Plumb et al., 2000). This approach was tested in a murine kidney fibrosis model. Folic acid-induced kidney fibrosis could be attenuated after application of 5-azacytidine (Bechtel et al., 2010). However, it must be considered that treatment with 5-azacytidine results in global non-specific hypomethylation (Issa und Kantarjian, 2009) of the DNA and thereby interferes substantially in the patient's methylome which could cause unpredictable side effects. Until targeted and specific modulation of PLK2 expression or function is safely applicable, we suggest to focus on the as well promising targets of the cardiac PLK2 signaling cascade.

4.6.2 p42/44 MAPK (ERK1/2) inhibition as therapeutic target

Similar to the PLK family, p42/44 MAPK (ERK1/2) also regulate cell proliferation and are therefore in the focus of oncological research. A recently published study revealed data on an orally administered ERK1/2 inhibitor given to patients with melanoma. The compound was tolerated by the patients and displayed antitumor activity in BRAFV600-mutant melanoma (Moschos et al., 2018). We found that basal phosphorylation of p42 MAPK was significantly elevated in KO fibroblasts and that pharmacological inhibition of p42/44 MAPK with 10 nM SCH772984 led to significantly reduced OPN protein abundance in PLK2 KO fibroblasts (Figure 33). Although p42/44 MAPK in the heart were shown to play a role in the response to pathological stimuli, the genetic inhibition of p42/44 MAPK had rather adverse effects in mice. The p42/44 MAPK-deficient animals were more prone to decompensation or heart failure due to pressure overload (Purcell et al., 2007). For this reason, the degree of p42/44 MAPK

inhibition in AF to prevent adverse effects of PLK2 downregulation must be well titrated and further explored to become a suitable treatment option.

4.6.3 OPN inhibition as therapeutic target

In contrast to PLK2 and ERK1/2, the elevated plasma OPN in AF appears to be a promising therapeutic target. In an approach of reverse translation, already existing and approved compounds could be tested in regard of counteracting OPN expression. Currently there are 2 available candidate groups. *1)* Soluble guanylate cyclase stimulators (sGCSs) like Riociguat® are a novel group of compounds relevant for the treatment of heart failure and cardiac fibrosis (Geschka et al., 2011; Sandner et al., 2017; Rai et al., 2018). Soluble guanylate cyclase stimulators enhance the availability of the second messenger cGMP which in turn stimulates antifibrotic pathways that are important for patients with heart failure (Gheorghiade et al., 2013). Experimental data has shown that Riociguat® reduces OPN expression in a heart failure animal model (Geschka et al., 2011). The positive effects of sGCSs are beyond doubt (Gheorghiade et al., 2013) and the indications for those new compounds are continuously being expanded (Gheorghiade et al., 2013; Sandner et al., 2017; Rai et al., 2018). If patients with newly diagnosed AF would receive testing of plasma OPN levels, pleiotropic sGCSs which can be orally administered could prevent the OPN-mediated contribution to cardiac fibrosis and diastolic dysfunction in AF. *2)* A second promising treatment option for OPN overload could be salicylic acid and its derivatives. Mesalazine which is approved for the treatment of chronic inflammatory bowel disease like foremost ulcerative colitis, was recently shown to be a potent inhibitor of OPN-release. Furthermore, it significantly reduced αSMA and TGF-β protein expression (Ramadan et al., 2018). The compound was tested in a model of pharmacologically induced liver fibrosis and it succeeded in reducing the expanse of fibrosis compared to control treatment (Ramadan et al., 2018). These findings support the existing knowledge about the antifibrotic properties of salicylates like acetyl salicylic acid (Aspirin®) (Abouzed et al., 2016). A great benefit of Mesalazine compared to other compounds counteracting OPN expression and release are the years of clinical experience and a profile of only moderate side effects such as gastrointestinal complaints (Shire Pharmaceutical Contracts Ltd, 2018). For all these reasons application of salicylates like Mesalazine appears to be a worthwhile and clinically relevant approach to counteract OPN-driven fibrosis in the heart.

4.7 General relevance of the PLK2-p42/44MAPK-OPN-axis in (non-cardiac) fibrosis

In order to draw conclusions about a general validity and importance of the newly identified PLK2-p42/44MAPK-OPN-axis in fibrosis in general, dermal fibroblasts from Control and RIM patients were characterized. We put particular emphasis on cellular functions such

as proliferation, migration and differentiation and the molecular pathways identified in the heart. Comparably to AF- and PLK2 KO-fibroblasts we found reduced proliferation and migration but increased differentiation into myofibroblasts in RIM cells. The PLK2 mRNA and protein expression were reduced, although the results did not reach the level of statistical significance. However, the protein abundance of OPN and αSMA were significantly elevated in RIM which was in line with significantly increased phosphorylation of p42 MAPK and SMAD2/3 being crucial for myofibroblast differentiation and OPN expression (Renault M.-A. et al., 2003; Ruiz et al., 2007; Lugenbiel et al., 2017). These findings are novel and clinically interesting, since there is no functional data on fibroblasts in RIM available, yet. For this reason, the therapeutic options are limited and unsatisfying (Spalek et al., 2015).

The similarities between cardiac and dermal fibroblasts imply that the PLK2 signaling cascade could be of general interest in dysregulated fibroblasts. Since OPN was so clearly elevated in RIM fibroblasts we wanted to test the potential of Mesalazine as OPN inhibitor as suggested by Ramadan and colleagues. The application of 10 mM Mesalazine markedly reduced OPN and αSMA protein abundance. In this respect the results confirmed the claim of Ramadan and colleagues. To clarify which molecular mechanism led to the reported antifibrotic effect of Mesalazine, we found evidence in the literature that Mesalazine can act as PPARγ stimulator (Schwab et al., 2008). There is evidence that selective PPARγ stimulation caused by amino salicylates such as Mesalazine inhibits fibrosis and inflammation (Mastrofrancesco et al., 2014). The selective activation of PPARγ inhibits the NFκB pathway and the AP1-regulated transcription of OPN (Renault M.-A. et al., 2003; Scirpo et al., 2015). So far we could show that 10 mM Mesalazine induced PPARγ protein expression (Figure 48 c) and contrariwise reduced p42 MAPK and SMAD2/3 phosphorylation significantly (Figure 48 a – b) which are requirements for myofibroblast differentiation and OPN expression. The cells tolerated the treatment well and displayed good viability and improved morphology.

In summary we identified several parallels between cardiac and dermal fibrosis mechanisms which refined our working hypothesis about the molecular PLK2-fibrosis-mechanism and a potential therapeutic intervention with Mesalazine (Figure 49).

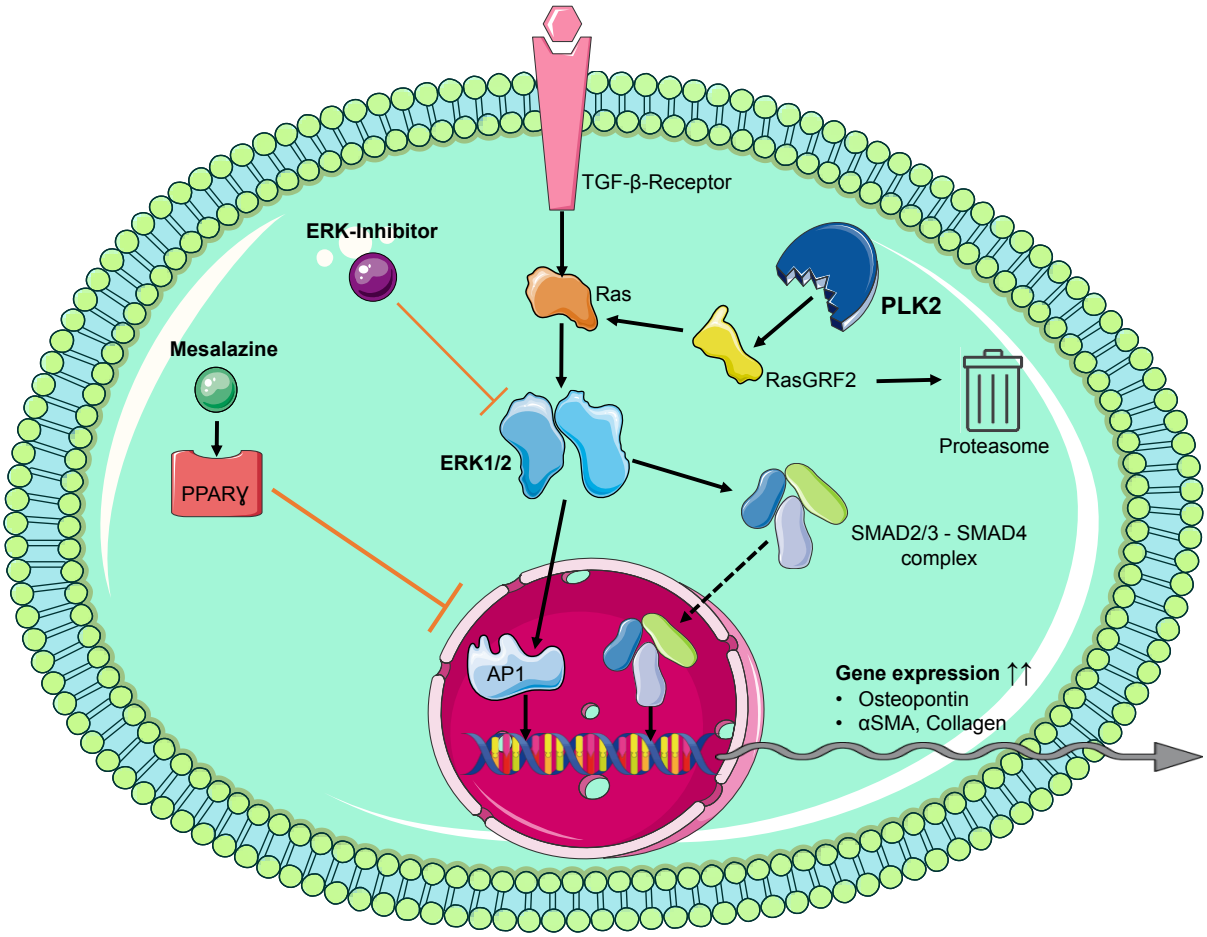

Figure 49. Working hypothesis about the PLK2-fibrosis-axis and therapeutic intervention with Mesalazine. Under physiological conditions, PLK2 phosphorylates RasGRF2, which is then degraded in the proteasome. With decreased PLK2 activity, RasGRF2 accumulates and stimulates the Ras signaling pathway. The Ras-pathway can also be stimulated via TGF-β. The central element of this cascade is p42/44 MAPK (ERK1/2) activation. ERK induces gene expression of osteopontin, αSMA, collagen as well as TGF-β via AP1 and SMAD phosphorylation, so that an autocrine amplification of this signaling pathway is possible. By selective modulation of the PPARɣ receptor with Mesalazine, AP1 is inhibited, thus preventing osteopontin transcription. As a result, the application of Mesalazine can potentially have an anti-fibrotic and anti-inflammatory effect in our experimental context. Images of Servier medical Art were used to create this graphic (https://smart.servier.com/; Creative Commons License).

4.8 Synopsis - the role of PLK2 in AF pathophysiology

Based on our experimental *in vitro* and *ex vivo* data we suggest the following role for PLK2 in AF pathophysiology: AF is accompanied by tissue hypoxia and ER stress. Chronic hypoxia leads to methylation of the *PLK2* promoter which corresponds with reduced PLK2 protein expression. ER stress on the other hand leads to upregulation of PRKRA expression and subsequent p53 downregulation. Lower p53 expression further lowers then PLK2 expression. Loss of PLK2 function activates fibroblasts that differentiate into myofibroblasts secreting various inflammation mediators such as OPN. Chronic OPN overload induces local inflammation and activates more fibroblasts resulting in interstitial fibrosis development.

Fibrosis worsens the cardiac performance of the patient mirrored in foremost diastolic dysfunction which can result in heart failure. The fibrotic remodeling disturbs coordinated excitation propagation in the atria and promotes AF maintenance in turn. Prolonged AF leads to further reduced PLK2 expression and the vicious circle continues (Figure 50).

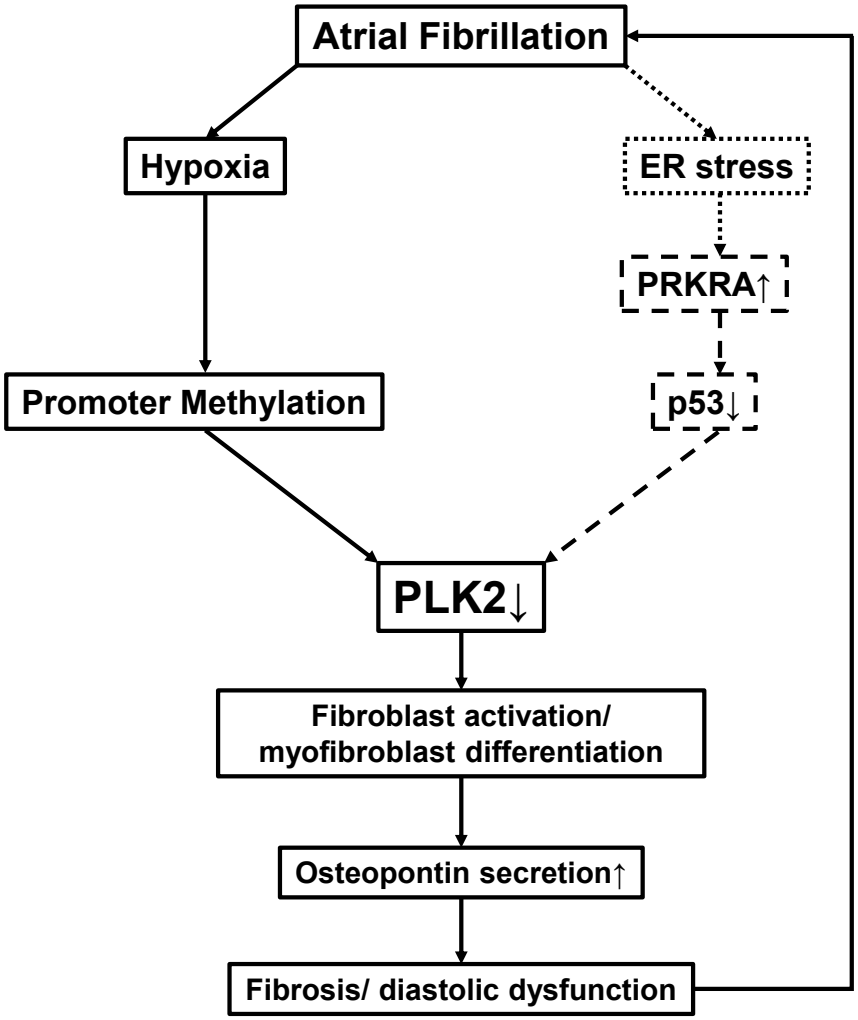

Figure 50. The role and regulation of PLK2 in AF pathophysiology. This scheme illustrates our suggested mode of PLK2 regulation and the downstream effects of PLK2 in the control of cardiac fibroblast activity, subsequent fibrosis development and AF maintenance. Continuous boxes indicate strong experimental evidence or strong support from primary literature sources. Hatched boxes indicate weaker experimental evidence from the Affymetrix® array only.

4.9 Experimental outlook

Further research on PLK2 and its regulation in the heart is required to fully understand this promising target to develop fibroblast-specific antifibrotic drugs. Modifying the PLK2 gene in primary human fibroblasts using CRISPR/cas could confirm the findings we obtained in the PLK2 KO mouse model. This model could be further improved by creating a heart-specific or even cardiac fibroblast specific KO of PLK2 using a Cre/loxP system (Bouabe und Okkenhaug, 2013). Similar fibroblast-specific KOs have recently been published (Jain et al., 2016; Woodall et al., 2016). Such a model could deliver useful information about the interplay between fibroblasts and cardiomyocytes and could clarify to which extent cardiac fibroblasts contribute to systemically elevated OPN. In contrast cardiac fibroblast-specific PLK2 overexpression would clarify the question whether PLK2 activation is desirable in preventing and treating fibrosis.

The next step to further characterize the PLK2 KO mouse model has to be a comprehensive functional analysis of the heart using echocardiography and implantable ECG telemetry. Our preliminary experiments already revealed a phenotype with diastolic dysfunction in PLK2 KO mice at 4 months of age. Higher numbers of experiments at 4 months and experiments in older animals (e.g. 8 months) will reveal whether the PLK2 KO mice develop a HFpEF like phenotype comparably to AF patients. Particular emphasis will be put on the development of the heart rate and arrhythmia induction. Subcutaneously implanted ECG telemeters can be used to record the ECG continuously over 2 weeks to gain insight on how PLK2 KO affects the cardiac electrophysiology.

Finally, *in vivo* interventions in mice could help to elucidate the therapeutic potential of either PLK2 activation or OPN inhibition. To test the effects of PLK2 activation, wild type mice could be given orally administered celastrol which was shown to enhance PLK2 expression (Kim et al., 2013, S. 2). A control group of littermates would be solely exposed to the physiological process of aging without drug application. Frequent echocardiography performed after e.g. 2, 4, 6 and 8 months could deliver data about the cardiac performance of the animals. After sacrificing the animals by bleeding out, histological sections could prove whether fibrosis was attenuated in the drug-treated group. The peripheral blood samples could deliver useful data about circulating OPN or other inflammation mediators. Further molecular biological analysis focusing on PLK2, αSMA, collagen and OPN expression would complete the experiments. Additionally, fibroblasts could be isolated from the tissue of both control and drug-treated animals to compare the extent of myofibroblast differentiation and the proliferation rates, respectively. Analogous experiments could be performed using PLK2 KO and Mesalazine to assess the effects of attenuated OPN expression on fibroblast function, cardiac performance and fibrosis. Mesalazine could be administered orally without retardation via the drinking water

of the animals over a prolonged period of several months. Mesalazine could be the most promising compound to test in the PLK2 KO animals since it is approved, well tolerated and cost-effective. In the course of reverse translation, this compound could be a promising candidate to effectively fight cardiac fibrosis that either causes or accompanies AF and heart failure.

4.10 Conclusions

Initially, the following 4 questions were addressed. The latter paragraph shall provide brief answers to them:

a) *What is the physiological function of PLK2 in cardiac fibroblasts and how is it altered in atrial fibrillation?*

   We found that PLK2 is a key mediator of cardiac fibroblast properties such as proliferation, differentiation and senescence induction. In the course of AF, PLK2 is downregulated likely due to chronic tissue hypoxia, leading to fibroblast dysfunction and fibrosis.

b) *Which molecular pathways are involved in the signaling of cardiac PLK2 and are there putative drug targets up- or downstream of PLK2?*

   Upstream of *PLK2* we found hypoxia-dependent promoter methylation, leading to reduced transcription of the *PLK2* gene. Downstream of PLK2, we identified the RasGRF2-p42/44 MAPK-pathway to be involved in excessive cardiac OPN expression which constitutes the most promising therapeutic target resulting from diminished PLK2 expression.

c) *Are there putative clinical implications by targeting PLK2 or its signaling cascade?*

   Based on the data obtained in this study, there are several potential options to influence PLK2 or its effectors like OPN to counteract fibrosis in the heart. Restoration of the physiological *PLK2* promoter methylation status with demethylating agents, or blockade of OPN using orally administered Mesalazine appear to be plausible approaches for further studies.

d) *Is the PLK2-signaling axis generally relevant in (non-cardiac) fibrotic remodeling?*

   This study identified a relevance for PLK2 and its signaling cascade in dermal fibrosis. Treating dysfunctional fibroblasts with Mesalazine resulted in significant improvement in fibroblast function, morphology and protein expression.

5 Summary

Background and aim. Atrial fibrillation (AF) is the most common and relevant arrhythmia in the clinical routine. AF is predicted to affect 6–12 million patients in the USA by 2050 and 18 million patients in Europe by 2060. Cardiac fibrosis and inflammation decisively determine the course of the disease and the clinical outcome of the patients. Despite the tremendous impact on human health, detailed understanding on the molecular mechanisms that contribute to fibrosis in AF is limited. This study provides further evidence for the current paradigm shift that atrial fibrillation is more of a systemic-inflammatory disease than a mere ion-channel dysfunction. The aim of this study was to investigate the role of polo-like kinase 2 (PLK2) and the pro-inflammatory cytokine osteopontin (OPN) with respect to fibroblast (dys)function and fibrosis formation in order to derive novel targets for targeted, fibroblast-specific pharmacotherapy.

Material and methods. All patients who participated in this study gave their written informed consent in accordance to the declaration of Helsinki. The study was approved by the local bioethics committee (Ethikkommission an der Technischen Universität Dresden). Human fibroblasts were isolated by outgrowth culture from right atrial biopsies of patients suffering from sinus rhythm (SR) and AF. Murine fibroblasts were isolated by whole-heart Langendorff-perfusion. Quantitative PCR and western blot were used to detect *PLK2* transcript expression and protein abundance, respectively. Functional assessment of cardiac function was done with transthoracic echocardiography and surface ECG recordings. Cell culture experiments were performed to evaluate the effects on functional fibroblast properties such as proliferation and differentiation after changing PLK2 activity by genetic knockout (KO) or pharmacological inhibition. A mass spectrometry based secretome analysis was performed by our collaborating laboratory of Prof. Manuel Mayr at King's College London. An enzyme-linked immunosorbent assay (ELISA) was done to measure OPN in the peripheral blood of patients in SR and with permanent AF.

Results. Right atrial appendage tissue and fibroblasts from AF patients displayed significantly lower expression of *PLK2* mRNA and protein due to increased DNA-methylation of the *PLK2* promotor when compared to sinus rhythm (SR) control patient atria or fibroblasts. This methylation was induced in cardiac fibroblasts by chronic hypoxia (1% O2) exposure for 96 h. Pharmacological inhibition as well as global KO of PLK2 in cardiac fibroblasts resulted in elevated myofibroblast differentiation and reduced fibroblast proliferation. *PLK2* KO mice

displayed vast interstitial fibrosis areas as observed from histological cross sections stained either with Sirius red or with Masson's trichrome staining. Transthoracic echocardiography revealed systolic and diastolic dysfunction in PLK2 KO mice and AF-typical ECG alterations such as prolonged PQ interval and QRS duration. Mass spectrometry proteomics revealed de novo expression of OPN in the PLK2-KO-fibroblast secretome. Furthermore, we found higher OPN plasma levels in AF patients correlated with electrophysiologically determined fibrosis compared to non-fibrosis control patients. Finally, we identified that the p42/44 MAPK signal transduction cascade is linking to reduced *PLK2* expression and enhanced OPN release. Specifically, we found that KO of PLK2 increase p42 MAPK phosphorylation which is known to stimulate OPN transcription. Thus inhibition of p42/44 MAPK resulted in diminished OPN expression. In a dermal fibrosis model the administration of Mesalazine *in vitro* resulted in reduced p42 MAPK and SMAD2/3 phosphorylation and thereby reduced OPN and αSMA expression. To explore the general validity and relevance of the PLK2 signaling pathway for fibrosis, a dermal model of radiation-induced fibrosis was used. This approach a) confirmed the observations that were made in the heart and b) showed that the use of Mesalazine *in vitro* led to a reduced p42 MAPK and SMAD2 / 3 phosphorylation and thus to a significantly reduced OPN and αSMA expression.

Conclusions and clinical significance. Fibroblasts from patients with permanent AF express less PLK2 than cells from SR control patients. The loss of physiological PLK2 activity coincides with marked changes in the proliferation and differentiation of cardiac fibroblasts. These changes favor fibrosis in the atrial tissues, which is further enhanced by the local and systemic increase of OPN. The present study identifies PLK2 as a novel regulator of cardiac fibroblast function and fibrosis. Restoration of the physiological methylation status of the *PLK2* promoter or the inhibition of OPN with Mesalazine could be of particular clinical interest. The tangible clinical and pharmacological feasibility will be subject of future investigations.

6 Zusammenfassung

Hintergrund und Zielstellung. Vorhofflimmern (VHF) ist die häufigste und bedeutsamste Arrhythmie in der täglichen klinischen Praxis. VHF wird bis 2050 voraussichtlich 6 -12 Millionen Menschen in den USA und bis 2060 zirka 18 Millionen Menschen in Europa betreffen. Fibrose und Entzündungsprozesse bestimmen entscheidend den Krankheitsverlauf und das klinische *Outcome* der Patienten. Trotz dieser großen Relevanz sind detaillierte Informationen zu den beteiligten molekularen Pathomechanismen weitgehend unklar. Diese Studie liefert weitere Evidenz für den aktuellen Paradigmenwechsel, dass Vorhofflimmern eher eine systemisch-entzündliche Erkrankung als eine bloße Ionenkanaldysfunktion ist. Ziel dieser Arbeit war es die Rolle der polo-like Kinase 2 (PLK2) und des proinflammatorischen Zytokins Osteopontin (OPN) im Hinblick auf Fibroblasten(dys)funktion und Fibroseentstehung zu untersuchen, um neuartige Angriffspunkte für zielgerichtete, Fibroblasten-spezifische Pharmakotherapie abzuleiten.

Material und Methoden. Alle Patienten wurden über die Teilnahme an der Studie aufgeklärt und gaben ihr schriftliches Einverständnis. Die vorliegende Studie ist konform mit der Deklaration von Helsinki und enthaltene Tierversuche erhielten ein positives Votum der lokalen Tierschutzbehörde. Humane Vorhoffibroblasten wurden mit der „*Outgrowth*“-Methode aus Gewebeproben von Patienten im Sinusrhythmus (SR) und im permanenten Vorhofflimmern isoliert. Murine Herzfibroblasten wurden aus dem Überstand nach Langendorff-Perfusion durch mehrere Zentrifugationsschritte gewonnen. Zur Detektion von PLK2 und anderen Markerproteinen wurden (quantitative) PCRs und Western Blots durchgeführt. Zur Beurteilung der Herzfunktion *in vivo*, wurde transthorakale Echokardiografie mit Oberflächen-EKG-Ableitung genutzt. Nachfolgende Zellkulturexperimente beleuchteten die Auswirkungen pharmakologischer PLK2 Inhibition oder genetischen Knock-Outs auf Fibroblasten im Hinblick auf Proliferation, Differenzierung, Seneszenzentwicklung und Sekretion. Eine Massenspektrometrie-basierte Untersuchung des Sekretoms PLK2-defizienter Fibroblasten wurde im Labor unseres Kollaborationspartners Prof. Manuel Mayr am King’s College London durchgeführt. OPN im peripheren Blut von Vorhofflimmerpatienten wurde mittels eines ELISAs gemessen. Ob die betreffenden Patienten Fibrose der Vorhöfe aufwiesen oder nicht, wurde in klinisch-elektrophysiologischen Untersuchungen, dem sogenannten *Mapping*, bestimmt.

Ergebnisse. Im Vergleich zu SR-Kontrollen, war die PLK2 mRNA- beziehungsweise Protein-Expression in isolierten Fibroblasten und auf Gewebeebene in VHF-Proben signifikant

erniedrigt. Dies korrelierte mit *PLK2*-Promotermethylierung in der Hälfte der VHF-Proben. In SR-Kontrollen konnten wir keine Methylierung des *PLK2* Promoters nachweisen. Die Herunterregulation der *PLK2* mRNA-Expression bzw. die Induktion der Promotermethylierung konnten in humanen kardialen Fibroblasten durch Exposition gegenüber chronischer Hypoxie (1% O_2) experimentell herbeigeführt werden. Pharmakologische Inhibition und der genetische Knockout (KO) von *PLK2* gingen *in vitro* mit erniedrigter Proliferation aber gesteigerter Differenzierung in Myofibroblasten einher. *PLK2*-KO-Mäuse entwickelten im Gegensatz zu ihren *Wildtyp*-Geschwistertieren ausgeprägte Areale interstitieller ventrikulärer Fibrose. Dies spiegelte sich in einer ausgeprägten systolischen und Diastolischen Funktionsstörung des Herzens bei 4 Monate-alten PLK2 KO Tieren wider. Die Sekretomanalyse deckte eine *de novo* Sekretion von OPN in PLK2-KO-Fibroblasten auf. Im Einklang mit diesem Ergebnis konnten wir höhere OPN-Plasmaspiegel auch bei VHF-Patienten messen, die mit dem Vorhandensein von elektrophysiologisch bestimmten Fibrosearealen korrelierte. Abschließend konnte der p42/44-MAPK-Signalweg als Bindeglied zwischen erniedrigter *PLK2*-Expression und erhöhter OPN-Freisetzung identifiziert werden. Verminderte PLK2 Expression beziehungsweise Aktivität gehen mit einer gesteigerten Proteinexpression und Phosphorylierung von p42/44 MAPK einher. P42/44 MAPK wiederum stimuliert dann die *OPN*-Transkription. Folgerichtig führte die Inhibition von p42/44 MAPK zu einer signifikant verminderten OPN-Expression. Um die Allgemeingültigkeit des PLK2-Signalweges für die Entstehung von Fibrose zu erforschen, wurde ein dermales Modell strahleninduzierter Fibrose benutzt. Darin bestätigten sich zum einen die Beobachtungen, die am Herzen gemacht wurden, und zum anderen führte der Einsatz von Mesalazin *in vitro* zu einer reduzierten p42 MAPK- und SMAD2 / 3-Phosphorylierung und damit zu einer deutlich verringerten OPN- und αSMA-Expression.

Schlussfolgerung. Fibroblasten von Patienten im permanenten Vorhofflimmern exprimieren weniger *PLK2* als Fibroblasten aus SR-Kontrollpatienten. Der Verlust der physiologischen PLK2-Aktivität geht mit ausgeprägten Veränderungen der Proliferation und Differenzierung von Fibroblasten im Herzen einher. Diese Veränderungen begünstigen eine profibrotische Situation auf Gewebeebene, welche durch die lokale als auch systemische Erhöhung des Plasmaosteopontins weiter begünstigt wird. Die vorliegende Studie identifiziert erstmalig PLK2 als neuen Regulator der Fibroblastenfunktion und Fibrose. Gleichzeitig stellen die Wiederherstellung des physiologischen Methylierungstatuses des *PLK2* Promoters oder die Inhibition von OPN mittels Mesalazin vielversprechende therapeutische Optionen im Kampf gegen die Fibrosierung des Herzmuskels dar. Die konkrete pharmakotherapeutische Umsetzbarkeit muss in künftigen Forschungsvorhaben überprüft werden.

7 References

Abouzed TK, Munesue S, Harashima A, Masuo Y, Kato Y, Khailo K, Yamamoto H, Yamamoto Y. 2016. Preventive Effect of Salicylate and Pyridoxamine on Diabetic Nephropathy. J Diabetes Res, 2016 DOI: 10.1155/2016/1786789.

Akay BN, Sanli H, Heper AO. 2010. Postirradiation linear morphoea. Clin Exp Dermatol, 35(4):e106-108 DOI: 10.1111/j.1365-2230.2009.03717.x.

Alberola-Ila J, Hernández-Hoyos G. 2003. The Ras/MAPK cascade and the control of positive selection. Immunological Reviews, 191(1):79–96 DOI: 10.1034/j.1600-065X.2003.00012.x.

Antzelevitch C, Burashnikov A. 2011. Overview of Basic Mechanisms of Cardiac Arrhythmia. Card Electrophysiol Clin, 3(1):23–45 DOI: 10.1016/j.ccep.2010.10.012.

Archambault V, Carmena M. 2012. Polo-like kinase-activating kinases. Cell Cycle, 11(8):1490–1495 DOI: 10.4161/cc.19724.

Ayrapetov MK, Xu C, Sun Y, Zhu K, Parmar K, D'Andrea AD, Price BD. 2011. Activation of Hif1α by the prolylhydroxylase inhibitor dimethyoxalyglycine decreases radiosensitivity. PLoS ONE, 6(10):e26064 DOI: 10.1371/journal.pone.0026064.

Bainbridge P. 2013. Wound healing and the role of fibroblasts. J Wound Care, 22(8):407–408, 410–412 DOI: 10.12968/jowc.2013.22.8.407.

Baudino TA, Carver W, Giles W, Borg TK. 2006. Cardiac fibroblasts: friend or foe? Am J Physiol Heart Circ Physiol, 291(3):H1015-1026 DOI: 10.1152/ajpheart.00023.2006.

Baum J, Duffy HS. 2011. Fibroblasts and myofibroblasts: what are we talking about? J Cardiovasc Pharmacol, 57(4):376–379 DOI: 10.1097/FJC.0b013e3182116e39.

Bechtel W, McGoohan S, Zeisberg EM, Müller GA, Kalbacher H, Salant DJ, Müller CA, Kalluri R, Zeisberg M. 2010. Methylation determines fibroblast activation and fibrogenesis in the kidney. Nat Med, 16(5):544–550 DOI: 10.1038/nm.2135.

Beck GR, Knecht N. 2003. Osteopontin regulation by inorganic phosphate is ERK1/2-, protein kinase C-, and proteasome-dependent. J Biol Chem, 278(43):41921–41929 DOI: 10.1074/jbc.M304470200.

Benetatos L, Dasoula A, Hatzimichael E, Syed N, Voukelatou M, Dranitsaris G, Bourantas KL, Crook T. 2011. Polo-like kinase 2 (SNK/PLK2) is a novel epigenetically regulated gene in acute myeloid leukemia and myelodysplastic syndromes: genetic and epigenetic interactions. Ann Hematol, 90(9):1037–1045 DOI: 10.1007/s00277-011-1193-4.

Biernacka A, Frangogiannis NG. 2011. Aging and Cardiac Fibrosis. Aging Dis, 2(2):158–173.

Bonner JC, Badgett A, Osornio-Vargas AR, Hoffman M, Brody AR. 1990. PDGF-stimulated fibroblast proliferation is enhanced synergistically by receptor-recognized alpha 2-macroglobulin. J Cell Physiol, 145(1):1–8 DOI: 10.1002/jcp.1041450102.

Boos CJ, Anderson RA, Lip GYH. 2006. Is atrial fibrillation an inflammatory disorder? Eur Heart J, 27(2):136–149 DOI: 10.1093/eurheartj/ehi645.

Boos CJ, Lip GYH. The role of inflammation in atrial fibrillation. International Journal of Clinical Practice, 59(8):870–872 DOI: 10.1111/j.1368-5031.2005.0599b.x.

Bouabe H, Okkenhaug K. 2013. Gene Targeting in Mice: a Review. Methods Mol Biol, 1064:315–336 DOI: 10.1007/978-1-62703-601-6_23.

Burlew BS, Weber KT. 2002. Cardiac fibrosis as a cause of diastolic dysfunction. Herz, 27(2):92–98.

Burns TF, Fei P, Scata KA, Dicker DT, El-Deiry WS. 2003a. Silencing of the novel p53 target gene Snk/Plk2 leads to mitotic catastrophe in paclitaxel (taxol)-exposed cells. Mol Cell Biol, 23(16):5556–5571.

Burns TF, Fei P, Scata KA, Dicker DT, El-Deiry WS. 2003b. Silencing of the novel p53 target gene Snk/Plk2 leads to mitotic catastrophe in paclitaxel (taxol)-exposed cells. Mol Cell Biol, 23(16):5556–5571.

Calkins H, Hindricks G, Cappato R, Kim Y-H, Saad EB, Aguinaga L, Akar JG, Badhwar V, Brugada J, Camm J, Chen P-S, Chen S-A, Chung MK, Nielsen JC, Curtis AB, Wyn Davies D, Day JD, d'Avila A, de Groot NMS (Natasja), Di Biase L, Duytschaever M, Edgerton JR, Ellenbogen KA, Ellinor PT, Ernst S, Fenelon G, Gerstenfeld EP, Haines DE, Haissaguerre M, Helm RH, Hylek E, Jackman WM, Jalife J, Kalman JM, Kautzner J, Kottkamp H, Kuck KH, Kumagai K, Lee R, Lewalter T, Lindsay BD, Macle L, Mansour M, Marchlinski FE, Michaud GF, Nakagawa H, Natale A, Nattel S, Okumura K, Packer D, Pokushalov E, Reynolds MR, Sanders P, Scanavacca M, Schilling R, Tondo C, Tsao H-M, Verma A, Wilber DJ, Yamane T. 2017. 2017 HRS/EHRA/ECAS/APHRS/SOLAECE expert consensus statement on catheter and surgical ablation of atrial fibrillation: executive summary. J Interv Card Electrophysiol, 50(1):1–55 DOI: 10.1007/s10840-017-0277-z.

Calvo D, Filgueiras-Rama D, Jalife J. 2018. Mechanisms and Drug Development in Atrial Fibrillation. Pharmacol Rev, 70(3):505–525 DOI: 10.1124/pr.117.014183.

Camelliti P, Borg TK, Kohl P. 2005. Structural and functional characterisation of cardiac fibroblasts. Cardiovasc Res, 65(1):40–51 DOI: 10.1016/j.cardiores.2004.08.020.

de Cárcer G, Manning G, Malumbres M. 2011. From Plk1 to Plk5. Cell Cycle, 10(14):2255–2262 DOI: 10.4161/cc.10.14.16494.

Cheng S, Keyes MJ, Larson MG, McCabe EL, Newton-Cheh C, Levy D, Benjamin EJ, Vasan RS, Wang TJ. 2009. Long-term Outcomes in Individuals with a Prolonged PR Interval or First-Degree Atrioventricular Block. JAMA, 301(24):2571–2577 DOI: 10.1001/jama.2009.888.

Cholewa BD, Liu X, Ahmad N. 2013. The role of polo-like kinase 1 in carcinogenesis: cause or consequence? Cancer Res, 73(23):6848–6855 DOI: 10.1158/0008-5472.CAN-13-2197.

Chung MK, Martin DO, Sprecher D, Wazni O, Kanderian A, Carnes CA, Bauer JA, Tchou PJ, Niebauer MJ, Natale A, Van Wagoner DR. 2001. C-reactive protein elevation in patients with atrial arrhythmias: inflammatory mechanisms and persistence of atrial fibrillation. Circulation, 104(24):2886–2891.

Cizmecioglu O, Krause A, Bahtz R, Ehret L, Malek N, Hoffmann I. 2012. Plk2 regulates centriole duplication through phosphorylation-mediated degradation of Fbxw7 (human Cdc4). J Cell Sci, 125(Pt 4):981–992 DOI: 10.1242/jcs.095075.

Cizmecioglu O, Warnke S, Arnold M, Duensing S, Hoffmann I. 2008. Plk2 regulated centriole duplication is dependent on its localization to the centrioles and a functional polo-box domain. Cell Cycle, 7(22):3548–3555 DOI: 10.4161/cc.7.22.7071.

Clay FJ, McEwen SJ, Bertoncello I, Wilks AF, Dunn AR. 1993. Identification and cloning of a protein kinase-encoding mouse gene, Plk, related to the polo gene of Drosophila. PNAS, 90(11):4882–4886.

Coley HM, Hatzimichael E, Blagden S, McNeish I, Thompson A, Crook T, Syed N. 2012a. Polo Like Kinase 2 Tumour Suppressor and cancer biomarker: new perspectives on drug sensitivity/resistance in cancer. Oncotarget, 3(1):78–83.

Coley HM, Hatzimichael E, Blagden S, McNeish I, Thompson A, Crook T, Syed N. 2012b. Polo Like Kinase 2 Tumour Suppressor and cancer biomarker: new perspectives on drug sensitivity/resistance in ovarian cancer. Oncotarget, 3(1):78–83.

Colilla S, Crow A, Petkun W, Singer DE, Simon T, Liu X. 2013. Estimates of current and future incidence and prevalence of atrial fibrillation in the U.S. adult population. Am J Cardiol, 112(8):1142–1147 DOI: 10.1016/j.amjcard.2013.05.063.

Collins AL, Rock J, Malhotra L, Frankel WL, Bloomston M. 2012. Osteopontin expression is associated with improved survival in patients with pancreatic adenocarcinoma. Ann Surg Oncol, 19(8):2673–2678 DOI: 10.1245/s10434-012-2337-z.

Conrad GW, Hart GW, Chen Y. 1977. Differences in vitro between fibroblast-like cells from cornea, heart, and skin of embryonic chicks. Journal of Cell Science, 26(1):119–137.

Cooper GM. 2000. Regulation of Transcription in Eukaryotes. In: The Cell: A Molecular Approach. 2nd edition. [Aufruf am: 06.07.2018] URL: https://www.ncbi.nlm.nih.gov/books/NBK9904/.

Coppé J-P, Patil CK, Rodier F, Sun Y, Muñoz DP, Goldstein J, Nelson PS, Desprez P-Y, Campisi J. 2008. Senescence-associated secretory phenotypes reveal cell-nonautonomous functions of oncogenic RAS and the p53 tumor suppressor. PLoS Biol, 6(12):2853–2868 DOI: 10.1371/journal.pbio.0060301.

Cowling RT. 2015. The aging heart, endothelin-1 and the senescent cardiac fibroblast. J Mol Cell Cardiol, 81:12–14 DOI: 10.1016/j.yjmcc.2015.01.018.

Cyganek L, Tiburcy M, Sekeres K, Gerstenberg K, Bohnenberger H, Lenz C, Henze S, Stauske M, Salinas G, Zimmermann W-H, Hasenfuss G, Guan K. 2018. Deep phenotyping of human induced pluripotent stem cell–derived atrial and ventricular cardiomyocytes. JCI Insight, 3(12) DOI: 10.1172/jci.insight.99941.

Das A, Monteiro M, Barai A, Kumar S, Sen S. 2017. MMP proteolytic activity regulates cancer invasiveness by modulating integrins. Scientific Reports, 7(1):14219 DOI: 10.1038/s41598-017-14340-w.

Deng S, Wang H, Jia C, Zhu S, Chu X, Ma Q, Wei J, Chen E, Zhu W, Macon CJ, Jayaweera DT, Dykxhoorn DM, Dong C. 2017. MicroRNA-146a Induces Lineage-Negative Bone Marrow Cell Apoptosis and Senescence by Targeting Polo-Like Kinase 2 Expression. Arterioscler Thromb Vasc Biol, 37(2):280–290 DOI: 10.1161/ATVBAHA.116.308378.

Dixon IMC, Davies JJL. 2011. Fibroblasts are coupled to myocytes in heart muscle by nanotubes: a bigger and better syncytium? Cardiovasc Res, 92(1):5–6 DOI: 10.1093/cvr/cvr216.

Doppler SA, Carvalho C, Lahm H, Deutsch M-A, Dreßen M, Puluca N, Lange R, Krane M. 2017. Cardiac fibroblasts: more than mechanical support. J Thorac Dis, 9(Suppl 1):S36–S51 DOI: 10.21037/jtd.2017.03.122.

El-Armouche A, Wittköpper K, Degenhardt F, Weinberger F, Didié M, Melnychenko I, Grimm M, Peeck M, Zimmermann WH, Unsöld B, Hasenfuss G, Dobrev D, Eschenhagen T. 2008. Phosphatase inhibitor-1-deficient mice are protected from catecholamine-induced arrhythmias and myocardial hypertrophy. Cardiovasc Res, 80(3):396–406 DOI: 10.1093/cvr/cvn208.

El-Tanani MK, Campbell FC, Kurisetty V, Jin D, McCann M, Rudland PS. 2006. The regulation and role of osteopontin in malignant transformation and cancer. Cytokine Growth Factor Rev, 17(6):463–474 DOI: 10.1016/j.cytogfr.2006.09.010.

Fan Z, Guan J. 2016. Antifibrotic therapies to control cardiac fibrosis. Biomater Res, 20 DOI: 10.1186/s40824-016-0060-8.

Fang L, Murphy AJ, Dart AM. 2017. A Clinical Perspective of Anti-Fibrotic Therapies for Cardiovascular Disease. Front Pharmacol, 8 DOI: 10.3389/fphar.2017.00186.

Gabbiani G. 2003. The myofibroblast in wound healing and fibrocontractive diseases. J Pathol, 200(4):500–503 DOI: 10.1002/path.1427.

Gao Y, Chu M, Hong J, Shang J, Xu D. 2014. Hypoxia induces cardiac fibroblast proliferation and phenotypic switch: a role for caveolae and caveolin-1/PTEN mediated pathway. J Thorac Dis, 6(10):1458–1468 DOI: 10.3978/j.issn.2072-1439.2014.08.31.

Georgescu SP, Komuro I, Hiroi Y, Mizuno T, Kudoh S, Yamazaki T, Yazaki Y. 1997. Downregulation of Polo-like Kinase Correlates with Loss of Proliferative Ability of Cardiac Myocytes. Journal of Molecular and Cellular Cardiology, 29(3):929–937 DOI: 10.1006/jmcc.1996.0334.

Geschka S, Kretschmer A, Sharkovska Y, Evgenov OV, Lawrenz B, Hucke A, Hocher B, Stasch J-P. 2011. Soluble guanylate cyclase stimulation prevents fibrotic tissue remodeling and improves survival in salt-sensitive Dahl rats. PLoS ONE, 6(7):e21853 DOI: 10.1371/journal.pone.0021853.

Gheorghiade M, Marti CN, Sabbah HN, Roessig L, Greene SJ, Böhm M, Burnett JC, Campia U, Cleland JGF, Collins SP, Fonarow GC, Levy PD, Metra M, Pitt B, Ponikowski P, Sato N, Voors AA, Stasch J-P, Butler J, Academic Research Team in Heart Failure (ART-HF). 2013. Soluble guanylate cyclase: a potential therapeutic target for heart failure. Heart Fail Rev, 18(2):123–134 DOI: 10.1007/s10741-012-9323-1.

Gigliotti JN, Sidhu MS, Robert AM, Zipursky JS, Brown JR, Costa SP, Palac RT, Steckman DA, Malenka DJ, Kono AT, Greenberg ML. 2017. The association of QRS duration with atrial fibrillation in a heart failure with preserved ejection fraction population: a pilot study. Clinical Cardiology, 40(10):861–864 DOI: 10.1002/clc.22736.

Glover DM, Hagan IM, Tavares ÁAM. 1998. Polo-like kinases: a team that plays throughout mitosis. Genes Dev, 12(24):3777–3787 DOI: 10.1101/gad.12.24.3777.

Goldsmith EC, Hoffman A, Morales MO, Potts JD, Price RL, McFadden A, Rice M, Borg TK. 2004. Organization of fibroblasts in the heart. Dev Dyn, 230(4):787–794 DOI: 10.1002/dvdy.20095.

Goncalves I, Bengtsson E, Colhoun HM, Shore AC, Palombo C, Natali A, Edsfeldt A, Dunér P, Fredrikson GN, Björkbacka H, Östling G, Aizawa K, Casanova F, Persson M, Gooding K, Strain D, Khan F, Looker HC, Adams F, Belch J, Pinnoli S, Venturi E, Kozakova M, Gan L-M, Schnecke V, Nilsson J, SUMMIT Consortium. 2015. Elevated Plasma Levels of MMP-12 Are Associated With Atherosclerotic Burden and Symptomatic Cardiovascular Disease in Subjects With Type 2 Diabetes. Arterioscler Thromb Vasc Biol, 35(7):1723–1731 DOI: 10.1161/ATVBAHA.115.305631.

Gramley F, Lorenzen J, Jedamzik B, Gatter K, Koellensperger E, Munzel T, Pezzella F. 2010. Atrial fibrillation is associated with cardiac hypoxia. Cardiovasc Pathol, 19(2):102–111 DOI: 10.1016/j.carpath.2008.11.001.

de Groot N, van der Does L, Yaksh A, Lanters E, Teuwen C, Knops P, van de Woestijne P, Bekkers J, Kik C, Bogers A, Allessie M. 2016. Direct Proof of Endo-Epicardial Asynchrony of the Atrial Wall During Atrial Fibrillation in Humans. Circ Arrhythm Electrophysiol, 9(5) DOI: 10.1161/CIRCEP.115.003648.

Guan L, Song Y, Gao Jian, Gao Jianjun, Wang K. 2016. Inhibition of calcium-activated chloride channel ANO1 suppresses proliferation and induces apoptosis of epithelium originated cancer cells. Oncotarget, 7(48):78619–78630 DOI: 10.18632/oncotarget.12524.

Guillen J. 2012. FELASA Guidelines and Recommendations. J Am Assoc Lab Anim Sci, 51(3):311–321.

Güneş HM, Babur Güler G, Güler E, Demir GG, Kızılırmak Yılmaz F, Omaygenç MO, İstanbullu Tosun A, Akgün T, Boztosun B, Kılıçarslan F. 2017. Relationship between serum osteopontin level and atrial fibrillation recurrence in patients undergoing cryoballoon catheter ablation. Turk Kardiyol Dern Ars, 45(1):26–32.

Gutteridge REA, Ndiaye MA, Liu X, Ahmad N. 2016. Plk1 Inhibitors in Cancer Therapy: From Laboratory to Clinics. Mol Cancer Ther, 15(7):1427–1435 DOI: 10.1158/1535-7163.MCT-15-0897.

Hadi HA, Alsheikh-Ali AA, Mahmeed WA, Suwaidi JMA. 2010. Inflammatory cytokines and atrial fibrillation: current and prospective views. J Inflamm Res, 3:75–97 DOI: 10.2147/JIR.S10095.

Hanna N, Cardin S, Leung T-K, Nattel S. 2004. Differences in atrial versus ventricular remodeling in dogs with ventricular tachypacing-induced congestive heart failure. Cardiovasc Res, 63(2):236–244 DOI: 10.1016/j.cardiores.2004.03.026.

He X, Dai J, Fan Y, Zhang C, Zhao X. 2017. Regulation function of MMP-1 downregulated by siRNA on migration of heat-denatured dermal fibroblasts. Bioengineered, 8(6):686–692 DOI: 10.1080/21655979.2016.1267885.

Heijman J, Guichard J-B, Dobrev D, Nattel S. 2018. Translational Challenges in Atrial Fibrillation. Circ Res, 122(5):752–773 DOI: 10.1161/CIRCRESAHA.117.311081.

Hickey FB, England K, Cotter TG. 2005. Bcr-Abl regulates osteopontin transcription via Ras, PI-3K, aPKC, Raf-1, and MEK. J Leukoc Biol, 78(1):289–300 DOI: 10.1189/jlb.1104655.

Hu B, Phan SH. 2013. Myofibroblasts. Curr Opin Rheumatol, 25(1):71–77 DOI: 10.1097/BOR.0b013e32835b1352.

Hu Y-F, Chen Y-J, Lin Y-J, Chen S-A. 2015. Inflammation and the pathogenesis of atrial fibrillation. Nat Rev Cardiol, 12(4):230–243 DOI: 10.1038/nrcardio.2015.2.

Inglis KJ, Chereau D, Brigham EF, Chiou S-S, Schöbel S, Frigon NL, Yu M, Caccavello RJ, Nelson S, Motter R, Wright S, Chian D, Santiago P, Soriano F, Ramos C, Powell K, Goldstein JM, Babcock M, Yednock T, Bard F, Basi GS, Sham H, Chilcote TJ, McConlogue L, Griswold-Prenner I, Anderson JP. 2009. Polo-like kinase 2 (PLK2) phosphorylates alpha-synuclein at serine 129 in central nervous system. J Biol Chem, 284(5):2598–2602 DOI: 10.1074/jbc.C800206200.

Issa J-PJ, Kantarjian HM. 2009. Targeting DNA Methylation. Clin Cancer Res, 15(12):3938–3946 DOI: 10.1158/1078-0432.CCR-08-2783.

Ivey MJ, Tallquist MD. 2016. Defining the Cardiac Fibroblast. Circ J, 80(11):2269–2276 DOI: 10.1253/circj.CJ-16-1003.

Jacobsen KS, Zeeberg K, Sauter DRP, Poulsen KA, Hoffmann EK, Schwab A. 2013. The role of TMEM16A (ANO1) and TMEM16F (ANO6) in cell migration. Pflugers Arch, 465(12):1753–1762 DOI: 10.1007/s00424-013-1315-z.

Jain N, Kalailingam P, Tan KW, Tan HB, Sng MK, Chan JSK, Tan NS, Thanabalu T. 2016. Conditional knockout of N-WASP in mouse fibroblast caused keratinocyte hyper proliferation and enhanced wound closure. Scientific Reports, 6:38109 DOI: 10.1038/srep38109.

Jalife J, Berenfeld O, Mansour M. 2002. Mother rotors and fibrillatory conduction: a mechanism of atrial fibrillation. Cardiovasc Res, 54(2):204–216.

Jeong SB, Im JH, Yoon J-H, Bui QT, Lim SC, Song JM, Shim Y, Yun J, Hong J, Kang KW. 2018. Essential Role of Polo-like Kinase 1 (Plk1) Oncogene in Tumor Growth and Metastasis of Tamoxifen-Resistant Breast Cancer. Mol Cancer Ther, 17(4):825–837 DOI: 10.1158/1535-7163.MCT-17-0545.

Jones SA, Yamamoto M, Tellez JO, Billeter R, Boyett MR, Honjo H, Lancaster MK. 2008. Distinguishing properties of cells from the myocardial sleeves of the pulmonary veins: a comparison of normal and abnormal pacemakers. Circ Arrhythm Electrophysiol, 1(1):39–48 DOI: 10.1161/CIRCEP.107.748467.

Jordana M, Särnstrand B, Sime PJ, Ramis I. 1994. Immune-inflammatory functions of fibroblasts. Eur Respir J, 7(12):2212–2222.

Kanisicak O, Khalil H, Ivey MJ, Karch J, Maliken BD, Correll RN, Brody MJ, Lin S-CJ, Aronow BJ, Tallquist MD, Molkentin JD. 2016. Genetic lineage tracing defines myofibroblast origin and function in the injured heart. Nature Communications, 7:12260 DOI: 10.1038/ncomms12260.

Kazemian P, Oudit G, Jugdutt BI. 2012. Atrial fibrillation and heart failure in the elderly. Heart Fail Rev, 17(4–5):597–613 DOI: 10.1007/s10741-011-9290-y.

Keating ST, Plutzky J, El-Osta A. 2016. Epigenetic Changes in Diabetes and Cardiovascular Risk. Circ Res, 118(11):1706–1722 DOI: 10.1161/CIRCRESAHA.116.306819.

Kendall RT, Feghali-Bostwick CA. 2014. Fibroblasts in fibrosis: novel roles and mediators. Front Pharmacol, 5:123 DOI: 10.3389/fphar.2014.00123.

Kim JH, Lee JO, Lee SK, Kim N, You GY, Moon JW, Sha J, Kim SJ, Park SH, Kim HS. 2013. Celastrol suppresses breast cancer MCF-7 cell viability via the AMP-activated protein kinase (AMPK)-induced p53-polo like kinase 2 (PLK-2) pathway. Cell Signal, 25(4):805–813 DOI: 10.1016/j.cellsig.2012.12.005.

Kirchhof P, Ammentorp B, Darius H, De Caterina R, Le Heuzey J-Y, Schilling RJ, Schmitt J, Zamorano JL. 2014. Management of atrial fibrillation in seven European countries after the publication of the 2010 ESC Guidelines on atrial fibrillation: primary results of the PREvention oF thromboemolic events--European Registry in Atrial Fibrillation (PREFER in AF). Europace, 16(1):6–14 DOI: 10.1093/europace/eut263.

Kirchhof P, Benussi S, Kotecha D, Ahlsson A, Atar D, Casadei B, Castella M, Diener H-C, Heidbuchel H, Hendriks J, Hindricks G, Manolis AS, Oldgren J, Popescu BA, Schotten U, Van Putte B, Vardas P, Agewall S, Camm J, Baron Esquivias G, Budts W, Carerj S, Casselman F, Coca A, De Caterina R, Deftereos S, Dobrev D, Ferro JM, Filippatos G, Fitzsimons D, Gorenek B, Guenoun M, Hohnloser SH, Kolh P, Lip GYH, Manolis A, McMurray J, Ponikowski P, Rosenhek R, Ruschitzka F, Savelieva I, Sharma S, Suwalski P, Tamargo JL, Taylor CJ, Van Gelder IC, Voors AA, Windecker S, Zamorano JL, Zeppenfeld K. 2016. 2016 ESC Guidelines for the management of atrial fibrillation developed in collaboration with EACTS. Eur J Cardiothorac Surg, 50(5):e1–e88 DOI: 10.1093/ejcts/ezw313.

Klesen A, Jakob D, Emig R, Kohl P, Ravens U, Peyronnet R. 2018. Cardiac fibroblasts : Active players in (atrial) electrophysiology? Herzschrittmacherther Elektrophysiol, 29(1):62–69 DOI: 10.1007/s00399-018-0553-3.

Kotecha D, Lam CSP, Van Veldhuisen DJ, Van Gelder IC, Voors AA, Rienstra M. 2016. Heart Failure With Preserved Ejection Fraction and Atrial Fibrillation: Vicious Twins. J Am Coll Cardiol, 68(20):2217–2228 DOI: 10.1016/j.jacc.2016.08.048.

Kuenzel SR, Sekeres K, Kaemmerer S, Kolanowski T, Meyer-Roxlau S, Piorkowski C, Tugtekin SM, Rose-John S, Yin X, Mayr M, Kuhlmann JD, Wimberger P, Gruetzmann K, Herzog N, Kuepper J-H, Guan K, Wagner M, Ravens U, Weber S, El-Armouche A. 2018. Hypoxia-induced epigenetic silencing of polo-like kinase 2 promotes fibrosis in atrial fibrillation. bioRxiv:445098 DOI: 10.1101/445098.

Künzel S. 2014. The regulatory role of Kv channels in fibroblasts isolated from patients in Sinus Rhythm and with chronic atrial fibrillation. Technische Universität Dresden, Dresden, Dissertation.

Lee KJ, Hoe H-S, Pak DT. 2011. Plk2 Raps up Ras to subdue synapses. Small GTPases, 2(3):162–166 DOI: 10.4161/sgtp.2.3.16454.

Lee KJ, Lee Y, Rozeboom A, Lee J-Y, Udagawa N, Hoe H-S, Pak DTS. 2011. Requirement for Plk2 in orchestrated ras and rap signaling, homeostatic structural plasticity, and memory. Neuron, 69(5):957–973 DOI: 10.1016/j.neuron.2011.02.004.

Li L, Deng B, Xing G, Teng Y, Tian C, Cheng X, Yin X, Yang J, Gao X, Zhu Y, Sun Q, Zhang L, Yang X, He F. 2007. PACT is a negative regulator of p53 and essential for cell growth and embryonic development. Proc Natl Acad Sci USA, 104(19):7951–7956 DOI: 10.1073/pnas.0701916104.

Lim DHK, Maher ER. 2010. DNA methylation: a form of epigenetic control of gene expression. The Obstetrician & Gynaecologist, 12(1):37–42 DOI: 10.1576/toag.12.1.037.27556.

Liu J, Xu K, Chase M, Ji Y, Logan JK, Buchsbaum RJ. 2012. Tiam1-regulated osteopontin in senescent fibroblasts contributes to the migration and invasion of associated epithelial cells. J Cell Sci, 125(Pt 2):376–386 DOI: 10.1242/jcs.089466.

Liu LY, Wang W, Zhao LY, Guo B, Yang J, Zhao XG, Hou N, Ni L, Wang AY, Song TS, Huang C, Xu JR. 2014. Mir-126 inhibits growth of SGC-7901 cells by synergistically targeting the oncogenes PI3KR2 and Crk, and the tumor suppressor PLK2. Int J Oncol, 45(3):1257–1265 DOI: 10.3892/ijo.2014.2516.

Liu X. 2015. Targeting Polo-Like Kinases: A Promising Therapeutic Approach for Cancer Treatment. Transl Oncol, 8(3):185–195 DOI: 10.1016/j.tranon.2015.03.010.

Lu Z, Nie L, He B, Yu L, Salim M, Huang B, Cui B, He W, Wu W, Jiang H. 2013. Increase in vulnerability of atrial fibrillation in an acute intermittent hypoxia model: importance of autonomic imbalance. Auton Neurosci, 177(2):148–153 DOI: 10.1016/j.autneu.2013.03.014.

Lugenbiel P, Wenz F, Govorov K, Syren P, Katus HA, Thomas D. 2017. Atrial myofibroblast activation and connective tissue formation in a porcine model of atrial fibrillation and reduced left ventricular function. Life Sci, 181:1–8 DOI: 10.1016/j.lfs.2017.05.025.

Ma S, Charron J, Erikson RL. 2003. Role of Plk2 (Snk) in mouse development and cell proliferation. Mol Cell Biol, 23(19):6936–6943.

Mandinov L, Eberli FR, Seiler C, Hess OM. 2000. Diastolic heart failure. Cardiovasc Res, 45(4):813–825 DOI: 10.1016/S0008-6363(99)00399-5.

March JT, Golshirazi G, Cernisova V, Carr H, Leong Y, Lu-Nguyen N, Popplewell LJ. 2018. Targeting TGFβ Signaling to Address Fibrosis Using Antisense Oligonucleotides. Biomedicines, 6(3):74 DOI: 10.3390/biomedicines6030074.

Marulanda-Londoño E, Chaturvedi S. 2017. The Interplay between Obstructive Sleep Apnea and Atrial Fibrillation. Front Neurol, 8 DOI: 10.3389/fneur.2017.00668.

Mastrofrancesco A, Kovacs D, Sarra M, Bastonini E, Cardinali G, Aspite N, Camera E, Chavatte P, Desreumaux P, Monteleone G, Picardo M. 2014. Preclinical studies of a specific PPARγ modulator in the control of skin inflammation. J Invest Dermatol, 134(4):1001–1011 DOI: 10.1038/jid.2013.448.

Masur SK, Dewal HS, Dinh TT, Erenburg I, Petridou S. 1996. Myofibroblasts differentiate from fibroblasts when plated at low density. Proc Natl Acad Sci USA, 93(9):4219–4223.

Midwood KS, Williams LV, Schwarzbauer JE. 2004. Tissue repair and the dynamics of the extracellular matrix. Int J Biochem Cell Biol, 36(6):1031–1037 DOI: 10.1016/j.biocel.2003.12.003.

Miyasaka Y, Barnes ME, Gersh BJ, Cha SS, Bailey KR, Abhayaratna WP, Seward JB, Tsang TSM. 2006. Secular trends in incidence of atrial fibrillation in Olmsted County, Minnesota, 1980 to 2000, and implications on the projections for future prevalence. Circulation, 114(2):119–125 DOI: 10.1161/CIRCULATIONAHA.105.595140.

Mochizuki M, Lorenz V, Ivanek R, Della Verde G, Gaudiello E, Marsano A, Pfister O, Kuster GM. 2017. Polo-Like Kinase 2 is Dynamically Regulated to Coordinate Proliferation and Early Lineage Specification Downstream of Yes-Associated Protein 1 in Cardiac Progenitor Cells. J Am Heart Assoc, 6(10) DOI: 10.1161/JAHA.117.005920.

Moreo Antonella, Ambrosio Giuseppe, De Chiara Benedetta, Pu Min, Tran Tam, Mauri Francesco, Raman Subha V. 2009. Influence of Myocardial Fibrosis on Left Ventricular Diastolic Function. Circulation: Cardiovascular Imaging, 2(6):437–443 DOI: 10.1161/CIRCIMAGING.108.838367.

Moschos SJ, Sullivan RJ, Hwu W-J, Ramanathan RK, Adjei AA, Fong PC, Shapira-Frommer R, Tawbi HA, Rubino J, Rush TS, Zhang D, Miselis NR, Samatar AA, Chun P, Rubin EH, Schiller J, Long BJ, Dayananth P, Carr D, Kirschmeier P, Bishop WR, Deng Y, Cooper A, Shipps GW, Moreno BH, Robert L, Ribas A, Flaherty KT. 2018. Development of MK-8353, an orally administered ERK1/2 inhibitor, in patients with advanced solid tumors. JCI Insight, 3(4) DOI: 10.1172/jci.insight.92352.

Nag AC. 1980. Study of non-muscle cells of the adult mammalian heart: a fine structural analysis and distribution. Cytobios, 28(109):41–61.

Nakaya M, Watari K, Tajima M, Nakaya T, Matsuda S, Ohara H, Nishihara H, Yamaguchi H, Hashimoto A, Nishida M, Nagasaka A, Horii Y, Ono H, Iribe G, Inoue R, Tsuda M, Inoue K, Tanaka A, Kuroda M, Nagata S, Kurose H. 2017. Cardiac myofibroblast engulfment of dead cells facilitates recovery after myocardial infarction. J Clin Invest, 127(1):383–401 DOI: 10.1172/JCI83822.

Nattel S, Burstein B, Dobrev D. 2008. Atrial remodeling and atrial fibrillation: mechanisms and implications. Circ Arrhythm Electrophysiol, 1(1):62–73 DOI: 10.1161/CIRCEP.107.754564.

Nattel S, Harada M. 2014. Atrial remodeling and atrial fibrillation: recent advances and translational perspectives. J Am Coll Cardiol, 63(22):2335–2345 DOI: 10.1016/j.jacc.2014.02.555.

Nihoyannopoulos P, Dawson D. 2009. Restrictive cardiomyopathies. European Heart Journal - Cardiovascular Imaging, 10(8):iii23–iii33 DOI: 10.1093/ejechocard/jep156.

Noda M. 1989. Transcriptional regulation of osteopontin production in rat osteoblast- like cells by parathyroid hormone. J Cell Biol, 108(2):713–718.

Omelchenko T, Vasiliev JM, Gelfand IM, Feder HH, Bonder EM. 2002. Mechanisms of polarization of the shape of fibroblasts and epitheliocytes: Separation of the roles of

microtubules and Rho-dependent actin–myosin contractility. PNAS, 99(16):10452–10457 DOI: 10.1073/pnas.152339899.

Opacic D, van Bragt KA, Nasrallah HM, Schotten U, Verheule S. 2016. Atrial metabolism and tissue perfusion as determinants of electrical and structural remodelling in atrial fibrillation. Cardiovasc Res, 109(4):527–541 DOI: 10.1093/cvr/cvw007.

Ou B, Zhao J, Guan S, Wangpu X, Zhu C, Zong Y, Ma J, Sun J, Zheng M, Feng H, Lu A. 2016. Plk2 promotes tumor growth and inhibits apoptosis by targeting Fbxw7/Cyclin E in colorectal cancer. Cancer Lett, 380(2):457–466 DOI: 10.1016/j.canlet.2016.07.004.

Pardo A, Gibson K, Cisneros J, Richards TJ, Yang Y, Becerril C, Yousem S, Herrera I, Ruiz V, Selman M, Kaminski N. 2005. Up-regulation and profibrotic role of osteopontin in human idiopathic pulmonary fibrosis. PLoS Med, 2(9):e251 DOI: 10.1371/journal.pmed.0020251.

Park J-E, Soung N-K, Yoshikazu J, Kang YH, Liao C, Lee KH, Park CH, Nicklaus MC, Lee KS. 2010. Polo-Box Domain: a versatile mediator of polo-like kinase function. Cell Mol Life Sci, 67(12):1957–1970 DOI: 10.1007/s00018-010-0279-9.

Petrov VV, Fagard RH, Lijnen PJ. 2002. Stimulation of collagen production by transforming growth factor-beta1 during differentiation of cardiac fibroblasts to myofibroblasts. Hypertension, 39(2):258–263.

Pfeffer JM, Fischer TA, Pfeffer MA. 1995. Angiotensin-converting enzyme inhibition and ventricular remodeling after myocardial infarction. Annu Rev Physiol, 57:805–826 DOI: 10.1146/annurev.ph.57.030195.004105.

Pinto AR, Ilinykh A, Ivey MJ, Kuwabara JT, D'Antoni ML, Debuque R, Chandran A, Wang L, Arora K, Rosenthal NA, Tallquist MD. 2016. Revisiting Cardiac Cellular Composition. Circ Res, 118(3):400–409 DOI: 10.1161/CIRCRESAHA.115.307778.

Piorkowski C, Arya A, Markovitz CD, Razavi H, Jiang C, Rosenberg S, Breithardt O-A, Rolf S, John S, Kosiuk J, Huo Y, Döring M, Richter S, Ryu K, Gaspar T, Prinzen FW, Hindricks G, Sommer P. 2018. Characterizing left ventricular mechanical and electrical activation in patients with normal and impaired systolic function using a non-fluoroscopic cardiovascular navigation system. J Interv Card Electrophysiol, 51(3):205–214 DOI: 10.1007/s10840-018-0317-3.

Plumb JA, Strathdee G, Sludden J, Kaye SB, Brown R. 2000. Reversal of drug resistance in human tumor xenografts by 2'-deoxy-5-azacytidine-induced demethylation of the hMLH1 gene promoter. Cancer Res, 60(21):6039–6044.

Porter KE, Turner NA. 2009. Cardiac fibroblasts: at the heart of myocardial remodeling. Pharmacol Ther, 123(2):255–278 DOI: 10.1016/j.pharmthera.2009.05.002.

Poulet C, Stephan Künzel, Büttner E, Lindner D, Westermann D, Ravens U. 2016. Altered physiological functions and ion currents in atrial fibroblasts from patients with chronic atrial fibrillation. Physiol Rep, 4(2) DOI: 10.14814/phy2.12681.

Purcell NH, Wilkins BJ, York A, Saba-El-Leil MK, Meloche S, Robbins J, Molkentin JD. 2007. Genetic inhibition of cardiac ERK1/2 promotes stress-induced apoptosis and heart failure but has no effect on hypertrophy in vivo. Proc Natl Acad Sci U S A, 104(35):14074–14079 DOI: 10.1073/pnas.0610906104.

Quinn TA, Camelliti P, Rog-Zielinska EA, Siedlecka U, Poggioli T, O'Toole ET, Knöpfel T, Kohl P. 2016. Electrotonic coupling of excitable and nonexcitable cells in the heart revealed by optogenetics. Proc Natl Acad Sci USA, 113(51):14852–14857 DOI: 10.1073/pnas.1611184114.

Rai N, Veeroju S, Schymura Y, Janssen W, Wietelmann A, Kojonazarov B, Weissmann N, Stasch J-P, Ghofrani HA, Seeger W, Schermuly RT, Novoyatleva T. 2018. Effect of Riociguat and Sildenafil on Right Heart Remodeling and Function in Pressure Overload Induced Model of Pulmonary Arterial Banding. Biomed Res Int, 2018 DOI: 10.1155/2018/3293584.

Ramadan A, Afifi N, Yassin NZ, Abdel-Rahman RF, Abd El-Rahman SS, Fayed HM. 2018. Mesalazine, an osteopontin inhibitor: The potential prophylactic and remedial roles in induced liver fibrosis in rats. Chem Biol Interact, 289:109–118 DOI: 10.1016/j.cbi.2018.05.002.

Ravens PDU. 2014. Neue Entwicklungen in der antiarrhythmischen Therapie des Vorhofflimmerns. Herzschr Elektrophys, 25(1):41–46 DOI: 10.1007/s00399-014-0302-1.

Renault M.-A., Jalvy S., Belloc I., Pasquet S., Sena S., Olive M., Desgranges C., Gadeau A.-P. 2003. AP-1 Is Involved in UTP-Induced Osteopontin Expression in Arterial Smooth Muscle Cells. Circulation Research, 93(7):674–681 DOI: 10.1161/01.RES.0000094747.05021.62.

Rima M, Daghsni M, De Waard S, Gaborit N, Fajloun Z, Ronjat M, Mori Y, Brusés JL, De Waard M. 2017. The β4subunit of the voltage-gated calcium channel (Cacnb4) regulates the rate of cell proliferation in Chinese Hamster Ovary cells. Int J Biochem Cell Biol, 89:57–70 DOI: 10.1016/j.biocel.2017.05.032.

Rittling SR, Chambers AF. 2004. Role of osteopontin in tumour progression. Br J Cancer, 90(10):1877–1881 DOI: 10.1038/sj.bjc.6601839.

Robinson CM, Neary R, Levendale A, Watson CJ, Baugh JA. 2012. Hypoxia-induced DNA hypermethylation in human pulmonary fibroblasts is associated with Thy-1 promoter methylation and the development of a pro-fibrotic phenotype. Respir Res, 13:74 DOI: 10.1186/1465-9921-13-74.

Rodier F, Campisi J. 2011. Four faces of cellular senescence. J Cell Biol, 192(4):547–556 DOI: 10.1083/jcb.201009094.

Rog-Zielinska EA, Norris RA, Kohl P, Markwald R. 2016. The Living Scar--Cardiac Fibroblasts and the Injured Heart. Trends Mol Med, 22(2):99–114 DOI: 10.1016/j.molmed.2015.12.006.

Rosenbloom J, Mendoza FA, Jimenez SA. 2013. Strategies for anti-fibrotic therapies. Biochimica et Biophysica Acta (BBA) - Molecular Basis of Disease, 1832(7):1088–1103 DOI: 10.1016/j.bbadis.2012.12.007.

Rudolph D, Steegmaier M, Hoffmann M, Grauert M, Baum A, Quant J, Haslinger C, Garin-Chesa P, Adolf GR. 2009. BI 6727, a Polo-like kinase inhibitor with improved pharmacokinetic profile and broad antitumor activity. Clin Cancer Res, 15(9):3094–3102 DOI: 10.1158/1078-0432.CCR-08-2445.

Rudolph V, Andrié RP, Rudolph TK, Friedrichs K, Klinke A, Hirsch-Hoffmann B, Schwoerer AP, Lau D, Fu X, Klingel K, Sydow K, Didié M, Seniuk A, von Leitner E-C, Szoecs K, Schrickel JW, Treede H, Wenzel U, Lewalter T, Nickenig G, Zimmermann W-H, Meinertz T, Böger RH, Reichenspurner H, Freeman BA, Eschenhagen T, Ehmke H, Hazen SL, Willems S, Baldus S. 2010. Myeloperoxidase acts as a profibrotic mediator of atrial fibrillation. Nat Med, 16(4):470–474 DOI: 10.1038/nm.2124.

Ruiz S, Santos E, Bustelo XR. 2007. RasGRF2, a Guanosine Nucleotide Exchange Factor for Ras GTPases, Participates in T-Cell Signaling Responses. Mol Cell Biol, 27(23):8127–8142 DOI: 10.1128/MCB.00912-07.

Sandner P, Berger P, Zenzmaier C. 2017. The Potential of sGC Modulators for the Treatment of Age-Related Fibrosis: A Mini-Review. Gerontology, 63(3):216–227 DOI: 10.1159/000450946.

Schott S, Wimberger P, Klink B, Grützmann K, Puppe J, Wauer US, Klotz DM, Schröck E, Kuhlmann JD. 2017. The conjugated antimetabolite 5-FdU-ECyd and its cellular and molecular effects on platinum-sensitive vs. -resistant ovarian cancer cells in vitro. Oncotarget, 8(44):76935–76948 DOI: 10.18632/oncotarget.20260.

Schwab M, Reynders V, Loitsch S, Shastri YM, Steinhilber D, Schröder O, Stein J. 2008. PPARgamma is involved in mesalazine-mediated induction of apoptosis and inhibition of cell growth in colon cancer cells. Carcinogenesis, 29(7):1407–1414 DOI: 10.1093/carcin/bgn118.

Scirpo R, Fiorotto R, Villani A, Amenduni M, Spirli C, Strazzabosco M. 2015. Stimulation of nuclear receptor PPAR-γ limits NF-kB-dependent inflammation in mouse cystic fibrosis biliary epithelium. Hepatology, 62(5):1551–1562 DOI: 10.1002/hep.28000.

Shamhart PE, Luther DJ, Adapala RK, Bryant JE, Petersen KA, Meszaros JG, Thodeti CK. 2014. Hyperglycemia enhances function and differentiation of adult rat cardiac fibroblasts. Can J Physiol Pharmacol, 92(7):598–604 DOI: 10.1139/cjpp-2013-0490.

Shen T, Li Y, Yang L, Xu X, Liang F, Liang S, Ba G, Xue F, Fu Q. 2012. Upregulation of Polo-like kinase 2 gene expression by GATA-1 acetylation in human osteosarcoma MG-63 cells. Int J Biochem Cell Biol, 44(2):423–429 DOI: 10.1016/j.biocel.2011.11.018.

Shire Pharmaceutical Contracts Ltd. 2018. Fachinformation - Mezavant 1200 mg magensaftresistente Retardtabletten.

Singh M, Foster CR, Dalal S, Singh K. 2010. Role of osteopontin in heart failure associated with aging. Heart Fail Rev, 15(5):487–494 DOI: 10.1007/s10741-010-9158-6.

Singh M, Fowlkes V, Handy I, Patel CV, Patel RC. 2009. Essential Role of PACT-Mediated PKR Activation in Tunicamycin-induced Apoptosis. J Mol Biol, 385(2):457–468 DOI: 10.1016/j.jmb.2008.10.068.

Spalek M, Jonska-Gmyrek J, Gałecki J. 2015. Radiation-induced morphea - a literature review. J Eur Acad Dermatol Venereol, 29(2):197–202 DOI: 10.1111/jdv.12704.

Stevenson IH, Roberts-Thomson KC, Kistler PM, Edwards GA, Spence S, Sanders P, Kalman JM. 2010. Atrial electrophysiology is altered by acute hypercapnia but not hypoxemia: implications for promotion of atrial fibrillation in pulmonary disease and sleep apnea. Heart Rhythm, 7(9):1263–1270 DOI: 10.1016/j.hrthm.2010.03.020.

Strebhardt K. 2010. Multifaceted polo-like kinases: drug targets and antitargets for cancer therapy. Nat Rev Drug Discov, 9(8):643–660 DOI: 10.1038/nrd3184.

Suna G, Wojakowski W, Lynch M, Barallobre-Barreiro J, Yin X, Mayr U, Baig F, Lu R, Fava M, Hayward R, Molenaar C, White SJ, Roleder T, Milewski KP, Gasior P, Buszman PP, Buszman P, Jahangiri M, Shanahan CM, Hill J, Mayr M. 2018. Extracellular Matrix Proteomics Reveals Interplay of Aggrecan and Aggrecanases in Vascular Remodeling of Stented Coronary Arteries. Circulation, 137(2):166–183 DOI: 10.1161/CIRCULATIONAHA.116.023381.

Syed N, Smith P, Sullivan A, Spender LC, Dyer M, Karran L, O'Nions J, Allday M, Hoffmann I, Crawford D, Griffin B, Farrell PJ, Crook T. 2006. Transcriptional silencing of Polo-like kinase 2 (SNK/PLK2) is a frequent event in B-cell malignancies. Blood, 107(1):250–256 DOI: 10.1182/blood-2005-03-1194.

Tallquist MD, Molkentin JD. 2017. Redefining the identity of cardiac fibroblasts. Nat Rev Cardiol, 14(8):484–491 DOI: 10.1038/nrcardio.2017.57.

Tekkeşin Aİ, Velibey Y, Türkkan C, Alper AT, Çakıllı Y, Güvenç TS, Tanık O, Kaya A, Yıldırımtürk Ö, Özbilgin N, Güzelburç Ö, Öz A, Zehir R, Gürkan K. 2017. Diastolic Electrocardiographic Parameters Predict Implantable Device Detected Asymptomatic Atrial Fibrillation. Balkan Med J, 34(5):417–424 DOI: 10.4274/balkanmedj.2016.0246.

Thijssen VLJL, van der Velden HMW, van Ankeren EP, Ausma J, Allessie MA, Borgers M, van Eys GJJM, Jongsma HJ. 2002. Analysis of altered gene expression during sustained atrial fibrillation in the goat. Cardiovasc Res, 54(2):427–437 DOI: 10.1016/S0008-6363(02)00260-2.

Thomas SM, DeMarco M, D'Arcangelo G, Halegoua S, Brugge JS. 1992. Ras is essential for nerve growth factor- and phorbol ester-induced tyrosine phosphorylation of MAP kinases. Cell, 68(6):1031–1040.

Travers JG, Kamal FA, Robbins J, Yutzey KE, Blaxall BC. 2016. Cardiac Fibrosis: The Fibroblast Awakens. Circulation Research, 118(6):1021–1040 DOI: 10.1161/CIRCRESAHA.115.306565.

Trueblood NA, Xie Z, Communal C, Sam F, Ngoy S, Liaw L, Jenkins AW, Wang J, Sawyer DB, Bing OH, Apstein CS, Colucci WS, Singh K. 2001. Exaggerated left ventricular dilation and reduced collagen deposition after myocardial infarction in mice lacking osteopontin. Circ Res, 88(10):1080–1087.

Warnke S, Kemmler S, Hames RS, Tsai H-L, Hoffmann-Rohrer U, Fry AM, Hoffmann I. 2004. Polo-like kinase-2 is required for centriole duplication in mammalian cells. Curr Biol, 14(13):1200–1207 DOI: 10.1016/j.cub.2004.06.059.

Watanabe T, Takeishi Y, Hirono O, Itoh M, Matsui M, Nakamura K, Tamada Y, Kubota I. 2005. C-reactive protein elevation predicts the occurrence of atrial structural remodeling in patients with paroxysmal atrial fibrillation. Heart Vessels, 20(2):45–49 DOI: 10.1007/s00380-004-0800-x.

Wenger RH, Kurtcuoglu V, Scholz CC, Marti HH, Hoogewijs D. 2015. Frequently asked questions in hypoxia research. Hypoxia (Auckl), 3:35–43 DOI: 10.2147/HP.S92198.

Whitbeck MG, Charnigo RJ, Shah J, Morales G, Leung SW, Fornwalt B, Bailey AL, Ziada K, Sorrell VL, Zegarra MM, Thompson J, Hosn NA, Campbell CL, Gurley J, Anaya P,

Booth DC, Biase LD, Natale A, Smyth S, Moliterno DJ, Elayi CS. 2014. QRS duration predicts death and hospitalization among patients with atrial fibrillation irrespective of heart failure: evidence from the AFFIRM study. Europace, 16(6):803–811 DOI: 10.1093/europace/eut335.

Wiersma M, Meijering RAM, Qi X, Zhang D, Liu T, Hoogstra-Berends F, Sibon OCM, Henning RH, Nattel S, Brundel BJJM. 2017. Endoplasmic Reticulum Stress Is Associated With Autophagy and Cardiomyocyte Remodeling in Experimental and Human Atrial Fibrillation. J Am Heart Assoc, 6(10) DOI: 10.1161/JAHA.117.006458.

Woodall MC, Woodall BP, Gao E, Yuan A, Koch WJ. 2016. Cardiac Fibroblast GRK2 Deletion Enhances Contractility and Remodeling Following Ischemia/Reperfusion Injury. Circulation Research:CIRCRESAHA.116.309538 DOI: 10.1161/CIRCRESAHA.116.309538.

Wu M, Assassi S. 2013. The Role of Type 1 Interferon in Systemic Sclerosis. Front Immunol, 4 DOI: 10.3389/fimmu.2013.00266.

Wu M, Schneider DJ, Mayes MD, Assassi S, Arnett FC, Tan FK, Blackburn MR, Agarwal SK. 2012. Osteopontin in Systemic Sclerosis and its Role in Dermal Fibrosis. J Invest Dermatol, 132(6):1605–1614 DOI: 10.1038/jid.2012.32.

Wynn TA. 2008. Cellular and molecular mechanisms of fibrosis. J Pathol, 214(2):199–210 DOI: 10.1002/path.2277.

Xie Z, Singh M, Singh K. 2004. ERK1/2 and JNKs, but not p38 kinase, are involved in reactive oxygen species-mediated induction of osteopontin gene expression by angiotensin II and interleukin-1β in adult rat cardiac fibroblasts. J Cell Physiol, 198(3):399–407 DOI: 10.1002/jcp.10419.

Yin FC, Spurgeon HA, Rakusan K, Weisfeldt ML, Lakatta EG. 1982. Use of tibial length to quantify cardiac hypertrophy: application in the aging rat. Am J Physiol, 243(6):H941-947 DOI: 10.1152/ajpheart.1982.243.6.H941.

Yoon J-H, Sudo K, Kuroda M, Kato M, Lee I-K, Han JS, Nakae S, Imamura T, Kim J, Ju JH, Kim D-K, Matsuzaki K, Weinstein M, Matsumoto I, Sumida T, Mamura M. 2015. Phosphorylation status determines the opposing functions of Smad2/Smad3 as STAT3 cofactors in T_H17 differentiation. Nature Communications, 6:7600 DOI: 10.1038/ncomms8600.

Yue L, Xie J, Nattel S. 2011. Molecular determinants of cardiac fibroblast electrical function and therapeutic implications for atrial fibrillation. Cardiovasc Res, 89(4):744–753 DOI: 10.1093/cvr/cvq329.

Zhao H, Chen Q, Alam A, Cui J, Suen KC, Soo AP, Eguchi S, Gu J, Ma D. 2018. The role of osteopontin in the progression of solid organ tumour. Cell Death Dis, 9(3):356 DOI: 10.1038/s41419-018-0391-6.

Zhao H, Wang W, Zhang Jie, Liang T, Fan G-P, Wang Z-W, Zhang P-D, Wang X, Zhang Jing. 2016. Inhibition of osteopontin reduce the cardiac myofibrosis in dilated cardiomyopathy via focal adhesion kinase mediated signaling pathway. Am J Transl Res, 8(9):3645–3655.

Zhu F, Li Y, Zhang J, Piao C, Liu T, Li H-H, Du J. 2013. Senescent cardiac fibroblast is critical for cardiac fibrosis after myocardial infarction. PLoS ONE, 8(9):e74535 DOI: 10.1371/journal.pone.0074535.

Zoni-Berisso M, Lercari F, Carazza T, Domenicucci S. 2014. Epidemiology of atrial fibrillation: European perspective. Clin Epidemiol, 6:213–220 DOI: 10.2147/CLEP.S47385.

8 Supplemental Data

Table 6 Patient data for OPN ELISA

	Healthy (n=4)	AF no fibrosis (n=8)	AF with fibrosis (n=9)
Average age (years)	54	71,3	71,4
Gender			
Male	2	5	5
Female	2	3	4
Disease			
Hypertension	1	8	9
Diabetes mellitus	0	4	3
Hyperlipidemia	0	5	5
Chronic kidney disease (GFR 40 – 90 ml/min)	0	2	3
Chronic lung disease	0	1	2
Thyroid disease	0	0	2
Adipositas	0	1	0
Current smoking	0	1	1
Atrial fibrillation characteristics			
Persistent AF	0	4	7
Paroxysmal AF	0	3	1
Atrial flutter	0	1	1
Drugs			
ACE inhibitors	1	0	6
AT1 receptor blockers	0	5	1
β-AR blockers	0	7	9
Calcium channel blockers (nifedipine)	0	2	4
Calcium channel blockers (verapamil)	0	1	0
Antiarrhythmic drugs	0	0	3
Glycosides	0	2	1
Statin	1	5	5

Allopurinol	0	1	3
Diuretics	0	5	6
Aldosterone inhibitor	0	1	1
Oral anticoagulants	0	7	9
Antidepressant	0	1	1
Oral antidiabetic drugs	0	3	2
α-AR blocker	0	1	0
PPI	1	7	9
NSAID	0	2	1
Insulin	0	3	1
Average osteopontin (ng/ml)	9,65	16,78	25,99

Table 7 Patient data for cell isolation, western blots and methylation analysis

	SR (n = 27)	**AF (n = 20)**
Average age (years)	68,8	72,4
Gender		
Male	21	12
Female	6	8
Average BMI	29,9	28,4
Disease		
Hypertension	24	15
Diabetes mellitus	9	7
Hyperlipidemia	18	6
Chronic kidney disease (GFR 40 - 90)	7	7
Chronic lung disease	5	2
Current smoking	11	4
Alcohol addiction	1	0
OSAS	2	2
Diagnosis		
ACB	18	7
Valvular replacement	11	16
Ablation	0	13
Echocardiography		
Ejection fraction	54,0	50,6
LV hypertrophy	12	7
Drugs		

ACE inhibitors	12	7
AT1 receptor blockers	6	4
β-AR blockers	15	17
Calcium channel blockers	4	2
Antiarrhythmic drugs	0	2
Glycosides	0	9
Statin	21	6
Allopurinol	2	5
Diuretics	12	11
Aldosterone inhibitor	1	3
Oral anticoagulants	3	14
Antidepressant	2	1
Oral antidiabetic drugs	4	2
α-AR blocker	2	2
PPI	2	3
ASS	14	1
Insulin	2	1

Table 8 Patient data for Affymetrix® RNA analysis and qPCR analysis

	SR (n = 7)	**AF (n = 5)**
Average age (years)	68,0	69,2
Gender		
(Male)	7	4
(Female)	0	1
Average BMI	28,0	30,2
Disease		
Hypertension	6	5
Diabetes mellitus	1	1
Hyperlipidemia	6	4
Chronic kidney disease (GFR 40 - 90)	2	2
Chronic lung disease	0	1
Current smoking	3	3
Epilepsy	1	0
OSAS	1	0
Diagnosis		
ACB	7	3

Valvular replacement	2	5
Ablation	0	3
Echocardiography		
Ejection fraction	47,3	36,3
LV hypertrophy	2	2
Drugs		
ACE inhibitors	5	4
AT1 receptor blockers	2	1
β-AR blockers	6	5
Nitrates	1	1
Calcium channel blockers	2	3
Antiarrhythmic drugs	0	1
Glycosides	1	2
Statin	6	4
Diuretics	2	4
Aldosterone inhibitor	0	1
Oral anticoagulants	1	3
Antidepressant	1	1
Oral antidiabetic drugs	1	1
PPI	2	1
ASS	4	3

Ultrasonic-augmented primary adult fibroblast isolation

1. Getting started – Preparing the setup, material and media

1.1. Prepare cell culture medium, PBS solution, Liberase stock solution (reconstitute 50 mg of lyophilized Liberase in 12 ml of sterile ultrapure water) and 0.25% trypsin solution.

1.2. Warm up the medium, the PBS and the trypsin solution to 37°C.

1.3. Preheat the ultrasonic water bath to 37°C.

1.4. Disinfect forceps, a stainless steel spatula, scalpels (2x scalpels per organ) and 2 glass beakers with 70% ethanol and place these materials under the cell culture hood.

1.5. Fill one beaker with 70% ethanol and the other with sterile water or PBS solution. These beakers are required to disinfect and wash the instrument after each organ procession.

1.6. Place sterile 15 ml plastic tubes containing cold PBS on wet ice. (The number of tubes depends on the number of organs you want to isolate fibroblasts from.)

2. Mouse dissection and organ removal

2.1. Wear **two pairs of gloves** one above the other, so the first pair can be removed as soon as the animal has been dissected. **Attention:** This procedure prevents bacteria from the animal's fell and skin from spreading over the organs.

2.2. Euthanize the mouse (e.g. via cervical dislocation) and pin the carcass with needles to every limb to a Styrofoam pad.

2.3. Disinfect the mouse carcass using 70% ethanol spray. Make sure the fur is soaked in ethanol so the hair will not swirl up.

2.4. Cut the fur right above the urogenital tract using surgical forceps and atraumatic scissors. Cut the skin alongside the middle line from the point of the initial incision to the neck (3 – 4 cm) and add relief cuts at the limbs. **Attention:** Do not perforate the muscular layer at this step to avoid bacterial contamination!

2.5. Pin the skin to the Styrofoam pad to have optimal access to the musculature covering the abdominal cavity.

2.6. Disinfect the abdominal musculature twice using 70% ethanol. Let the ethanol dry before continuing to the next step.

2.7. Remove the first pair of gloves. Use a new, sterile set of forceps and scissors.

2.8. Open the abdominal cavity and the thorax by incising the muscular layer with surgical scissors to gently remove the organs of choice.

2.9. Put the organs into the sterile tubes containing cold PBS. Close the tubes tightly. Place the tubes on wet ice until you continue with step 3.1.

3. Tissue mincing, digestion and cell extraction

3.1. Transfer the tubes under the sterile cell culture hood. **Attention:** Wear a fresh pair of gloves and disinfect the tubes with 70% ethanol before transferring them under the hood!

3.2. Take the organ out of the 15 ml tube using sterile forceps. Place the organ onto one half of a sterile 6 cm Petri dish and wash the organ briefly with PBS to remove excess blood. Transfer the organ to the second half of the Petri dish, remove excess PBS.

3.3. Mince the tissue using two sterile scalpels. The remaining tissue fragments should not be larger than 1 – 2 mm.

3.4. Transfer the minced tissue into a new sterile 15 ml tube using the sterile spatula and add 2 ml of 0.25% trypsin solution. Place the tube into a cell culture incubator at 37°C for 5 min.

3.5. Vortex the tube gently (circa 1400/ min) for 10 s.

3.6. Stop the trypsin reaction under the cell culture hood by adding 4 ml FCS-containing cell culture medium (Dulbecco's Modified Eagle Medium (DMEM), e.g.).

3.7. Add 250 µl of Liberase solution to each tube containing heart or lung tissue and 100 µl for kidney or liver, respectively.

3.8. Place the tubes into an ultrasound water bath (37°C) and activate the ultrasonic for 10 min.

3.9. Vortex the tubes gently (circa 1400/ min) for 10 s.

3.10. Place the tubes again into the ultrasonic water bath for 10 min.

3.11. Vortex gently (circa 1400/ min) for 10 s.

3.12. Disinfect the tubes with 70% ethanol and transfer them under the sterile cell culture hood.

3.13. Filter the solution with a 40 µm mesh into a new sterile 15 ml tube.

3.14. Centrifuge the tube at 500xg for 5 min.

3.15. Remove the supernatant and resuspend the pellet in 1 ml fresh medium.

3.16. Transfer the cells into a suitable cell culture vessel (6-well plate, e.g.) and place the vessel into the cell culture incubator overnight at 37°C and 5% CO_2.

3.17. The next day, remove the medium, wash 3 times with PBS, then add fresh medium (the added volume depends on the cell culture vessel of choice, 2 ml per well of a 6-well plate e.g.).

3.18. Change the medium every other day.

3.19. Fibroblasts can be splitted after reaching optical confluence of 90% (usually after 5-7 days).

Table 9 Material list for ultrasonic-augmented primary adult fibroblast isolation

Position	Company
0.25% Trypsin-EDTA	Sigma-Aldrich, St. Louis, USA
Antibiotics	Gibco-Life Technologies, Carlsbad, USA
Cell culture hood	Thermo Fisher Scientific, Waltham, USA
Cell culture incubator	Thermo Fisher Scientific, Waltham, USA
Cell culture plates	Thermo Fisher Scientific, Waltham, USA
Cell culture suction	VACUUBRAND GMBH + CO KG, Wertheim, Germany
Cell strainer (mesh)	Corning, Tewksbury, USA
Centrifuge	Thermo Fisher Scientific, Waltham, USA
Cordless pipetting controller	Hirschmann, Eberstadt, Germany
Disposable pipette tips	Sigma-Aldrich, St. Louis, USA
Disposable plastic pipettes	Sigma-Aldrich, St. Louis, USA
Disposable sterile scalpel	Myco Medical, Cary, USA
Dulbeccos Modified Eagle Medium (DMEM)	Thermo Fisher Scientific, Waltham, USA
Eppendorf tubes	Eppendorf, Hamburg, Germany
Fetal calf serum (FCS)	Sigma-Aldrich, St. Louis, USA
Liberase	Sigma-Aldrich, St. Louis, USA
Petri dish 6 cm	Sigma-Aldrich, St. Louis, USA
Phosphate Buffered Saline (PBS)	Sigma-Aldrich, St. Louis, USA
Senescence detection kit	Abcam, Cambridge, UK
Shaker/ Vortex	IKA, Staufen im Breisgau, Germany
Sterile plastic tubes	Thermo Fisher Scientific, Waltham, USA
Ultrasonic water bath	BANDELIN electronic GmbH & Co. KG, Berlin, Germany

Surgical scissors (atraumatic)	Aesculap AG, Tuttlingen, Germany
Surgical scissors	Aesculap AG, Tuttlingen, Germany
Surgical forceps	Aesculap AG, Tuttlingen, Germany

9 Acknowledgements

When something makes you the happiest and the saddest person at the same time, that's when it's real.

That's when it's worth something.

-Anonymous-

Curiosity, excitement, frustration, success and relief – it was a long way to complete the present work and I would like to take the opportunity to express my heartfelt gratitude.

I am grateful to my supervisor, mentor and friend Prof. Ali El-Armouche for giving me the chance to develop my independent research project and to pursue it with all scientific freedom in his laboratory. His continuous support, constructive criticism and mentoring made this dissertation possible.

Furthermore, I would like to thank Dr. rer. medic. Susanne Kämmerer and my TAC members PD. Dr. med. Michael Wagner and Dr. rer. nat. Silvio Weber for their continuous scientific and more importantly personal input. They shared a great deal of their experience with me from which I will permanently benefit.

I am grateful to Prof. Dr. med. Claudia Günther for inspiring scientific discussions, being my clinical mentor within the Else Kröner-Forschungskolleg (Dresden Clinician Scientist Program) and for the provision of dermal fibroblasts to this study.

I also would like to thank my former mentor Prof. Dr. med. Dr. h.c. Ursula Ravens for providing the basis of this work by granting me access to the data of the Affymetrix® RNA sequencing. Besides the scientific achievements, Ursula Ravens contributed decisively to my personal and professional development.

Additionally, I would like to thank Prof. Dr. rer. nat. Günter Vollmer for important input and criticism which profoundly improved this thesis.

I would like to thank the scientists in our laboratory for their support, input and encouragement. Prof. Dr. rer. nat. Kaomei Guan, Prof. Christopher Antos and Dr. rer. medic. Stefanie Meyer-Roxlau – thank you!

Nowadays it is nearly impossible to conduct scientific research in a single laboratory without support. I would like to thank our cooperation partner Prof. Dr. med. Manuel Mayr, Ph.D. for introducing me to the technique of mass spectrometry in his laboratory at King's College London. Eloi Haudebourg, Marc Lynch and Dr. med. Tom Herschel made the time in London unforgettable.

A special and heartfelt thank you goes to Mrs. Annett Opitz and Ms. Romy Kempe who helped me enormously with western blotting and general assistance.

I am glad the laboratory offered me the chance to meet Dr. med. des. Julius Joos. I particularly enjoyed the lunch times in our social room and your fine sense of humor.

I am extraordinarily glad about my friends Pia Vahlefeld, Martin Dschietzig and Sascha Hill. You are the best. Thank you for your friendship, humor and encouragement.

The "Förderverein der Dresdner Herz-Kreislauf-Tage" is gratefully acknowledged for funding.

Last, but not least, I am grateful to my parents Kerstin and Reinhard Künzel and to my fiancée Karolina. Thank you for your love and support. I am especially grateful to my dear grandmother Regina Leeder and my uncle Dr. med. Rolf Künzel who sadly will not be able to celebrate the accomplished with me.

10 Declarations

10.1 Erklärung über die Eigenständigkeit

1. Hiermit versichere ich, dass ich die vorliegende Arbeit ohne unzulässige Hilfe Dritter und ohne Benutzung anderer als der angegebenen Hilfsmittel angefertigt habe; die aus fremden Quellen direkt oder indirekt übernommenen Gedanken sind als solche kenntlich gemacht.

2. Bei der Auswahl und Auswertung des Materials sowie bei der Herstellung des Manuskripts habe ich Unterstützungsleistungen von folgenden Personen erhalten:

- Herr Prof. Dr. med. Ali El-Armouche,
- Herr Dr. rer. nat. Silvio Weber,
- Herr PD. Dr. med. Michael Wagner,
- Frau Dr. rer. medic. Susanne Kämmerer,
- Herrn Prof. Dr. med. Manuel Mayr, Ph.D. (King's College London),
- Frau Prof. Dr. med. Dr. h.c. Ursula Ravens,
- Frau Prof. Dr. med. Claudia Günther.

3. Weitere Personen waren an der geistigen Herstellung der vorliegenden Arbeit nicht beteiligt. Insbesondere habe ich nicht die Hilfe eines kommerziellen Promotionsberaters in Anspruch genommen. Dritte haben von mir weder unmittelbar noch mittelbar geldwerte Leistungen für Arbeiten erhalten, die im Zusammenhang mit dem Inhalt der vorgelegten Dissertation stehen.

4. Die Arbeit wurde bisher weder im Inland noch im Ausland in gleicher oder ähnlicher Form einer anderen Prüfungsbehörde vorgelegt.

5. Die Inhalte dieser Dissertation wurden in folgender Form veröffentlicht:

Kongressbeiträge (Poster/ Vorträge/ Preise von Fachgesellschaften)

2017	DGK Jahrestagung, Mannheim (Vortrag)
2017	Dresdner Herz-Kreislauf-Tage (Forschungspreis)
2017	DGPT, Heidelberg (Poster)
2019	DGK Jahrestagung, Mannheim (Vortrag)

Originalarbeiten

Kuenzel SR, Sekeres K, Kaemmerer S, Kolanowski T, Meyer-Roxlau S, Piorkowski C, Tugtekin SM, Rose-John S, Yin X, Mayr M, Kuhlmann JD, Wimberger P, et al. 2018. Hypoxia-induced epigenetic silencing of polo-like kinase 2 promotes fibrosis in atrial fibrillation. bioRxiv 445098.

Stephan R. Kuenzel, Charlotte Schaeffer, Karolina Sekeres, Carola S. Mehnert, Stephanie M. Schacht Wall, Manja Newe, Susanne Kämmerer, Ali El-Armouche. Ultrasonic-augmented primary adult fibroblast isolation. Journal of Visualized Experiments. 2019 (Currently in minor revision)

6. Ich bestätige, dass es keine zurückliegenden erfolglosen Promotionsverfahren gab.

7. Ich bestätige, dass ich die Promotionsordnung der Medizinischen Fakultät der Technischen Universität Dresden anerkenne.

8. Ich habe die Zitierrichtlinien für Dissertationen an der Medizinischen Fakultät der Technischen Universität Dresden zur Kenntnis genommen und befolgt

Dresden, den (Dr. med. Stephan R. Künzel)

.

10.2 Erklärung über die Einhaltung der aktuellen gesetzlichen Vorgaben im Rahmen der Dissertation

Hiermit bestätige ich die Einhaltung der folgenden aktuellen gesetzlichen Vorgaben im Rahmen meiner Dissertation:

- Das zustimmende Votum der Ethikkommission bei Klinischen Studien, epidemiologischen Untersuchungen mit Personenbezug oder Sachverhalten, die das Medizinproduktegesetz betreffen. Aktenzeichen der zuständigen Ethikkommission: EK 114082202, EK 465122013

- Die Einhaltung der Bestimmungen des Tierschutzgesetzes: T 2014/5; TVA 25/2017, TVV 64/2018

- Die Einhaltung des Gentechnikgesetzes: Az. 55-8811.72/46

- Die Einhaltung von Datenschutzbestimmungen der Medizinischen Fakultät und des Universitätsklinikums Carl Gustav Carus.

Dresden, den (Dr. med. Stephan R. Künzel)